Early Expression of CACNA2D1 in Satellite Cells Promotes Myogenicity and Repair of Dystrophic Muscle

BY

TAMMY ROCÍO SMITH TAMAYO
B.S. University of California, Davis, 2005
B.S. University of California, Davis, 2005
M.S. University of California, Davis, 2008

THESIS

Submitted as partial fulfillment of the requirements for the degree of Doctor of Philosophy in Physiology and Biophysics in the Graduate College of the University of Illinois at Chicago, 2015

Chicago, Illinois

Defense Committee:

Ahlke Heydemann PhD, Chair
Jesús García-Martínez MD, PhD, Advisor
David Geenen, PhD
John Kennedy PhD
Timothy Koh PhD, Nutrition and Kinesiology

ACKNOWLEDGMENTS

Each of my committee members directly impacted my graduate education at UIC. John Kennedy consistently provided me with thorough feedback to help me develop a scientific sensibility while not stifling my personal approach. David Geenen regularly encouraged me to think two or three experiments ahead in an effort to sharpen my scientific sensibilities. Timothy Koh was always willing to share his expansive knowledge of regeneration. The chair of my committee, Ahlke Heydemann, was always willing to trouble-shoot experiments, lend reagents, and work out data management presentation. My advisor, Jesús García-Martínez, played many roles, but the two roles he most often employed were that of coach and comedian. Habits that I developed in his lab will keep me working hard and laughing aloud.

The five committee members provided me with expertise in *in vivo* muscle testing and characterization, muscle metabolism, cellular implantation in non-native tissue, interaction of inflammatory cells and muscle regeneration, and ion channel involvement in cell signaling. I would be honored if our career paths cross again.

Kelly Garcia, Liliana Grajales, Eben Eno, Omar Jawaid, and Carlos Madrigal have earned my gratitude as they provided support during experiments, many of which are presented here.

For the past six years, Roberta Bernstein, Larry Tobacman, Nancy Freitag and Karen Colley of the MSTP supported me wholeheartedly, and for that I will always be grateful.

An NIH training grant (PI Solaro) and an MDA grant (PI García) supported this work.

TRST

CONTRIBUTION OF AUTHORS

Each chapter of this written work was improved with the help of Jesús Garcia-Martínez MD, PhD. Chapter 1 sets the context of this work with the published work of other laboratories. I did the literature review and wrote this chapter. Chapter 2 is a statement of my hypothesis and specific aims, which I developed collaboratively with my advisor. Chapter 3 is slightly modified from a published work that is primarily reflective of my own efforts. Liliana Grajales, PhD obtained data for figures 3.4 and 3.5, and is a coauthor of this paper. I obtained and managed the rest of the data shown in all other figures of this chapter. Jesús Garcia-Martínez played a large role in writing the manuscript. Chapter 4 contains data about the cell signaling experiments. I designed and either conducted or supervised all of the experiments represented in this chapter and analyzed the data. I supervised the work of Carlos Madrigal who helped with experiments shown in figure 4.4. I was the driver behind all data in Chapter 5. Eben Eno, MD, helped analyze data for this chapter. This work was recently submitted for publication, and Eben Eno MD and Jesús Garcia-Martínez MD, PhD are both coauthors of this work. Chapter 6 was a very collaborative work. Kelly García, DVM, PhD, helped with the design of the grafting protocol. Omar Jawaid, MS, helped with very long muscle grafting procedures and muscle function tests. Finally, I wrote the Conclusions and Future Directions chapters with the continued help of Jesús Garcia-Martínez MD, PhD.

TABLE OF CONTENTS

Acknowledgments ii

Contribution of Authors iii

Table of Contents iv

List of Figures iv

List of Abbreviations ix

Summary x

Chapter 1: Background and significance 1
- Duchenne Muscular Dystrophy 1
- Satellite cell grafts in humans 4
- CD34 6
- Thrombospondin-1 6
- Figures 8
  - Figure 1.3: Organization of domains of Thrombospondin subgroups A and B 10

Chapter 2: Hypothesis and specific aims 11

Chapter 3: *In vitro* characterization of four subpopulations 13
- Methods 15
  - Isolation of satellite cells 15
  - Fluorescence-activated cell sorting 16
  - Real-time quantitative polymerase chain reaction (RT-qPCR) 16
- Results 17
  - Presence of α2δ1 protein in isolated satellite cells 17
  - The α2δ1 protein is expressed earlier than the other calcium channel subunits 18
  - Quantification of cell size 19
  - Distinct myogenic regulatory factors profiles in satellite cell subpopulations 20
- Discussion 21
- Figures 24

Chapter 4: Signaling through the α2δ1 receptor 31
- Methods 33
  - Migration assay 33
  - Protein Quantification 34
  - Western Blot 35
  - Bromodeoxyuridine (proliferation) assay 36
- Results 36
  - Thrombospondin is expressed from bone-marrow derived macrophage-like cells. 36
  - Treatment with TSP accelerates expression of Jnk 37
  - Treatment with thrombospondin increases proliferation rate in C2C12 cells 37
  - Treatment with either thrombospondin and/or gabapentin augments migration rate. 38
- Discussion 38
- Figures 41

TABLE OF CONTENTS (CONTINUED)

Chapter 5: *In vivo* characterization of skeletal muscle 45
Methods 47
Partial *in situ* mouse tibialis anterior characterization protocol 47
Anesthesia 47
Stimulation of muscle contraction 48
Moisture Maintenance 48
Muscle Preparation 48
Optimization of passive tension and voltage 49
Twitch 49
Fatigue 49
Force-Frequency 50
Passive Tension Tolerance 50
Results: 51
Fatigue 51
Force-Frequency 53
Passive Tension Tolerance 54
Discussion 54
Fatigue 56
Force-Frequency 57
Passive Tension Tolerance 58
Figures 61
Chapter 6: Restoration of skeletal muscle function in muscles treated with satellite cells that express α2δ1 74
Methods: 75
Satellite Cell Isolation and Storage: 75
Anesthesia: 75
Irradiation of hindlimbs: 75
Muscle stimulation protocol: 76
Injection of sorted cells 76
Re-exercise challenge 76
Statistics: 77
Results 77
Muscles treated with cells that express α2δ1 are significantly heavier than the contralateral muscle 77
No difference in force, force generation rate or relaxation rate in muscles control or treated muscles during the fatigue protocol 78
Muscles treated with cells that express α2δ1 are significantly stronger than the contralateral muscle 78
Muscles treated with cells that express α2δ1 contract faster than the contralateral muscle 78
Muscles treated with either cell subpopulation relax more quickly than contralateral muscle 79
Discussion: 81
Re-exercise challenge 83
Figures 85

TABLE OF CONTENTS (CONTINUED)

Conclusions **95**

Future directions **98**

REFERENCES **101**

VITA **109**

Appendix **112**

Permission to Reprint Copyright Material 112

LIST OF FIGURES

Figure 1.1: The dystrophin-glycoprotein complex…… 8
Figure 1.2: The structure of α2δ1 provides clues to its function…… 9
Figure 1.3: Organization of domains of thrombospondin subgroups A and B…… 10
Figure 3.1: Satellite cells sorted for CD34…… 24
Figure 3.2 Satellite cells sorted for CD34 and α2δ1…… 25
Figure 3.3: Cell sorting was performed to create the populations of study…… 26
Figure 3.4: Expression of calcium channel subunits in satellite cells…… 27
Figure 3.5: Changes in subunit mRNA expression during the first week after plating…… 28
Figure 3.6: Morphological dimensions of sorted satellite cells…… 29
Figure 3.7: Expression of myogenic transcription factors in satellite cells…… 30
Figure 4.1: Thrombospondin is secreted from macrophage-like cells…… 41
Figure 4.2 Treatment with TSP accelerates expression of Total Jnk1…… 42
Figure 4.3 Treatment with TSP increases proliferation rate of C2C12 cells *in vitro*…… 43
Figure 4.4: Migration of satellite cells not treated, treated with TSP, GBP, or both……44
Figure 5.1: Myomechanical testing protocol……61
Figure 5.2: Muscle testing platform……62
Figure 5.3: TA wet mass and maximal force by age……63
Figure 5.4: Force is not predictive of force generation rate……64
Figure 5.5: The mean force, force generation rate, and relaxation rate of 6-8 week old *mdx* muscles……65
Figure 5.6: Fatigue of force among groups……66
Figure 5.7: Initial, maximal and minimal force during fatigue……67
Figure 5.8: Initial, Maximal and Minimal force generation rates during fatigue……68
Figure 5.9: Initial, maximal and minimal relaxation rates during fatigue……69
Figure 5.10: *Mdx* versus WT mini-tetanti of fatigue……70
Figure 5.11: Maximal and minimal force generation rates in force frequency protocols……71
Figure 5.12: Maximal and minimal relaxation rates in force frequency protocols……72
Figure 5.13: Passive tension tolerance of force, force generation rate, and relaxation rate……73
Figure 6.1: Irradiation of hindlimbs of mdx host mice……85
Figure 6.2: Mass of treated and control muscles……86
Figure 6.3: Fatigue behavior of muscles treated with satellite cells that express surface α2δ1 and muscles treated with cells that do not express surface α2δ1……87
Figure 6.4: Force of muscles treated with satellite cells that express surface α2δ1 (A and B) and muscles treated with satellite cells without α2δ1 (C and D) in a less challenging force-frequency protocol (A and C) and a more challenging force-frequency protocol (B and D) ……88

Figure 6.5: Force generation rate of muscles treated with satellite cells that express surface α2δ1 (A and B) and muscles treated with satellite cells without α2δ1 (C and D) in a less challenging force-frequency protocol (A and C) and a more challenging force-frequency protocol (B and D)……..……..……**89**
Figure 6.6: Relaxation rate of muscles treated with satellite cells that express surface α2δ1 (A and B) and muscles treated with satellite cells without α2δ1 (C and D) in a less challenging force-frequency protocol (A and C) and a more challenging force-frequency protocol (B and D) ……..……...**90**
Figure 6.7: Passive tension tolerance of muscles treated with cells that have α2δ1 are capable of maintaining their contraction with significantly greater passive tension……...**91**
Figure 6.8: Mass of treated muscles 10 days after re-exercise challenge……...……..**92**
Figure 6.9: Mass decline after irradiation and re-exercise…….....….….…**93**
Figure 6.10: Exercised and non-exercised mass of tibialis anterior treated with vehicle at 10 weeks……...……..**94**

LIST OF ABBREVIATIONS

ANOVA	Analysis of Variance
AON	Anti-sense Oligonucleotides
CD	Cluster of Differentiation
DHPR	Dihydropyridine Receptor
DMD	Duchenne Muscular Dystrophy
DMSO	Dimethyl Sulfoxide
EDL	Extensor Digitorum Longus
EGPF	Enhanced Green Fluorescence Protein
FACS	Fluorescence Activated Cell Sorting
FAK	Focal Adhesion Kinase
FF	Force Frequency
FGR	Force Generation Rate
GBP	Gabapentin
GPI	Glycophosphatidylinositol
HRP	Horseradish Peroxidase
MHC	Major Histocompatibility Complex
MIDAS	Metal-ion Dependent Adhesion Site
PCR	Polymerase Chain Reaction
PMO	Morpholino Phosphorodiamidate
PVDF	Polyvinlyidene fluoride
PTT	Passive Tension Tolerance
RR	Relaxation Rate
RT-PCR	Reverse Transcription Polymerase Chain Reaction
RT-qPCR	Real Time Quantitative Polymerase Chair Reaction
TSP	Thrombospondin
TA	Tibialis Anterior
VWA	vonWillebrand A
WT	Wild Type

SUMMARY

Young boys with Duchenne Muscular Dystrophy suffer from early, profound, and progressive muscle degeneration. As damaged muscle regenerates, new muscles form from resident myogenic cells, called satellite cells. Replacement of the patient's own satellite cells with grafted satellite cells without this genetic mutation could potentially lead to the generation of muscle that is not predisposed to progressive muscle damage characteristic of Duchenne Muscular Dystrophy. Previous trials of myoblast transfer have shown that these efforts are limited by the lack of capability of the donor cells to attach and migrate into host muscle. It has been demonstrated that the surface protein α2δ1 aids in the attachment and migration of satellite cell-like cells *in vitro*. We characterized satellite cells from wild type mice and contrasted the morphology and myogenic transcription factor expression profiles of four subpopulations of satellite cells *in vitro*. These four populations of satellite cells were created based on the presence or absence of α2δ1 and CD34, a marker of primitive satellite cells. The creation of four subpopulations of cells was achieved by fluorescence activated cell sorting (FACS). We found that there are some differences in the behavior of these subpopulations of cells. For example, we showed that cells that express α2δ1 early elongate earlier than cells that did not express α2δ1, and that cells that express α2δ1 but not CD34 continued to elongate throughout the first week. Cells with α2δ1 at the time of FACS expressed more myogenin than MyoD, consistent with a population of cells that are more advanced in the process of differentiation. Next, we examined the differences in the ability of these cells to regenerate muscle *in vivo*. Subpopulations of satellite cells were injected into the tibialis anterior of dystrophic mice. We waited three to four weeks to allow the cells to integrate into the host

muscle tissue and then characterized the muscles that were treated with each population of cells. We found that, after three weeks, the muscles that were treated with cells that express α2δ1 were larger, stronger, and contracted and relaxed at a faster rate than the contralateral muscle treated with vehicle only. Muscles that were treated with cells without α2δ1 exhibit a greater relaxation rate, but there were no differences in mass, force, or force generation rate compared to the contralateral muscle treated with vehicle only.

We believed it was important to know whether these cells would be able to withstand further exercise. We subjected some mice to our intensive exercise protocol three weeks after the graft and then waited ten days to measure mass and muscle performance. In these experiments, we found that *all* muscles decreased in mass, demonstrating that the graft did not compensate for the irradiation damage. There was no significant preservation of mass in muscles treated with cells that expressed α2δ1. However, there was a significant preservation of mass in muscles that had been treated with cells that expressed CD34. This was an unexpected result, and led us to conclude that cells that express both CD34 and α2δ1 may be optimal for grafting.

Demonstration that cells with α2δ1 behave differently both *in vitro* and *in vivo* warrants further study of the mechanism of action during early development. Thrombospondin was shown to be a ligand to α2δ1 in neurons, but the mechanism is still not well understood. We investigated the role of thrombospondin in signaling through the α2δ1 receptor by using thrombospondin constructs and measuring critical signaling proteins, such as Akt, FAK, and Jnk and the phosphorylated counterparts. We did not find a difference in the phosphorylation

rates of these proteins, but we did observe a brief increase in total Jnk expression 24 hours after treatment. We also measured the proliferation rate and the rate of migration of cells treated with thrombospondin, gabapentin, both, or only vehicle. Gabapentin was used because previous experiments from other labs show that gabapentin is specific to the α2δ1 receptor, acting as a competitive inhibitor or partial agonist. Thrombospondin treatment did increase both proliferation rate and rate of migration. However, gabapentin alone increased the migration rate as much as thrombospondin and both thrombospondin together. Therefore, we were unable to conclude that thrombospondin was acting at the α2δ1 receptor. However, as gabapentin did have an effect on migration, we believe that α2δ1 is a critical component in this process. The particular mechanism was not made clear here.

Additionally, in order to have confidence in the power of the muscle function testing results, we designed a partial *in situ* testing protocol that tested more than strength of muscle, but also force generation rate and relaxation rate during twitch, fatigue, force-frequency, and passive tension tolerance protocols. We validated this protocol by performing this test on six to eight week old wild type and *mdx* mice from four to sixty-seven weeks old. We found that pattern of change of force, force generation rate and relaxation rates do not respond proportionally during these protocols. Further, the comparison of these measurements among the testing groups moved in opposing ways, not together as one would expect if it was believed that these were redundant measurements. This led us to conclude that thorough functional testing of muscles must include all three measurements in order to demonstrate the result of a treatment, or the progression of a disease.

CHAPTER 1: BACKGROUND AND SIGNIFICANCE

Duchenne Muscular Dystrophy

Duchenne Muscular Dystrophy (DMD) is a devastating condition that is characterized by early, progressive, and profound muscle wasting. DMD is caused by a genetic mutation that interferes with the expression of dystrophin, a protein that links contractile actin to the sarcoglycan complex on the sarcolemma (Figure 1.1). This lack of a linkage leaves the myofibers vulnerable to microtears in the membrane, resulting in tissue injury and cell death(Allen, Zhang et al.). Skeletal muscle regenerates via activation of muscle resident myogenic satellite cells, but in DMD, these cells also lack a viable copy of the dystrophin gene and the new muscle is just as vulnerable to contraction induced damage and necrosis, especially during lengthening contraction. In addition to increased vulnerability to death, it is believed that satellite cells cannot maintain viability after rapid rounds of degeneration and regeneration. When healthy muscle regenerates, an inflammatory cascade accompanies the early regeneration process. In DMD, the inflammatory condition permanently exacerbates degeneration.

In the clinic, therapy for DMD is largely aimed on supportive care and reducing the downstream effects of the lack of dystrophin. Weak muscles are supported by orthotics(Heckmatt, Rodillo et al. 1989; Taktak and Bowker 1995). Corticosteroids reduce the inflammation that accompanies the constant state of muscle injury(Hoffman, Reeves et al.). Advances in ventilation have prolonged the lifespan of these patients(Manzur and Muntoni 2009). Newer therapies reduce cardiac contractility, as cardiac complications are becoming the most common cause of death in these patients(Politano and Nigro). There is a great need to

find effective methods to introduce dystrophin into dystrophic muscle and reduce the rate of myofiber death. Strategies to target the root of the problem include pharmacologic, genetic, and cellular approaches.

Pharmacological strategies aim to provoke errors in reading a premature stop codon. Premature stop codons account for 10-15% of the mutations that lead to DMD. Aminoglycosides are a set of antibiotics that function by interfering with ribosomal function. Application of the aminoglycoside gentamicin increases the number of dystrophin positive fibers, but gentamicin is ototoxic and nephrotoxic at the doses needed to impact dystrophin expression. Atalurin increases dystrophin expression by a similar mechanism and is not associated with severe side effects. Unlike gentamicin, atalurin can be administered orally. There is potential for this to be used as part of a treatment strategy.

Over half of the mutations that lead to DMD occur within one of the exons that code for the repeated globular structures of dystrophin. If the exon with the mutation were skipped, the resulting protein would include one less of these repeated structures. This is the strategy known as exon skipping. Anti-sense oligonucleotides (AONs) mask a site where transcription is initiated on a specific exon, causing transcription of the exon to be skipped. In this strategy, the specific location of the mutation determines the pharmaceutical applied(Foster, Foster et al. 2006). Exon 51, the site of 20% of mutations that lead to DMD, requires the use of the molecule called 2'-O-methyl-phosphorothioate. The skipping of exon 23 requires the use of morpholino phosphorodiamidate (PMO). Application of PMO led to an increase in dystrophin expression in 25% of fibers biopsied. The site specificity of AONs would limit its widespread use, but this has potential to contribute to a multi-faceted clinical strategy to increase dystrophin expression(Govoni, Magri et al.).

Introduction of an exogenous copy of dystrophin is limited by the size of the dystrophin gene(Garside, Kowalik et al.). At 2.2 Mb, the dystrophin gene is one of the largest genes known. Proponents of gene therapy have engineered genes that will generate smaller versions of dystrophin, but which have a reduced mechanical dampening capacity.

Another approach to providing a dystrophic muscle with dystrophin is cell therapy, in which myogenic, dystrophin$^+$ MHC matched cells are either injected intramuscularly, where they migrate away from the injection point to a damaged site, or intravascularly, where they home to damaged tissue and migrate into the tissue by diapedesis. In native tissue, satellite cells migrate to injured sites where they either fuse to existing myofibers or fuse with other satellite cells and form a new myofiber. It is hoped that these cells will function similarly in donor tissue. Initial results are promising, as it has been shown that dystrophic muscles injected with dystrophin$^+$ cells actively transcribe dystrophin(Partridge, Morgan et al. 1989). Subsequent animal experiments showed that the grafts are limited by their poor survival and migration(Dimchev, Al-Shanti et al.).

The most commonly used animal model to study DMD is the *mdx* mouse, which also lacks dystrophin due to a spontaneous mutation. The *mdx* model has a histological profile similar to human DMD. The functional consequence of the lack of dystrophin in skeletal muscle is diminished in the *mdx* model(Turk, Sterrenburg et al. 2005). DMD is also studied using dystrophin$^-$ canines, which have a pathology more similar to humans(Banks and Chamberlain 2008). In mice, knockout of other proteins in the dystrophin-glycoprotein complex leads to a histological and pathological profile very similar to human DMD(Hack, Groh et al. 2000).

Satellite cell grafts in humans

In 1995, twelve boys with DMD received one transfer per month for six months. This study used passaged donor cells from unaffected fathers or brothers of the patient. The authors concluded that, though this treatment with satellite cells did not provide additional strength compared to the contralateral muscle, dystrophin expression increased in the treated biceps brachii(Mendell, Kissel et al. 1995).

Results from the San Francisco Study were published in 1997. In this study, ten boys with DMD received $10x10^6$ myoblasts transferred into one tibialis anterior, while the contralateral muscle was used as control. After one month and again in six months, there was no difference in the strength of the treated leg to the other, though both legs increased in strength, potentially due to the cyclosporine that was used as an immunosuppressive. This study also used PCR to look for evidence of donor cells. Donor cells were present in three patients after one month, and in only one patient after six months(Miller, Sharma et al. 1997).

In 2003, three patients with DMD received parallel injections in one tibialis anterior. Tacrolimus was used for immunosuppression, and the $30x10^6$ cells were delivered by 25 parallel injections. Four weeks later, biopsies taken from the treated area showed that each injected muscle was expressing dystrophin in 9, 6.8, and 11% of the sampled fibers.

Satellite cells were chosen for therapy because of their regenerative functions in muscle. In each of these studies, mononuclear cells were isolated by mechanically separating the satellite cells by mincing, digesting, and filtering out the myofiber debris. The non-specificity of cell selection is a major criticism of this work.

One limitation to myoblast transfer is that myoblasts only migrate 0.5 mm from the injection site (Tremblay and Vilquin 2001). Improved results have been demonstrated by injecting cells

every 1 mm, but this is impractical when scaling up the size of the muscle. Alternatively, one could endeavor to select myoblasts with enhanced capability to migrate.

α2δ1

Coded by the gene called CACNA2D1, this first-expressed subunit of the dihydropyridine receptor, α2δ1 confers properties to satellite cells that are unrelated to its role with the DHPR(Dolphin ; Tamayo, Grajales et al. ; Garcia, Nabhani et al. 2008). When α2δ1 is knocked down by siRNA in C2C12 cells, migration and attachment are reduced by nearly two-thirds.

The structure of α2δ1 provides clues to its function. A schematic of the subunits of α2δ1 is displayed in figure 1.2. A signaling peptide on the N-terminal side guides the protein to the membrane. The complete von Willebrand A (VWA) domain contains a metal ion dependent adhesion site. There are two *cache* domains, which are so named for their homology to calcium channel and chemotaxis receptors in prokaryotes. Cysteine-rich regions provide many available sites for cystine bonds to form between the α2 and δ components of the protein after cleavage. There is a purported transmembrane region in the delta domain(Douglas, Davies et al. 2006). In at least some cases, the delta domain is involved in GPI anchoring, rather than spanning the membrane(Bauer, Tran-Van-Minh et al.).

The pharmaceuticals gabapentin and pregabalin are ligands of α2δ1. Gabapentin treatment has different effects on the function of the protein, depending on the time course of treatment and the experimental conditions(García, Grajales et al. 2011). Shuttling of the pore forming subunit of the DHPR, α1s, is performed by association with the MIDAS domain on α2δ1. Chronic treatment with gabapentin has been shown to reduce the trafficking of α1s from the endoplasmic reticulum to the surface membrane. The reduction of trafficking results in decreased calcium current amplitude (Hoppa, Lana et al. ; Hendrich, Van Minh et al. 2008).

CD34

There are many cell types in skeletal muscle tissue including myofibers, endothelial cells, fibroblasts and satellite cells. Cell surface markers are used to identify which cells are myogenic. CD34 is a cell surface glycoprotein and a marker of primitive satellite cells. In 2000, Beauchamp et al reported that CD34 positive cells define the majority of quiescent satellite cells and that after commitment to myogenic lineage, CD34 is alternatively spliced, and downregulated early in differentiation(Beauchamp, Heslop et al. 2000). Myotubes or myofibers do not express CD34.

Thrombospondin-1

Thrombospondin-1 (Figure 1.2), a member of a family of secreted proteins has been shown to be a ligand of α2δ1 in the CNS(Risher and Eroglu). There is reason to believe that this interaction plays a role in skeletal muscle development. Two confirmed sources of TSP-1 that are proximal to muscle are tendons and macrophages. Macrophages secrete TSP-1 and are present in skeletal muscle at the time of satellite cell activation. The presence of TSP-1 correlates with the regeneration after injury(Watkins, Lynch et al. 1990).

The thrombospondins are comprised of multiple repeated domains that allow binding to a variety of growth factors and enzymes (Figure 1.3). TSR domains, or Type-1 repeats, are directly involved in anti-angiogenic activity, and proteins that contain this domain are anti-angiogenic. Type 2 repeats are endothelial growth factor-like repeats, and it is this region that binds to α2δ1(Eroglu, Allen et al. 2009). Toward the C-terminal side, Type 3 domains change conformation upon binding to calcium, and along with the L-lectin domain, are often called the calcium wire. The N-terminal domains of TSP play a role in attachment and migration(Adams and Tucker 2000), functions critical to satellite cell development, and

treatment of myogenic cell line C2C12 cells with TSP-1 results in characteristic pattern of spreading and migration(Adams and Lawler 1994).

All members of TSP family evolved from a single TSP that is still present in drosophila melanogaster. In this system, a deletion of TSP results in complete disassociation of skeletal muscle from tendon, promoting severe embryonic lethality.

TSP-1 is upregulated in muscular dystrophies (De Luna, Gallardo et al. ; Spurney, Sali et al.). This may be exploited for therapeutic strategies by introducing cells enriched with the receptor for TSP-1, α2δ1.

FIGURES

Figure 1.1: The dystrophin-glycoprotein complex
Dystrophin anchors sarcomeric actin of the contractile filaments to β-dystroglycan embedded in the sarcolemma of a muscle fiber. Genetic mutations of the dystrophin gene may lead to the absence of linkage between the contractile proteins and the membrane of the myofiber. The dystrophin gene is located on the x-chromosome, and is inherited in an x-linked pattern. Absence of dystrophin leads to Duchenne's Muscular Dystrophy (DMD) in human boys, or an *mdx* phenotype in mice. Some mutations of the dystrophin gene lead to the expression of a truncated dystrophin. This results in Becker's Muscular Dystrophy and is much less severe than DMD.

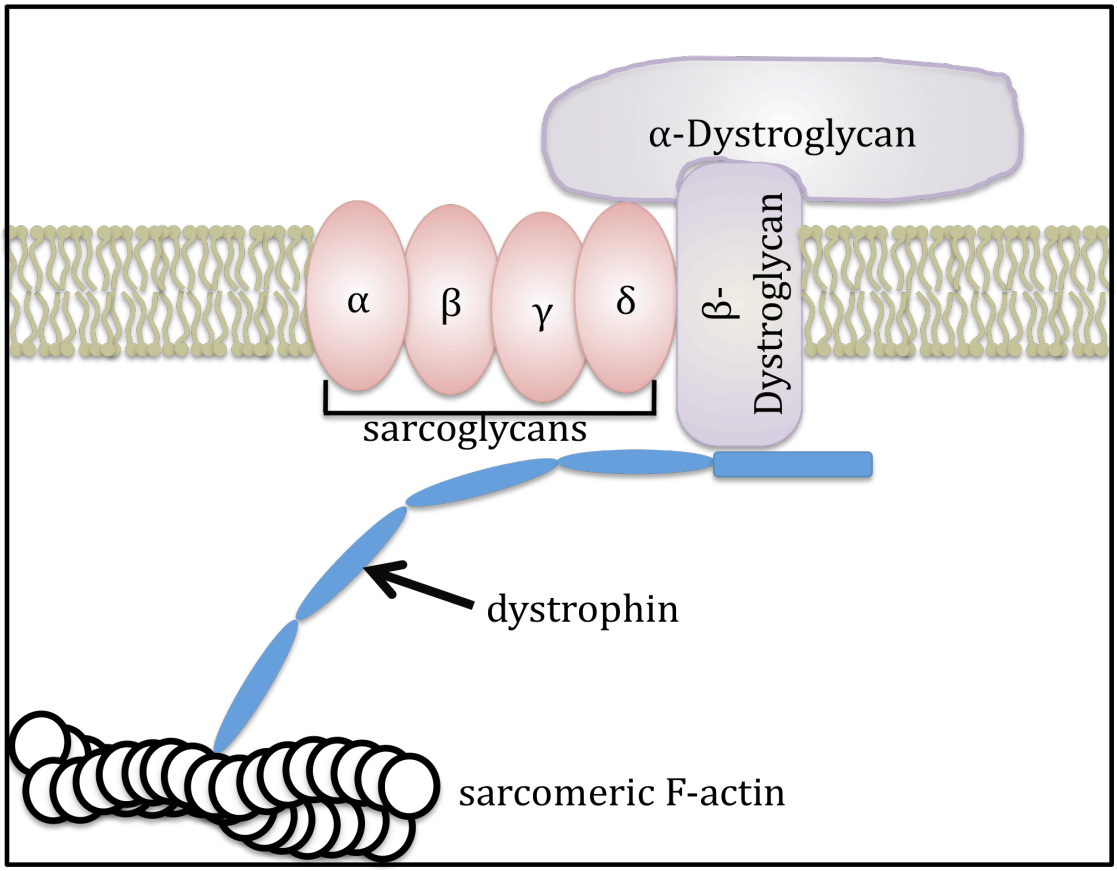

Figure 1.2: The structure of α2δ1 provides clues to its function
Alpha2 is entirely extracellular. The delta subunit anchors the protein onto the plasma membrane. Alpha2 and delta1 are transcribed from one gene, cleaved, and then bound by cystine bonds. MIDAS is the metal ion dependent adhesion site. VWA is the complete vonWillebrand A domain. SP is the signaling peptide. Cache domains are named for their homology to calcium channel chemotaxis receptors in prokaryotes. TM is the transmembrane region.

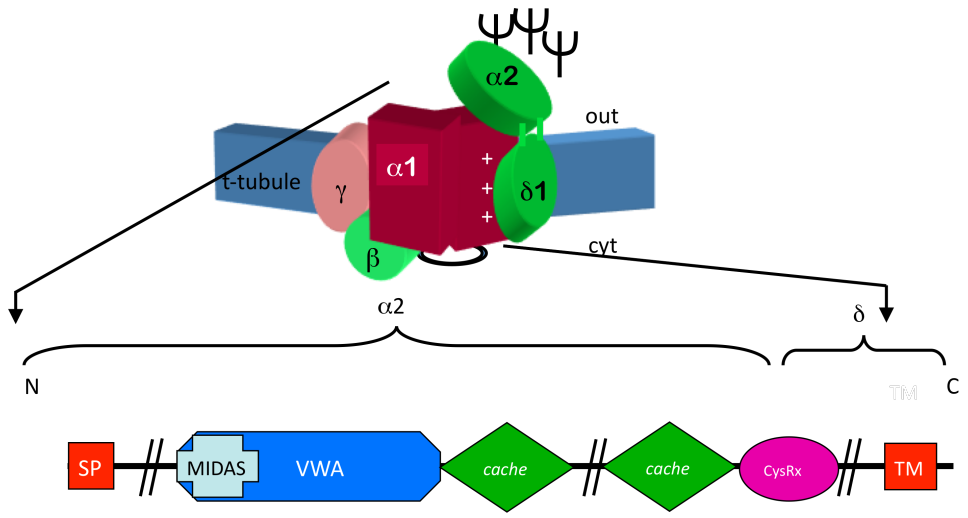

Figure 1.3: Organization of domains of Thrombospondin subgroups A and B

The top image represents TSP subgroup A, which contains TSP-1 and TSP-2. The lower represents subgroup B, which contains TSP-3, TSP-4 and TSP-5. TSP-5 is also called cartilage oligomeric matrix protein (COMP). Members of subgroup A form trimers. Members from subgroup B form pentamers. All domains shown here have been conserved throughout metazoa. Further description of these domains is found in the text.

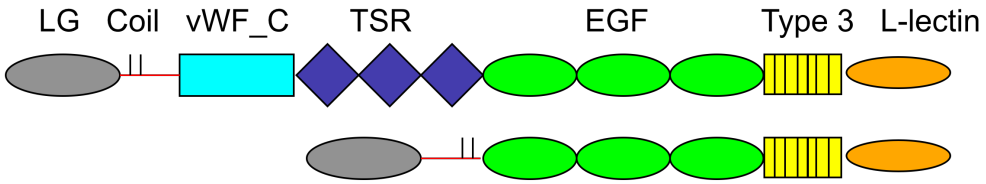

CHAPTER 2: HYPOTHESIS AND SPECIFIC AIMS

Satellite cell grafts are limited because of the lack of migration into donor tissue. The surface protein α2δ1 improves the attachment rates and enhances migration of C2C12 cells. In primary cells, α2δ1 can be localized on the leading edges of elongating myotubes. We submit that cells that express α2δ1 have an advantage over cells that do not express early α2δ1. Further, we assert that this advantage would be critical to the outcome of satellite cell grafts.

The presence of α2δ1 on surface of satellite cells may be well suited for therapy of dystrophic muscle where there is an abundance of a ligand of α2δ1, TSP-1(De Luna, Gallardo et al. ; Spurney, Sali et al.). We believe that a satellite cell population that express α2δ1 will integrate more effectively into dystrophic muscle than cells that do not express α2δ1. We hypothesize that **satellite cells with α2δ1 will be more efficacious for use in satellite cells grafts into dystrophic muscle than cells without this surface protein.**

Specific Aim 1: We aim to measure the differences *in vitro* among populations of cells that have been created based on the presence or absence of α2δ1, and on the presence or absence of CD34. Myotube formation can be visualized by characteristic morphology. We measure cell size and shape through the first week of differentiation of each of the four subpopulations. We perform RT-PCR two days after plating for two well-studied myogenic transcription factors, MyoD and myogenin. We also investigate the time course of the expression of DHPR subunit expression.

Specific Aim 2: We aim to understand the signaling mechanism of α2δ1. As macrophages are present in skeletal muscle at the time of satellite cell activation, we probe media conditioned by macrophages for TSP-1. We treat C2C12 cells with the N-terminal fragment of the TSP protein and measure proliferation rate and expression of Jnk over three days. Primary satellite cells were treated with the TSP fragment, gabapentin, or both and the distance of migration is measured over 4 days. These results contextualize the interaction between TSP and α2δ1.

Specific Aim 3: We aim to measure the functional differences of muscles treated with cells with and without α2δ1 *in vivo*. Three weeks after irradiation, exercise, and injection, we measure the force, force generation rate and relaxation rate of treated muscles and controls. In this myotest, three protocols are applied to the muscle: fatigue, force frequency, and passive tension tolerance. Three weeks after treatment, some subjects undergo a second challenge of lengthened contractions, and measurements of muscle mass are obtained 10 days later.

CHAPTER 3: *IN VITRO* CHARACTERIZATION OF FOUR SUBPOPULATIONS

Parts of this chapter was previously published as Commitment of Satellite Cells Expressing the Calcium Channel alpha2delta1 Subunit to the Muscle Lineage" in the Journal of Signal Transduction, in 2012.

Satellite cells are found between the plasma membrane of the muscle fiber and the basal lamina(Mauro 1961). They are responsible for the growth, maintenance, and repair of skeletal muscle. They remain in a mitotically quiescent state under normal physiological conditions but can be activated during exercise or muscle damage, aiding with the repair of muscle. Satellite cells can maintain or repair muscle because they possess stem cell properties; they can differentiate into other cell types(Asakura, Komaki et al. 2001) and can also divide and maintain their population. Activated satellite cells undergo several rounds of cell division and some of them will differentiate and fuse to form the typical multinucleated skeletal muscle fiber. Due to the regenerative capacities provided by satellite cells, they are a valuable option for cell therapy. Cells used for therapy are selected based on specific markers present in the plasma membrane. In the case of satellite cells the function of those markers ranges from regulation of proliferation to cell cycle entry to fusion(Kuang and Rudnicki 2008). Although many markers have been identified, there is a need to find a marker indicative of the cells that will commit to the muscle lineage and that is expressed at different states; that is, activated, quiescent, or differentiated cell. Furthermore, the marker has to be present in human tissue. Here we examined the $\alpha 2\delta 1$ protein, a subunit of calcium channels, that fulfills those requirements.

The α2δ1 subunit forms part of the L-type voltage-dependent calcium channel (or dihyropyridine receptor, DHPR) in adult skeletal muscle. In addition to α2δ1, the skeletal muscle DHPR contains α1 (Cav1.1), β, and γ subunits. The α1 subunit is the voltage sensor and contains the channel pore (Tanabe, Beam et al. 1988), while the role commonly assigned to the other subunits is to regulate the activity of α1. However, recent evidence has shown that the β and the α2δ1 subunits have roles independent from calcium channels. The β subunit is an intracellular protein involved in regulation of gene expression in different cell types including myoblasts(Zhang, Yamada et al. ; Hibino, Pironkova et al. 2003). The α2δ1 protein is an extracellular protein involved in cell attachment and migration and possibly cell signaling in myoblasts(Garcia ; Garcia, Nabhani et al. 2008). We recently found that the α2δ1 subunit localizes at the leading ends of myotubes with little or no association with α1 subunits 2 days after induction of differentiation(Garcia, Nabhani et al. 2008) suggesting that, in addition to attachment and migration, α2δ1 may play a role in the elongation process required of myotubes. With longer times in differentiation medium, the localization of α2δ1 gradually becomes homogeneous until it co-localizes almost completely with α1. However, some α2δ1 subunit does not co-localize with α1 even at later times in a number of myotubes. Interestingly, experiments performed in dysgenic muscle (which lack the α1 subunit) have shown that the α2δ1 subunit is normally expressed but that its distribution patterns are abnormal in the absence of α1(Flucher, Phillips et al. 1991). In dysgenic muscle cells, α2δ1 was found in the plasma membrane, around the nucleus, and in the transverse tubular membrane in a diffuse pattern. Accordingly, the localization pattern of α2δ1 in dysgenic cells closely resembles our findings in immature muscle where there is little or no α1 subunit to

associate with α2δ1. These data indicate that the α2δ1 subunit is not only part of the DHPR but that it may be important for other cellular functions in muscle precursor cells or satellite cells. Thus, the purpose of the present study was to determine whether the α2δ1 subunit is present in satellite cells and if so, when the α2δ1 subunit first appears in those cells. We also sought to determine the fate of satellite cells expressing α2δ1. We found that the α2δ1 subunit is expressed in the majority of newly isolated satellite cells and that it appears earlier than the α1 subunits and at higher levels than the β or γ subunits. We also found that those cells that expressed α2δ1 would differentiate into muscle cells. This evidence indicates that the α2δ1 may be used as a marker of satellite cells that will differentiate into muscle.

METHODS

Isolation of satellite cells

All experiments using animals were approved by the Institutional Animal Care and Use Committee at the University of Illinois at Chicago. Skeletal muscle of newborn mice (<72 hours postnatal) was dissociated for fluorescence-activated cell sorting (FACS) and cultured for patch clamp experiments or were used for extraction of total RNA (see below). Dissociation of muscle was performed in Ca2+-, Mg2+-free Rodent Ringer (in mM): 155 NaCl, 5 KCl, 11 glucose, 10 HEPES, pH 7.4 containing 0.3% trypsin type XI, 0.01% DNAse I, and 1 mg/ml collagenase type IA (Sigma), as previously reported(Alden and Garcia 2002).

Fluorescence-activated cell sorting

Cells were suspended in sorting media (phosphate-buffered saline (PBS with 10 mM HEPES and 0.5%BSA) and labeled with antibodies against CD34 (anti-mouse CD34 conjugated with Alexa Fluor 700; eBiosciences) and α2δ1 (monoclonal antibody 20A from Pierce ThermoScientific and a secondary pac blue goat anti-mouse antibody from Invitrogen). Collection tubes contained plating media (high-glucose DMEM supplemented with L-glutamine with 20% serum, 1% penicillin/streptomycin and 1% amphotericin-b). Immediately after the sort was completed, the cells were centrifuged, resuspended in Dulbecco's modified essential medium supplemented with 4.5 g/l glucose, 10% horse serum, and 10% fetal calf serum, and plated at a density of 26,000 cells per square centimeter on 35 mm primaria dishes.

Real-time quantitative polymerase chain reaction (RT-qPCR)

Total RNA was obtained from satellite cells from two 35 mm culture plates for each day (0-6). RNA extractions were done following Qiagen RNeasy mini-kit followed by DNAse treatment to avoid amplification of genomic DNA. The RNA density for each sample was measured (Thermo Scientific: spectrophotometer NanoDrop 8000) and normalized to the lowest RNA density found in the sample group and reverse-transcribed to cDNA using ImProm-II kit from Promega with a random primer. RT-qPCR was performed (Applied Biosystems 7500) using 10 μl of Fast SYBR® Green Master Mix, 7 μl of molecular grade water, 1 μl of forward and 1 μl of reverse gene specific primer, plus 1 μl of cDNA . All genes except 18s were run between 59-60ºC annealing temperature and dissociation curves were obtained for all gene/cDNA mixes and for the primer without cDNA for control and comparison. The 18s gene was run at 55º C. The number of independent cell cultures analyzed was a minimum of

three and the same gene/cDNA mix was analyzed three times in qPCR 96 well plates. All genes were referenced to the geometric mean of at least two control genes selected from YWHAZ, 18s, and HPRT1(Grajales, Garcia et al. ; Vandesompele, De Preter et al. 2002). The primer sequences are given in Table 1.

Statistics – Data are expressed as means ± SEM. To determine statistical significance, we used one-way ANOVA followed by Tukey's multiple comparison test or two-way ANOVA followed by Dunn's multiple comparison test.

RESULTS

Presence of α2δ1 protein in isolated satellite cells

Satellite cells were isolated from hind limb muscles from newborn mice and separated by FACS for the presence of the accepted marker CD34(Beauchamp, Heslop et al. 2000). CD34+ and CD34- cells were plated separately on primaria culture dishes and allowed to grow. CD34- cells divided, fused and developed into myotubes, while most of the CD34+ cells remained mononucleated after 7 days in culture, as shown in Fig 3.1. Differentiation of CD34- cells into myotubes is consistent with other current studies showing that CD34 is lost after satellite cells are activated and that CD34+ cells experience little division and remain in a quiescent state(Ieronimakis, Balasundaram et al.). We then performed a double gating and examined freshly isolated cells for the presence of α2δ1 since we had previously reported that this protein is expressed early in development of muscle cells and that it is involved in attachment and migration(Nabhani, Shah et al. 2005; Garcia, Nabhani et al. 2008). We found

that more than 50% of satellite cells expressed α2δ1 protein upon isolation and the majority of these cells were CD34+, as shown in Figure 3.3. The four groups were plated separately in growth media (DMEM, 10% horse serum, 10% fetal bovine serum) and examined at different times in culture. Cells expressing α2δ1+ (CD34-) produced myotubes early (2-3 days) and persisted for longer times in culture (>21 days) than the other three groups (Fig 3.2). Cells α2δ1+/CD34+ produced myotubes and also fibroblast-like cells; these myotubes did not last as long in culture as the ones produced in the absence of CD34. Cells α2δ1-/CD34+ produced mostly fibroblast-like cells. The α2δ1-/CD34- cells produced myotubes at later times (>5 days) and did not last more than a few days in culture. Cells that were α2δ1-/CD34- at the time of the sort were then examined for the presence of α2δ1 with RT-PCR. It was observed that α2δ1-/CD34- cells started expressing α2δ1 after plating and that they expressed α2δ1 only during the time when the cells were differentiating into myotubes, supporting the idea that α2δ1 is linked to differentiation of the cells.

The α2δ1 protein is expressed earlier than the other calcium channel subunits

We further characterized the temporal expression of α2δ1 in satellite cells at different times after isolation and compared it with expression of α1, β and γ subunits. The message for the α2δ1 subunit was present in freshly isolated satellite cells (D0) while the message for the other subunits was very low. To provide an objective comparison among the levels of expression of the different calcium channel subunits, Fig. 3.4 shows the ratios of expression of α1, β, and γ subunits in relation to the expression of α2δ1 at D0. All values were normalized to the expression of α2δ1 since this subunit had the highest level of expression. The ratios of expression were 0.26 ± 0.04%, 2.89 ± 0.38%, and 5.89 ± 0.34% for α1, β, and γ subunits, respectively. These values were significantly lower than those of α2δ1 at D0 ($p<0.001$).

Because the levels of expression of the subunits were so different at D0, it was expected that the expression for each subunit would not increase proportionately with differentiation. For the α2δ1 subunit its levels were significantly higher (6-fold) by D5 compared to D0 and remained high by D6 (Fig 3.5). In contrast, levels of α1 were barely detected at D0. Low levels of α1 were detected by D1 but increased significantly (~70-fold) by D4 and stayed around this level through D6. Similarly to α1, the levels of β subunit increased more than 10-fold by D4 compared to D0. The γ subunit levels increased with time to reach a maximum 147-fold increase at D4 compared to D0. Thus, the fold increase in the levels of α1, β, and γ were substantially higher than for α2δ1. Overall, the mRNA data demonstrate that α2δ1 is expressed earlier than α1 and at higher levels than β or γ subunits in satellite cells, and are consistent with studies detecting different protein levels of α2δ1 and α1 subunits early in development(Garcia ; Morton and Froehner 1989).

Quantification of cell size

In order to obtain an objective aspect of cell morphology and development of each of the four subpopulations of sorted cells, we measured cell dimensions at several days after initial plating. Wide-field images were recorded from several random places in culture dishes. The maximum width and length were measured with Image J software. The maximum width varied between 8 and 12 μm for all cell groups at days 2 and 4 after plating. After 7 days in culture, the width increased in the α2δ1+/CD34-, α2δ1-/CD34+, and α2δ1-/CD34- groups, with the increase being more significant in the later ($p<0.001$). The width showed a small decline in the α2δ1+/CD34+ group (Fig 3.6a). Since myoblasts align end to end to form the typical myotubes, we measured the length of the cells and estimated its relation to cell width. The

aspect ratio length:width, a measure of elongation, is shown in Fig 3.6b for the four subpopulations at 4 and 7 days. A ratio of 1 would represent a spherical cell. The ratio at day 2 was close to 1 in all groups and is not plotted in the graph. The populations expressing α2δ1 at the time of sorting had the largest aspect ratios of the four groups at day 4 (α2δ1+/CD34+, 18.1 ± 6.3; α2δ1+/CD34-, 11.7 ± 1.5; α2δ1-/CD34+, 4 ± 0.7; α2δ1-/CD34-, 6.4 ± 0.8) and the ratio was even larger for the α2δ1+/CD34- group at day 7 (α2δ1 +/CD34+, 15.8 ± 2.9; α2/δ1 +/CD34-, 20.2 ± 3.4; α2/δ1 -/CD34+, 4.8 ± 0.3; α2δ1 -/CD34-, 6.4 ± 0.8). These measurements are consistent with the idea that cells expressing α2δ1 form mytoubes, as noted above. By day 7 few α2δ1-/CD34- cells had formed myotubes and instead had an appearance of a compact multinucleated cell. The results are also consistent with the appearance of α2δ1 at the leading edges of immature muscle cells(Garcia, Nabhani et al. 2008).

Distinct myogenic regulatory factors profiles in satellite cell subpopulations

To further determine the differentiation state of the sorted satellite cells and the relationship with α2δ1 expression, total RNA was isolated from each of the four groups of cells two days after plating in growth media to measure the levels of the myogenic regulatory factors MyoD and myogenin. The values were normalized to the expression of 18S (Fig 3.7). The presence of the two regulatory factors was detected in the four groups although in different proportions. Cells expressing α2δ1 had significantly larger expression of myogenin than MyoD (α2δ1+/CD34+, MyoD 0.29 ± 0.02, myogenin 0.54 ± 0.07, $p<0.01$; α2δ1+/CD34-, MyoD 0.16 ± 0.03, myogenin 0.49 ± 0.05, $p<0.01$). The difference in MyoD expression between the α2/δ1 +-expressing cells was also significant ($p<0.05$). Cells without expression of α2/δ1 at the time of the sort had a larger amount of MyoD message than myogenin (α2/δ1 -/CD34+, MyoD 0.48 ± 0.04, myogenin 0.02 ± 0.01, $p<0.01$; α2/δ1 -/CD34-, MyoD 0.81 ± 0.07,

myogenin 0.44 ± 0.03, $p<0.01$). However, as mentioned above, α2δ1-/CD34- started expressing α2δ1 after plating and thus the differentiation of these cells into muscle cells was delayed in comparison to the cells that expressed α2δ1 during sorting. Levels of MyoD were also significantly different between the α2δ1- cells ($p<0.001$). In contrast, the levels of myogenin were significantly different only in the α2δ1-/CD34+ population compared to the other three subgroups ($p<0.001$). The presence of MyoD and low myogenin is indicative of a population of proliferating cells, while high myogenin and low MyoD, suggests that these cells are in the process of differentiation(Kottlors and Kirschner). These results agree with the different capacity of the cells in each of the four groups to form myotubes as described above and further support the idea that expression of the α2δ1 subunit is a good indicator of the fate of satellite cells.

DISCUSSION

Satellite cells are involved in the maintenance and repair of skeletal muscle. This function of satellite cells is of paramount significance in patients with muscular dystrophy. In order to improve the repair of dystrophic muscle, it is necessary to supply muscle with an adequate number of satellite cells with an intact copy of the affected gene. Thus, it is evident that the population of satellite cells used for therapy needs to be enriched with a marker that is indicative of the commitment of the cells to become muscle. Here we have shown that satellite cells that express the α2δ1 protein are more likely to differentiate into muscle cells *in vitro*.

Satellite cells that expressed α2δ1 at the time of sorting showed earlier signs of differentiation (elongation and transcription factor profile) than the cells devoid of this protein. Some of the

α2δ1-/CD34- cells, however, also differentiated into muscle cells but at a much later time than cells expressing α2δ1. The α2δ1-/CD34- cells expressed α2δ1 after they had been in culture for several days, effectively turning into α2δ1+/CD34- cells; the absence of CD34 alone was not enough for the cells to commit to the muscle lineage. This result suggests that it may be optimal to induce the expression of α2δ1 prior to cell sorting in order to obtain a larger population of cells that will differentiate into skeletal muscle.

Commitment of cells to the muscle lineage in the presence of α2δ1 was also demonstrated by the expression of the myogenic regulatory factors MyoD and myogenin two days after plating. α2δ1-expressing cells at time of sorting expressed relatively higher levels of myogenin that MyoD. In contrast, the levels of MyoD were higher than those of myogenin in cells without α2δ1 at the time of sorting. The myogenic regulatory factor profile of cells expressing α2δ1 and not CD34 is consistent with myoblasts that are not only committed but also actively differentiating into muscle.

Further support for a role for the assertion that the α2δ1 subunit is a marker of muscle commitment of satellite cells is provided by the fact that α2δ1 appears earlier than the α1, β, and γ subunits and its levels remain high through the differentiation process. This suggests that α2δ1 is a harbinger of the DHPR, which is necessary and required in all myocytes. These results also indicate that the assembly of the skeletal muscle DHPR as a complex occurs later in development than it was previously believed(Flucher and Franzini-Armstrong 1996; Protasi, Franzini-Armstrong et al. 1997) since not all the subunits are expressed initially and simultaneously. The early abundance of α2δ1 may suggest a role for the subunit that is independent of calcium channel, as previously described.

An important property of cells expressing α2δ1 is that they exhibit improved adhesion and migration *in vitro* compared to cells without α2δ1, as previously demonstrated(Garcia, Nabhani et al. 2008). Interestingly, this capability imparted to the cells by the α2δ1 is not limited to muscle cells and has been confirmed by another laboratory using bone cells and bone matrix (Thompson & Farach-Carson, personal communication). Involvement of α2δ1 in attachment and migration is a significant attribute for the selection of this protein as a marker of satellite cells since few satellite cells have been shown to migrate great distances from the site of injection in dystrophic muscle. Further experiments must be performed to test the ability of α2δ1-expressing satellite cells to attach and migrate away from the site of delivery in dystrophic muscle. We previously observed that α2δ1 is found on the leading edges of cells, and here we show that cells that exhibit early expression of α2δ1 elongate faster than cells without α2δ1. In addition to migration and attachment, α2δ1 may be actively involved in elongation of myotubes.

FIGURES

Figure 3.1: Satellite cells sorted for CD34.
CD34- (left) and CD34+ (right) cells were plated in growth medium (20% serum). CD34- fused to form myotubes while CD34+ remained mononucleated after 7 days in culture. Images are 623 μm x 623 μm.

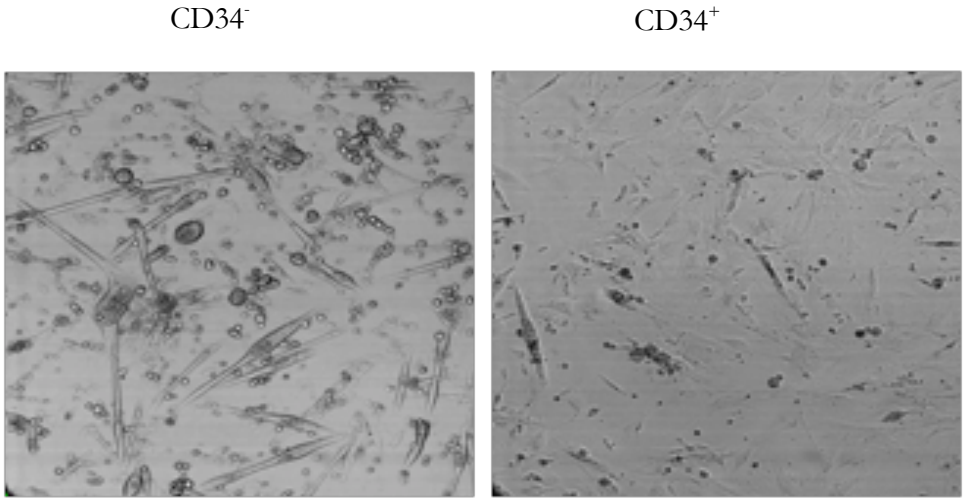

Figure 3.2 Satellite cells sorted for CD34 and α2δ1.
Satellite cells were sorted in four subpopulations and plated in growth medium (20%). Although both subpopulations of cells expressing α2δ1+ differentiated into myotubes, the α2δ1+/CD34- cells formed longer and thicker myotubes at 7 and 21 days. α2δ1-/CD34- cells transiently produced myotubes but they did not last past 10 days in culture. α2δ1-/CD34+ cells did not produce myotubes at any time. Images correspond to day 21 in culture. Image sizes are 623 μm x 623 μm.

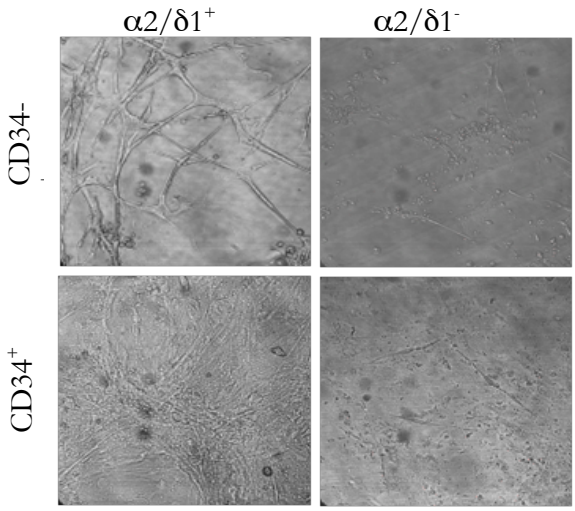

Figure 3.3: Cell sorting was performed to create the populations of study.
On the left is a characteristic sort and on the right is the mean percentage and standard error of the mean of each population. The surface protein α2δ1 is present in over 50% of the cells.

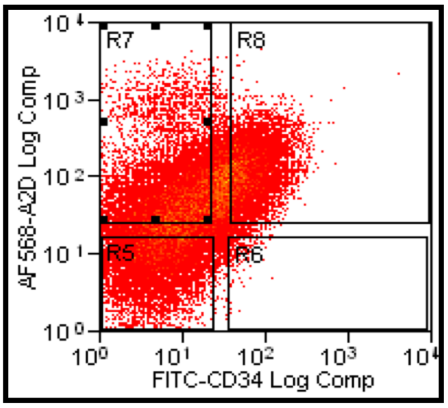

α2δ1+ CD34- 21 ± 3.7%	α2δ1+ CD34+ 32 ±4.5%
α2δ1- CD34- 44± 5.3%	α2δ1- CD34+ 3.0 ±1.2%

Figure 3.4: Expression of calcium channel subunits in satellite cells.
The α2δ1 subunit is expressed at significantly higher levels than the α1, β, and γ subunits in freshly isolated satellite cells. Expression of α1, β, and γ subunits was normalized to α2δ1 levels for comparison. The asterisk indicates statistically significant difference with all other data points ($p<0.001$). Bars represent mean ± sem of three independent cultures measured in triplicate in the qPCR plate. Differences between data points are represented by lines. The asterisk represents differences with all other bars except those ones with an asterisk. For all graphs, the p value was <0.05. All genes were referenced to the geometric mean of at least two control genes selected from YWHAZ, 18s, and HPRT1.

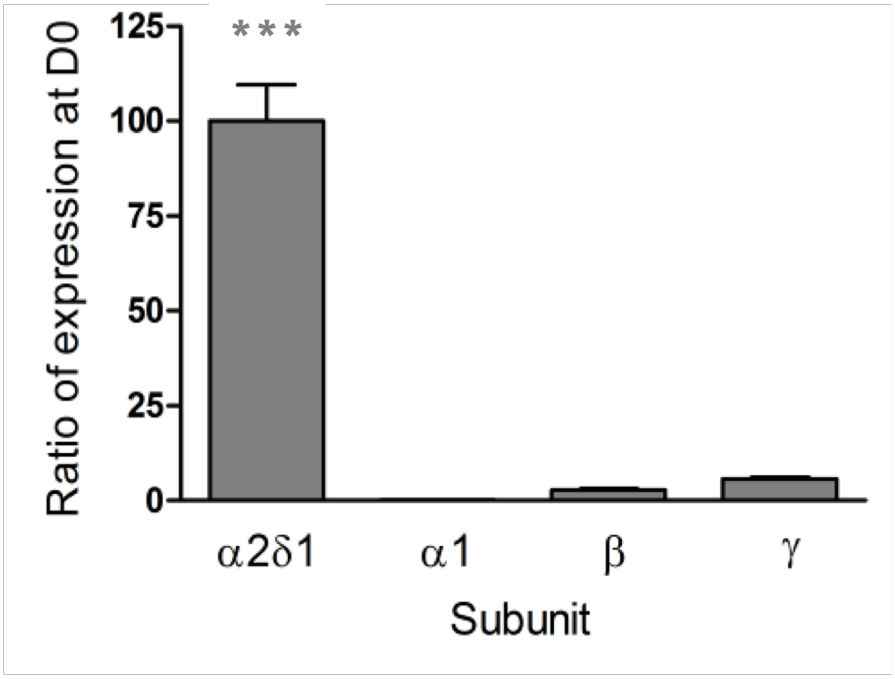

Figure 3.5: Changes in subunit mRNA expression during the first week after plating. B, temporal expression of calcium channel subunits in satellite cells cultured for 0-6 days in 20% serum. For each subunit, the fold change was calculated with their respective level at D0. The α2δ1 subunit showed a smaller fold change with time in culture when compared to the other three subunits, followed by the β subunit. The α1 and the γ subunits showed a large fold change of expression. Bars represent mean ± sem of three independent cultures measured in triplicate in the qPCR plate. Differences between data points are represented by lines. The asterisk represents differences with all other bars except those ones with an asterisk. For all graphs, the p value was <0.05. All genes were referenced to the geometric mean of at least two control genes selected from YWHAZ, 18s, and HPRT1.

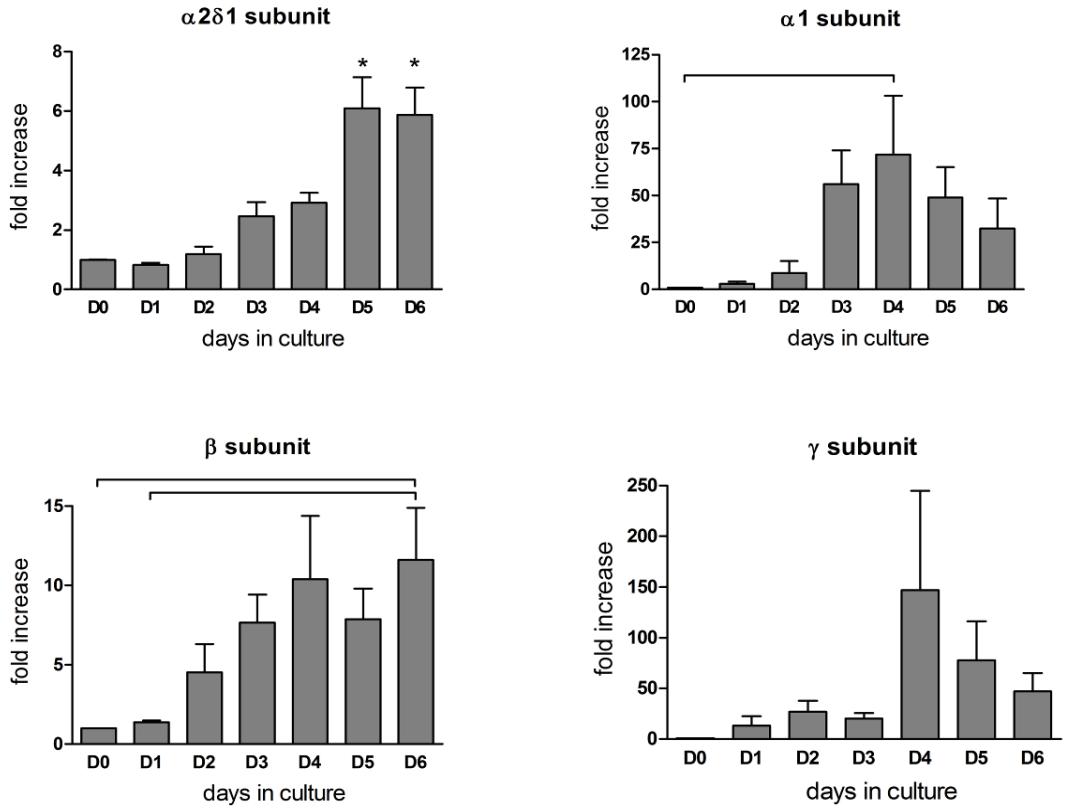

Figure 3.6: Morphological dimensions of sorted satellite cells.
A, maximum width was recorded from several random fields for each subpopulation of cells, at 2, 4, and 7 days after culture in 20% serum. The number of cells measured for each subpopulation at each day is indicated below each bar. Statistical differences between data points are represented by lines ($p<0.05$). The asterisk indicates statistically significant difference with all other data points ($p<0.001$). B, aspect ratio length:width measured from the four subpopulations at days 4 and 7 in culture. The number of cells for each condition is indicated below each bar. The populations expressing α2δ1+ at the time of sorting had the largest aspect ratios of the four groups at day 4 and the ratio was even larger for the α2δ1+/CD34- group at day 7. Statistical differences between data points are represented by lines ($p<0.01$). The discontinuous line with an asterisk represents a statistically significant difference between α2δ1- cells and α2δ1+ cells ($p<0.001$).

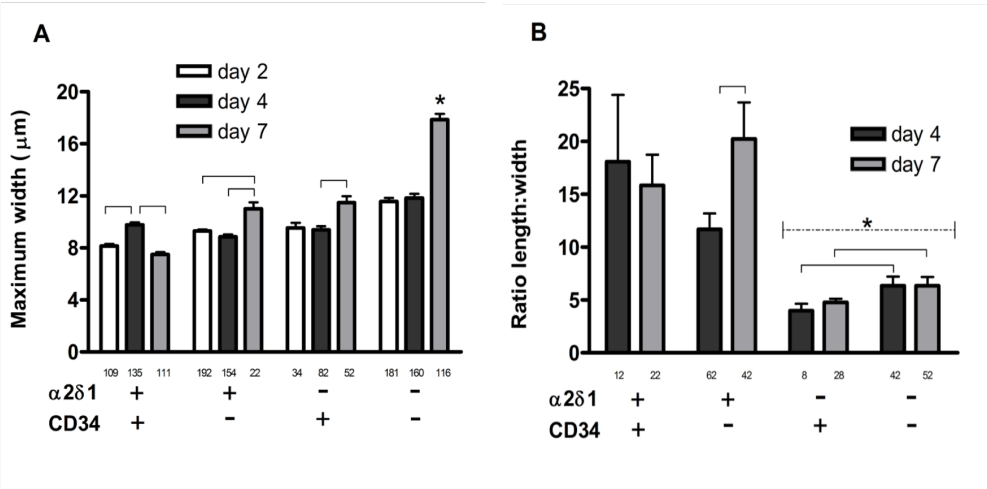

Figure 3.7: Expression of myogenic transcription factors in satellite cells.
Expression levels of MyoD and myogenin were measured in the four subpopulations after two days in culture. Cells expressing α2δ1+ had significantly larger expression of myogenin than MyoD, while α2δ1- cells expressed larger levels of MyoD than myogenin. Statistical differences between data points are represented by lines ($p<0.01$). The asterisks represent significant differences of that value with respect to all other data points.

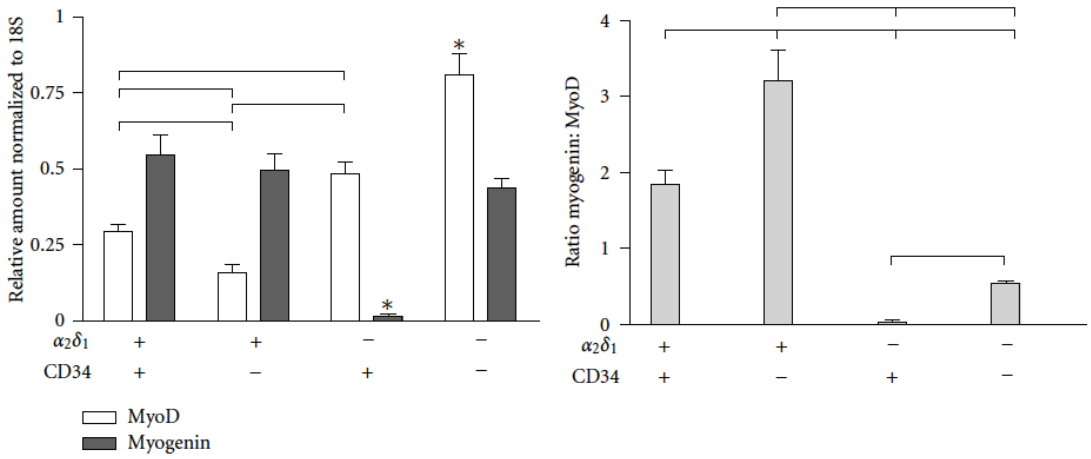

CHAPTER 4: SIGNALING THROUGH THE α2δ1 RECEPTOR

The role of α2δ1 in myogenesis has been as elusive as it is alluring. The discovery of α2δ1 coincided with the discovery and sequencing of DHPR subunits(De Jongh, Warner et al. 1990). The direct function of α2δ1 in association with the calcium channel has been difficult to define, as association with features of calcium current is inconsistent. It was proposed in the late 1990's that a critical function of α2δ1 is to traffic calcium pores to the membrane(Dolphin, Wyatt et al. 1999). In 2005, Dolphin's group from University College in London showed that α2δ1 traffics α1s, the pore-forming subunit of the DHPR, to the membrane(Canti, Nieto-Rostro et al. 2005). Pharmaceuticals target α2δ1 for pain relief and a reduction of neuroexcitability, but the mechanism is unknown(Kukkar, Bali et al.). Expression of α2δ1 takes place much earlier than expression of pore forming subunits of the DHPR, which suggests that signaling through α2δ1 does not involve the calcium channel (García, Grajales et al. 2011). More recent evidence shows that α2δ1 is a receptor for thrombospondin-1, and is involved in synaptogenesis(Eroglu, Allen et al. 2009). Here, we investigate the relationship between α2δ1 and TSP-1 in skeletal muscle.

Inflammatory cells migrate into the tissue within minutes after injury to skeletal muscle. Neutrophils and polarized macrophages secrete cytokines that provide signals to satellite cells and fibroblasts. The first cells to the site are neutrophils, which peak in concentration at 24 hours and remove debris by phagocytosis. On the second day, proinflamatory phagocytotic M1 macrophages are in largest concentration. M1 macrophages secrete signals that favor proliferation of satellite cells(Arnold, Henry et al. 2007). Anti-inflammatory M2a and M2c

macrophages are in the majority by day 3 (M2a slightly ahead of M2c). Of all inflammatory cells, M2 macrophages reside in the muscle for the longest time, where they secrete signals that favor differentiation of satellite cells(Arnold, Henry et al. 2007).

TSP-1 is one of the secretions of macrophages. This is of particular interest because interaction between TSP-1 and α2δ1 has been demonstrated(Eroglu, Allen et al. 2009), but the importance of this relationship in skeletal muscle is not understood. Despite recent interest in the role of TSP-1 and α2δ1, not much is known about the cell signaling mechanism that results from their interaction in any system. Published literature about the effects of α2δ1 on satellite cells occasionally coincides with the effect of TSP on skeletal muscle-like cell line or similar tissues, and this offers some guidance in discovering potential targets for investigation. TSP-1 supports adhesion and migration, and α2δ1 augments the same biological processes(Majack, Cook et al. 1986; Garcia, Nabhani et al. 2008). Perhaps the similarity of these findings is the result of TSP-1 acting through α2δ1.

Skeletal muscle satellite cells adhere to and migrate on purified TSP *in vitro*(Adams and Lawler). C2C12 cells that attach to TSP-1 have a particular phenotype. This interaction results in fascin microspikes and actin ruffles, which are morphologically distinct from the stress fibers of C2C12 cells after binding to fibronectin. In elongating myotubes, α2δ1 is distributed at the leading edges. These fascin microspikes require signaling through Cdc42 and Rac(Adams and Lawler 1994).

Gabapentin, a ligand of α2δ1, is used as a specific α2δ1 blocker in CNS experiments(Dooley, Taylor et al. 2007) and applied here in some of our experiments. Gabapentin has been shown to have low-level mitogenic activity. Its effects on satellite cells are not known.

Jnk and Akt are both strongly implicated in migration and proliferation, and regulated primarily by phosphorylated fraction. Jnk and Akt activation seem to have opposing effects. Jnk promotes proliferation and inhibits differentiation(Meriane, Roux et al. 2000; Perdiguero, Ruiz-Bonilla et al. 2007; Perez-Ruiz, Gnocchi et al. 2007), while Akt inhibits proliferation and promotes differentiation(Glass ; Blaauw, Canato et al. 2009). Treatment with TSP-1 may activate proliferation, differentiation, or may activate both(Elia, Madhala et al. 2007), like Sonic Hedgehog.

Here we treat C2C12 cells with TSP and measure proliferation and protein content. We treat primary cells with TSP, TSP and gabapentin, and gabapentin alone, and compare to the distance migrated over time to the distance migrated by untreated cells. The TSP used was provided by Deane Mosher at the University of Wisconsin. The protein construct includes the EGF-repeats, a type 3 repeat the LG and coil domains (see figure 1.2).

METHODS

Migration assay

Cells were plated on 35mm Falcon primary dishes in media with 20% serum for two days. The cells were split and re-plated in media with 20% serum for an additional two days, at which time they were 80-95% confluent. Cells were then placed in DMEM with 1%FBS, 1%AmphotericinB and 1%PenStrep. Media for TSP-treated cells also contained 25 nM TSP. Media for cells treated with gabapentin included 25mM gabapentin. Gabapentin was provided by Parke Davis Pharmaceutical Research.

Cells from a small, linear portion of the surface were removed by a cell scraper by pressing down firmly and moving very slightly in the direction of the long axis of the scraper. This method allows for a clearly delineated denuded- and nearly-confluent region with minimal floating debris. A scratch just outside of the field of view was used to find the identical area for each subsequent measurement. Images (10x and 20x) were acquired at t=0, 6, 9, 12, 24, 36, 48, 60, 72, 84 and 96 hours. Images taken at t=0 were used to identify a reference (starting) line. This line was used as a mask in all subsequent images ($t \neq 0$) in order to determine the initial position of the cells. Ten equally spaced points were placed on the reference line, and were used to draw evenly spaced perpendicular lines. The distance from the reference point to the furthest cell on the line was recorded. The ten distances were averaged for each time point, and each treatment for three independent experiments.

Protein Quantification

Whole lysates were suspended in phosphate-buffered saline and spun down. Supernatant was aspirated and cells were resuspended in protein isolation buffer (20mM HEPES, 50mM b-glycerol phosphate, 2mM EGTA, 10mM NaF, 1%Triton X-100, 10% Glycerol, pH 7.4) phosphatase inhibitor, protease inhibitor and sodium orthrvanadate. Cells were ultrasonicated to break up DNA and reduce viscosity.

Pierce™ BCA Protein Assay Kit was used as directed. In short, 100μL of reagent B was added to every 5mL of reagent A. 200μL of this mixture was added to each well of a 96-well plate. Bovine serum albumin from a standard sample provided in the kit was diluted and used to create a standard curve. 5 μL of each protein sample was added to three wells. Protein in the sample binds to the bicinchoninic acid resulting in a change of color from green to purple.

The 96-well plate was placed in a microplate reader (BioTek) capable of measuring the light absorption at a wavelength of 550nm of the solution in each well. The standard curve allows for interpretation of this data.

Western Blot

M1-like, M2a-like and M2c-like macrophages were polarized from bone marrow cells as previously described(Novak and Koh). Protein from media conditioned by bone marrow derived cells untreated, treated to be M1-like, M2a-like or M2C-like (provided by Dr. Timothy Koh) was concentrated using Amicon Ultra-0.5mL Centrifugal Filters by Millipore. Concentrated protein, dithiothreitol (to a total concentration of 1mM), and Laemmli Buffer (BioRad) were separated by a SDS/PAGE gel, transferred to a PVDF membrane. The membrane was probed with an antibody to TSP-1 (Pierce MA5-13385), rinsed, incubated with an anti-mouse secondary conjugated with HRP, and developed using SuperSignal West Femto Detection Kit (Pierce).

The time-course of expression of focal adhesion kinase (FAK), Akt, and Jnk and their phosphorylated counterparts (pFAKY397, pAktY473 and pJnkT183/Y185) were measured at 8, 24, 48, and 72 hours after plating. Tested cultures were treated with TSP or GBP at the time of plating. After protein quantification, protein concentrations were normalized and 25 μgrams of protein was added to each well. Dithiothreitol (DTT) and Laemmli buffer (BioRad, #161-0737) were added to proteins and loaded into wells of pre-cast 4-20% SDS-Page gels (BioRad, #456-1094). Precision Plus Protein Standards (BioRad, #161-0373) were loaded into the first well on the SDS-PAGE gel.

Jnk, FAK, Akt antibodies and the corresponding phospho antibodies were purchased from Cell Signaling. The catalog numbers for Jnk primary antibody and phospho-Jnk are #9252 and #9251 Numbers for Akt and pAkt are #9272 and #4060, and FAK and pFAK catalog numbers are #3285 and #8556 respectively.

Bromodeoxyuridine (proliferation) assay

C2C12 cells were plated in collagen-coated 4-chamber slides at 25,000 cells per chamber in media with 10% serum for 24 hours. At this time, the cells were approximately 70% confluent. The cells were rinsed with PBS and treated with media with 1% serum alone or with 25nM TSP construct for 24hours. BrdU was added in the last hour of treatment. Cells were rinsed, fixed with 4% paraformaldehyde for 10 minutes, and delivered to the UIC COM Histology core for labeling of nuclei by ToPro3 and BrdU by a primary antibody conjugated to Alexa-Fluor® 488.

RESULTS

Thrombospondin is expressed from bone-marrow derived macrophage-like cells.

The differentiation of macrophages from bone-marrow derived cells is well characterized. Here, we test to see whether these macrophage-like cells can also secrete TSP-1, as macrophages have been reported to do. Conditioned media from undifferentiated bone-marrow derived cells, and those polarized as M1-like, M2a-like, and M2c-like macrophages were probed for pan TSP secretion. All groups of polarized macrophages secreted significantly more TSP than the undifferentiated bone marrow cells (Figure 4.1). The M1-like macrophages

secrete 2.0±0.5 times the quantity of TSP-1 that is secreted from undifferentiated bone marrow cells. M2a-like and M2c-like macrophages secrete 1.7±0.08 and 1.3±0.09 times the quantity of TSP-1 that is secreted from bone marrow cells. This sets the stage for the study of TSP-1 and α2δ1 in co-culture with these cells types. We expect that rate of migration and attachment would mirror the relative amounts of TSP-1 secretion. Further, we expect that our measurements would be severely reduced by knocking out TSP-1 and recovered after treatment with exogenous TSP-1.

Treatment with TSP accelerates expression of Jnk

There is a steady increase in total Jnk protein in both treatment and control lysates. At twenty-four hours, there is a significant increase in total Jnk in the treated group compared to control, which is consistent with an accelerated activation from quiescence of the C2C12 cells (Figure 4.2). This suggests that signaling of TSP at least partially takes place as the signaling machinery is being developed, and that TSP is responsible for activation of satellite cells from a quiescent state.

Treatment with thrombospondin increases proliferation rate in C2C12 cells

We measured the proliferation rate in control and treated cells 24 hours after treatment with TSP, the same time that we found that total Jnk expression is accelerated. C2C12 cells treated with 25 nM thrombospondin in 1% media showed a proliferation rate double that of cells in 1% media alone (Figure 4.3). Of treated cells, 24.78 ± 1.84% were labeled with BrdU. In the control group, only 12.35 ± 2.9% were labeled with BrdU.

Treatment with either thrombospondin and/or gabapentin augments migration rate. Untreated cells migrate 470μm in four days, while cells treated with TSP and/or gabapentin migrate 704μm in the same amount of time (Figure 4.4). There is no difference between the migration distance of TSP-treated, GBP-treated, and cells treated with both. The group that is treated with both TSP and GBP may migrate faster initially. No significant difference is measured before 36 hours.

DISCUSSION

The concentration of macrophages in skeletal muscle peaks on the second day after injury, at the same time that satellite cells are proliferating and in the early stages of migration. Satellite cells proliferate asymmetrically, migrate to the site of injury, and fuse with myofibers and/or other satellite cells and differentiate. Macrophages aid the satellite cells in these functions(Lesault, Theret et al.). In this chapter, we show that thrombospondin is secreted from macrophages (Figure 4.1) and contributes to proliferation and migration. We glimpse at a potential signaling component, Jnk1, which may play a role in this contribution.

Total Jnk expression is hastened (Figure 4.2) in C2C12 cells after treatment with TSP. As Jnk is implicated in the proliferation of C2C12 cells, the increase of Jnk at 24 hours and the 24-hour treatment with TSP are in agreement. Our preliminary results did not show a difference in the fraction of phosphorylated to total Jnk (data not shown). This suggests that Jnk is at least partly regulated by expression levels rather than phosphorylation, as has been shown previously. It is possible that TSP acts before the machinery of signaling transduction pathways are established. Whereas Jnk levels are usually constant, here we see a gradual

increase in both treated and control in the first three days, reinforcing the concept that the signaling system is being established, and that treatment with TSP accelerates this process.

After being plated, C2C12 cells express CD34, which is a marker of quiescent cells(Beauchamp, Heslop et al. 2000). These experiments test the very early stages of myocyte activation following quiescence when the molecular framework for signaling is being established. Treatment of C2C12 cells with TSP for 24 hours doubles the proliferation rate (Figure 4.3). This strong evidence of activation guides us to find signaling pathway components that are likely to be involved in proliferation in early development or regeneration of skeletal muscle.

Enhanced migration of primary satellite cells treated with TSP (figure 4.4) is in agreement with previous reports. Gabapentin did not block the effect of TSP treatment in the migration experiment and no dose- dependence experiments were conducted. As such, no conclusion can be made about whether the effect of TSP was specific to α2δ1, nor can it be ruled out. The signaling experiments were intended to allow us to disambiguate whether differences in subpopulation were directly due to α2δ1 or if the presence of α2δ1 was a byproduct of a pre-existing differences. These results do not allow us to conclude that TSP acts on the same receptor as gabapentin but they do provide context for the role of TSP in regenerating skeletal muscle.

Together, the secretion of TSP by macrophages, the increase in proliferation of C2C12 cells after TSP treatment and an increase in migration of primary satellite cells in addition to the

hastening of Jnk expression upon treatment with TSP, strongly suggest an important role of endogenous TSP in activation of satellite cells from a quiescent state.

FIGURES

Figure 4.1: Thrombospondin is secreted from macrophage-like cells. Polarized macrophages derived from bone marrow show an increase in TSP-1 secretion compared to undifferentiated bone marrow-derived cells. The levels were 2.0 ± 0.5 fold, 1.7 ± 0.08 fold, and 1.3 ± 0.09 fold higher than control, in M1-, M2a- and M2c-conditioned media, respectively.

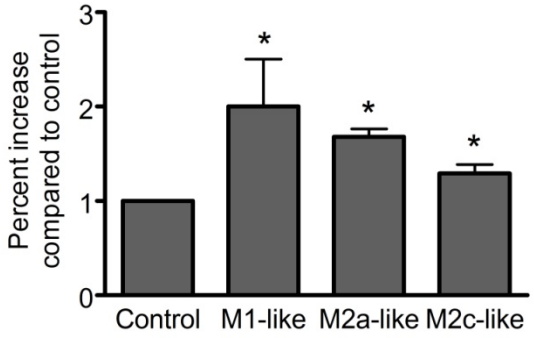

Figure 4.2 Treatment with TSP accelerates expression of Total Jnk1. C2C12 cells were plated in DMEM + 1% serum with or without TSP. RPL26 was used as a loading control. Expression of Jnk did not increase until 48 hours in control. At 24 hours, Jnk was significantly more abundant in the cells treated with 25 nM. The error bars represent the sem. For time points 8, 24, and 48 hours, n=4, and for time point at 72 hours, n=3.

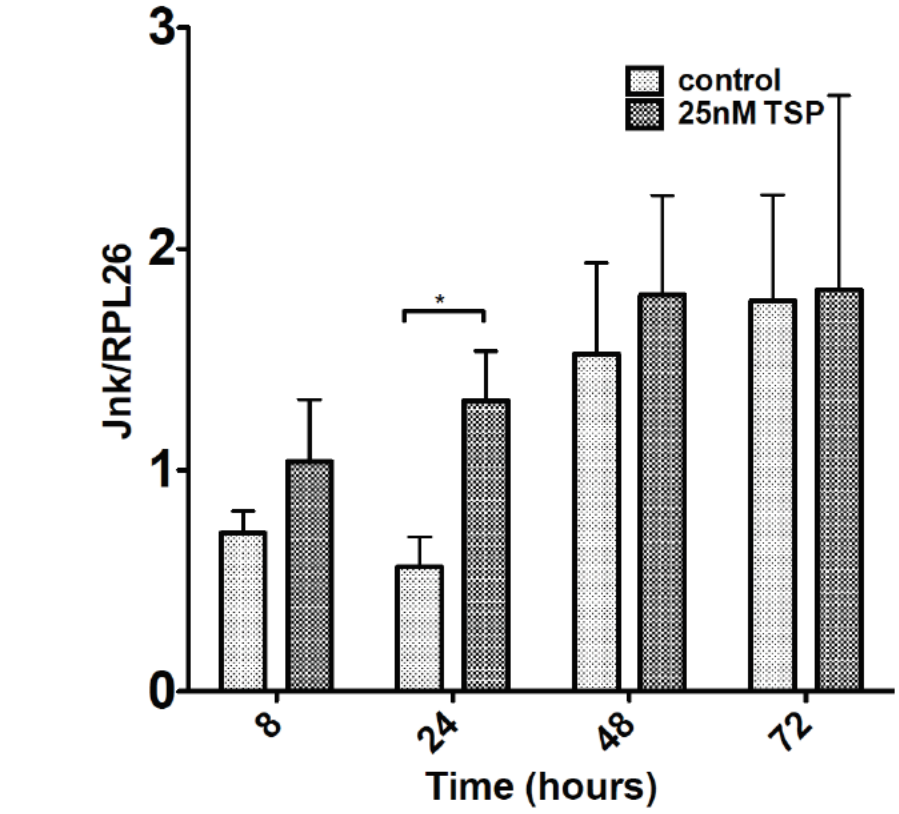

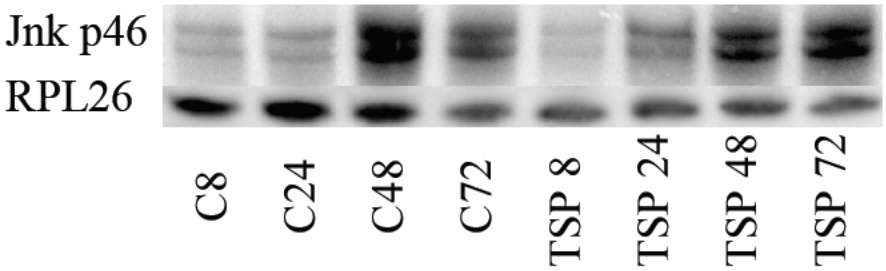

Figure 4.3 Treatment with TSP increases proliferation rate of C2C12 cells *in vitro*. The nuclei are stained by ToPro3 and BrdU is labeled with a primary antibody and visualized with a secondary AF488 antibody. Images are 310x310mm. Error bars represent sem.

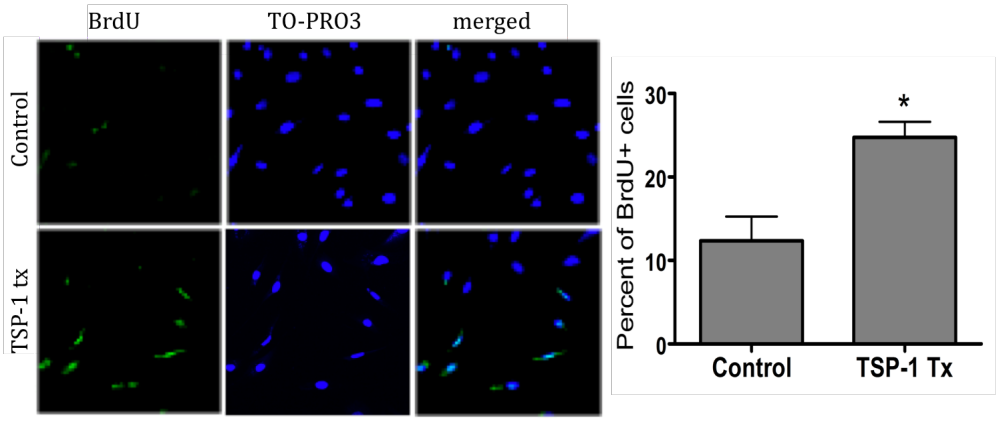

Figure 4.4: Migration of satellite cells not treated, treated with TSP, GBP, or both. Treatment of primary satellite cells with augments migration by 35%. GBP does not block the treatment by TSP. Error bars show sem. The dashed lines represent the actual data (n=3), and the solid lines represent the best fit.

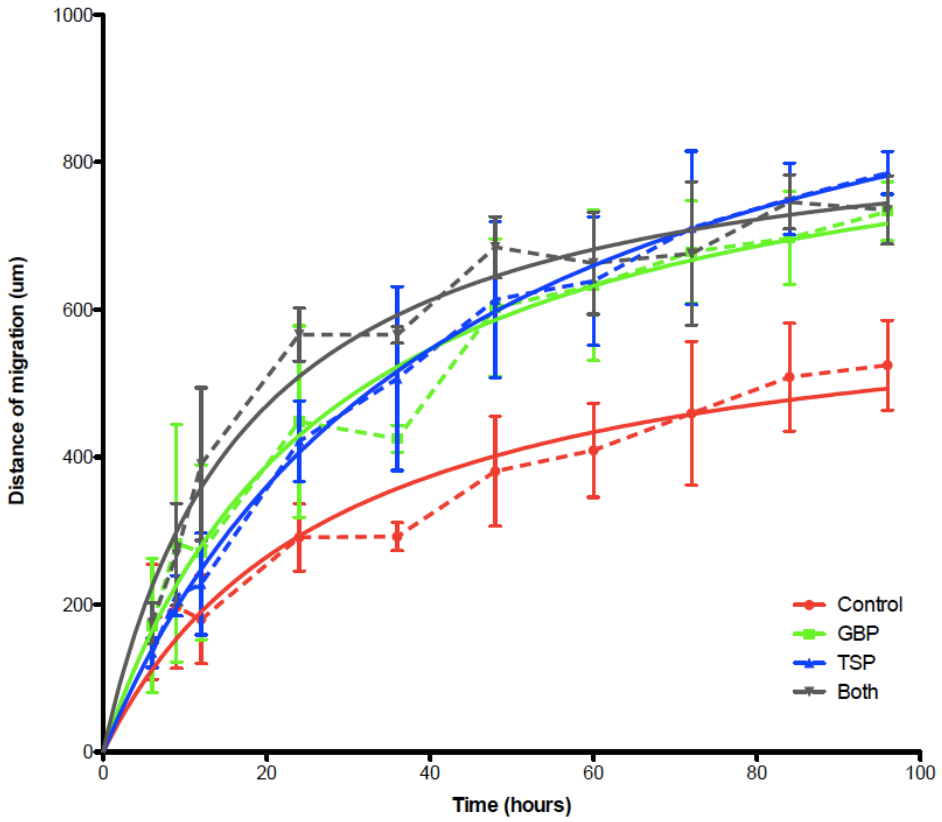

CHAPTER 5: *IN VIVO* CHARACTERIZATION OF SKELETAL MUSCLE

Excitation-contraction coupling is a complex, multifactorial process by which an action potential of a motor neuron is transduced to mechanical contraction of a muscle. After release from a motor neuron, acetylcholine binds to the nicotinic receptor on a muscle fiber, causing an influx of sodium that depolarizes the membrane and activates surrounding sodium channels. The resulting wave of depolarization moves along the sarcolemma into t-tubules, where activation of voltage sensitive calcium channels allows an influx of calcium into the cytoplasm. The conformational change that accompanies depolarization of these channels causes a physical interaction with ryanodine receptors on a proximal portion of the sarcoplasmic reticulum. This physical contact results in opening of the calcium channel of the ryanodine receptor. As calcium pours into the cytoplasm increasing the intracellular concentration from 100nM to more than 10uM, calcium binds to troponin C, causing a conformational change that shifts tropomyosin away from the myosin binding site on actin. Binding of myosin to this exposed site triggers a conformational change known as a powerstroke. Myosin is released when ATP binds to myosin. The additive effect of millions of powerstrokes is a muscle contraction. In neuromuscular disease, one or more of these processes are altered.

Despite this complex nature of excitation contraction coupling, reports from *in vivo* or *in situ* skeletal muscle tests are limited to maximal force generation elicited by a single stimulation (twitch), an ongoing series of mini tetani (fatigue) or well-spaced tetani at increasing stimulation frequencies (force-frequency). These reports are offered as a way to understand the disease progression or efficacy of treatment. Treatment may not result in an increase of

contractile force from the muscle, but may modify the kinetics of muscle contraction. Rates of contraction and relaxation are altered even when the muscle exerts the same maximal force, and they may be altered by aging, disease progression or treatment(Stodieck, Greybeck et al.)These measurements offer an improved understanding of the capability of the muscle, and they are readily offered by the same protocol used to obtain force measurements.

Non-invasive *in vivo* tests such as rotating rod, voluntary wheel running, and forced treadmill running tests do not account for central fatigue or learning. *Ex vivo* tests will examine the muscle, but not the muscle capability under neural control. Here, we provide a detailed experimental protocol for an *in situ* muscle test that challenges many aspects of muscle function. This test has several advantages. The muscle is intact, with intact vasculature and innervation that will make it possible to test larger muscles. We elicit contraction by stimulating the nerve, which allows us to bypass central fatigue and at the same time stimulate all of the motor neuron axons to avoid gradation of motor pool recruitment. We report trends of contractile force, force generation rate and relaxation rate throughout a 90-minute protocol. The test includes classic fatigue, repeated twitch, two force-frequency sequences, and a novel protocol that challenges the ability of the muscle to tolerate increasing amounts of passive tension.

Data presented here are derived from common control groups. We test the tibialis anterior of 6-8 week old wild type mice, 6-8 week old *mdx* mice, aged (43 weeks) *mdx* mice, and 6-8 week old *mdx* mice that have been irradiated at 3-4 weeks. All groups are comparable to the 6-8 week old *mdx* mice. The WT muscles are age- and sex-matched to the 6-8 week old *mdx* mice. The 43 week-old mice are from the same colony of the 6-8 week old *mdx* mice, and are representative of the aging process of *mdx* mice. The irradiated *mdx* muscles are age matched,

and results from these subjects demonstrate the result of withdrawal of the contribution to muscle function made by satellite cells.

We present data from whole muscle *in situ* experiments. We demonstrate that force generation rate is not predictive of force (and vice versa) in any of the groups tested. We show that differences among control groups are demonstrated by optimal testing conditions. Our tests show that during a fatigue test, the patterns of force generation, rate of force generation and rate of relaxation are distinct. We show that the force generation rate in young, untreated *mdx* muscles is greater than that for age-matched WT controls, even though the force is reduced. In addition, we show that although the total force produced is greater in 43-week old *mdx* mice, the relaxation rate is attenuated when compared to younger mice in the same colony.

METHODS

Partial *in situ* mouse tibialis anterior characterization protocol

The stimulation protocols are arranged from least energy demanding (twitch) to most demanding, so that the fatigue or damage that results from one test will not affect the results of another test. The order remains consistent for every muscle tested and is as shown in Figure 5.1. As the tests were developed over time, the number of subjects in each test is not the same.

Anesthesia

Mouse subjects were anesthetized with 0.2ml of ketamine (10mg/ml) and 0.05ml of xylazine (2mg/ml) and redosed as needed throughout the procedure, usually 0.2ml of the ketamine xylazine mixture after the preparation and another 0.2ml before the protocol was performed

on the second tibialis anterior. Appropriate anesthetic plane was determined by toe pinch. All *mdx* animals used in this study were C57Bl/10ScSn-Dmd*mdx*/J from Jackson Laboratories. The WT mice were from a C57Bl/10 colony.

Stimulation of muscle contraction

The tibialis anterior muscle was stimulated via the deep fibular nerve, as it arises from the sciatic nerve. The sciatic nerve was freed from fascia, tied with silk suture just distal to the spine and severed between the suture and spine. The sciatic or deep fibular nerve was rested over the hooked electrode.

Moisture Maintenance

During the procedure, the muscle was kept moist by continuous drip of Kreb's Henseleit solution (130mM NaCl, 5mM KCl, 1mM CaCl2, 1.1mM KH2PO4, 0.85mM MgSO4, 0.6 MgCl2, 25mM HEPES, 25mM NaCO3, 11mM glucose bubbled with 95%O2 and 5%CO2). A peristaltic pump was used to drip the solution over the muscle. The impact of the drip did not alter the measurements of muscle function. The flow rate of the pump was 2.0-2.5 mL per minute.

Muscle Preparation

At the anterior ankle, the attachment of the tibialis anterior (TA) runs over that of the extensor digitorum longus (EDL), and great care was taken to not include the EDL in the surgical isolation of the TA. This was achieved by severing the attachment distal to the ankle as the TA tendon passes medially to the inferior surfaces of the cuneiform and metatarsals, thus loosening only the TA tendon above the ankle and separating it from the EDL. The tendon was tied with silk suture, wrapped back over the knot and tied again to minimize slipping. The leg was fixed at the knee to the testing stage by needles, with the length of the limb parallel to

the direction of force but without impeding contraction. The heating pad and a heat lamp were adjusted to keep the temperature at 37°C at the level of the subject. The positioning and orientation of the subject to other components of the testing platform can be seen in figure 5.2.

Optimization of passive tension and voltage

Optimal passive tension was determined by eliciting 100 ms contractions at 50 Hz every 6 seconds. The passive tension was increased every three twitches. When the force either remained the same or began to decrease, the passive tension was recorded and we proceeded with the test.

To ensure proper voltage, a set of twitches was elicited at 2.0 volts, and then again at 3.5 volts. If an increase in twitch force was observed, the positioning of the electrodes was adjusted. In the reported data, 2.0 volts were used to stimulate the sciatic of each test. Optimal voltage was re-determined after each test. When the optimal voltage changed, the data from the previous test were discarded, and the test was repeated.

Twitch

After optimal voltage and length were determined, the nerve was stimulated every three seconds at 1 ms 10 times. The amplitude of the twitches was reported along with the standard deviation. The force generation rates and relaxation rates were also reported.

Fatigue

A 300 ms, 50 Hz burst of stimulation was applied to the nerve every three seconds for ten minutes. Fatigue was reported as the minimum force, usually at 10 minutes, as a fraction of the reference force. The reference force was recorded from the second contraction. In these

measurements, a smaller number shows greater fatigue. Potentiation was reported as the maximal force, usually within the first 40 seconds of the test, as a percent of reference force.

Force-Frequency

Bursts of 300ms at varying frequencies were stimulated at increasing frequencies every 3 minutes. The testing frequencies ranged from 10 to 250 Hz. This test is referred to as force-frequency 1 (FF1). A second force-frequency protocol was performed with 3-second bursts every one minute at the same frequencies. These tests were referred to as force-frequency 2 (FF2). As the stimulations are ten times longer and the resting time in between is shorter, the FF2 protocol is a more demanding protocol.

Passive Tension Tolerance

The ability of the muscle to maintain constant active contractile force with increasing passive tension was measured by eliciting 0.5 second bouts of twitches every 5.7 seconds for 100 seconds. Under constant passive tension at this rate of stimulation, no fatigue was observed in any of the muscles. The passive tension was increased and more bouts of twitches were provoked for another 100 seconds. At this time, the passive tension was increased again for another increment. This continued until a passive tension of 50 g was reached. After the last set of active twitches was stimulated at the greatest passive tension, the passive tension was set to the original optimal passive tension. Stimulation of twitches continued while the muscle recovered for at least 8 minutes.

RESULTS:

Figures 5.3A and B show data from the *mdx* colony that was tested. The mass of the tibialis anterior (TA) increases with age to a mean of 80 mg but declines after 40 weeks. The mean TA mass of the oldest mice tested, 67 weeks, was 60 mg. The isometric force of the TA also reaches a maximum at 40 weeks, but only declines slightly. The maximum mean force for the tested age groups is 51 grams. At 67 weeks, the mean force is 48 grams. This difference is not significant.

Fatigue

Data in figures 5.4-5.10 are extracted from the fatigue protocol. Figure 5.3 shows the force of each muscle plotted against the force generation rate. We found that, while there is a positive correlation with force generation rate, it is not predictive of force. Furthermore, we found that data from wild type muscles are clustered outside of the 95% confidence interval representative of *mdx* muscles, with the wild type muscles having lower force generation rate but greater force.

The mean force, force generation rate, and relaxation rate, of 6-8 week old *mdx* muscles are displayed in Figure 5.5. Measurement of force shows potentiation in the first few seconds of the test, reaching a maximum at 26 seconds and a minimum at the completion of the test. The total change of force is 24% of the initial value. The force generation rate quickly increases to 11% over initial value at 36 seconds, and maintains the same magnitude so that by the end of the test it is 12% greater than it was initially. Initially, the magnitude of the relaxation rate is 90% larger than the magnitude of the force generation rate, but declines to 54% initial value in 168 seconds. The magnitudes of force generation rate and relaxation rate are equal 78 seconds

into the test. Classic fatigue, defined as a decrease in force, force generation rate and relaxation rate, is not observable in this test.

Next, we look at the common control groups of animals. We calculated fatigue as the ratio of minimal force to initial force. There are no significant differences in this calculation of fatigue among these groups (Fig. 5.6). However, there are significant differences in other measurements of fatigue from these tests. Force, force generation rate and relaxation rates were recorded at initial, maximal and minimal values (figures 5.7-5.9). Figure 5.7 shows that differences are significant in the initial force during fatigue between age- and sex-matched WT and *mdx* mice. Force is also greater in 43 week-old *mdx* mice. This difference is not significant for the end of the test.

Surprisingly, the force generation rate was 15%-25% smaller in the WT mice when compared to non-irradiated *mdx* mice. This was significant throughout the test. There was no significant difference in force generation rates among 43 week of *mdx* mice and 6-8 week old *mdx* mice (Figure 5.8).

Measurement of relaxation rates show that the 6-8 week old WT and *mdx* mice are the not different, while the relaxation rate of 43-week old mice is over 50% reduced (Figure 5.9) compared to their younger counterparts.

Figure 5.10 allows careful comparison of representative submaximal unfused mini-tetani from the fatigue protocols of age-matched *mdx* and WT (Figure 10a) and young and old *mdx* (Figure 10b). The top panels show active force during the 300 ms submaximal, unfused tetanus. The lower panels show the change of force over time, or the derivative of the top panels. Some features that have been reported are directly observable. In the *mdx* mice, the force is lower but the force generation rate is higher, and the relaxation rate is statistically the same at WT. A

closer look shows that after the last stimulation in the 300 ms bout, the WT muscle levels off for roughly 25 ms, resulting in a delayed return to relaxation. There is a greater range of rates of contraction in the *mdx* muscle compared to the WT muscle. On the left, a comparison of the young and old *mdx* muscle shows that, while the force is higher, the rate of force generation is not significantly different and the relaxation rate of the older *mdx* mice is significantly slower. During contraction, there is a slow decline in the force of the 43-week old *mdx* muscle, even while the relaxation rate is slower than for 6-8 week old *mdx* mice.

Force-Frequency

Figures 5.11 and 5.12 represent the force generation rate and relaxation rate (respectively) during the force-frequency protocol. In the first force frequency test (FF1), the muscle is stimulated for 0.3 s with a 3-minute recovery period before the next stimulation. In the second test (FF2), the muscle is stimulated for 3 seconds with only one minute to recover.

Upon increasing stimulation frequency, force, relaxation rate, and force generation rate increase in magnitude and then decline after some optimal frequency. Here, we report force generation rates and relaxation rates at maximal values and minimal reduced value. The minimal reduced value was obtained at frequencies greater than the frequency that provoked max value. We show the difference of these values for the less demanding (FF1) and more demanding (FF2) protocols.

Figure 5.11 shows the maximal (A and C) and minimal (B and D) force generation rate in the less challenging (A and B) and more challenging (C and D) protocols. We can observe that for every group, the force generation rate declines at the end of the test, but actually increases from the less to the more challenging protocol. The force generation rate of 43-week old mice

declines slightly less than other groups, so that it was significantly greater than the force generation rate of 6-8 week old mice of the same colony (Figure 5.11D).

Passive Tension Tolerance

Figure 5.13 shows the force, force generation and relaxation rate as passive tension was incrementally increased, for all four groups tested. In each group, relaxation rate was the most sensitive to increases in passive tension. The wild type muscle, figure 5.13d, shows that there may be some increase in both force and force generation rate even after the passive tension was optimized for greatest force generation. The decrement in force and the decrement in force generation rate are more closely matched, but are significantly different in irradiated muscle (13a) and wild type muscle (13d).

DISCUSSION

Reporting the force capability is not sufficient for understanding the functional biophysical properties of skeletal muscle. The kinetics of whole muscle contraction are also important. For example, the force generation rate declines in patients with sarcopenia. Reduced force generation rate is a predictor of traumatic fall in elderly adults. In these patients, the rate of force is more critical than the total force generated, since movements during gait take place in less time than the maximal force can be generated. The relaxation rate is important for efficiency of energy usage. The ability of muscle force to sum (and produce more force) depends on the fine-tuning of the rates of contraction and relaxation. Finally, these measurements of force generation rate and relaxation rate provide additional methods of monitoring disease progression or effect of treatment.

Data from irradiated muscles are shown here. Irradiation of muscles prevents the proliferation of satellite cells. Irradiation is performed in grafting experiments because the reduction in host satellite cell pool results in a reduction of inhibition of donor cells and improvement of donor cell viability. As irradiated muscles are used as a control group in satellite cell graft or myoblast transfer studies, the data are included here. In this study, muscles were irradiated at 3-4 weeks of age, which was 3-4 weeks before these measurements were taken. In every measure here, irradiated muscles were not as fast or as strong as the non-irradiated control. Irradiation affected the force, FGR and RR equally. When normalized for force, the irradiated muscle did not demonstrate greater FGR or RR than the non-irradiated age matched muscles.

These results clearly demonstrate that force is not predictive of force generation rate. Figure 5.4 shows force as a function of force generation rate for 25 *mdx* muscles. While the best-fit line does show a positive correlation, more than half of the data points are outside of the 95% confidence interval. Data representative of wild type muscles are clustered in a region of the graph outside of the 95% confidence interval. These WT muscles exhibit greater force but reduced force generation rate. This indicates that these measurements are not redundant, and suggests that reporting both measurements may be helpful in diagnosing myopathies, comparing animal models of disease, and in monitoring the effect of treatment.

Figure 5.6 shows that when measured by the classical definition of fatigue, there is no difference among the control groups tested. Differences in fatigue have been reported between *mdx* and WT muscles. The lack of difference here may be due to the age of the muscles tested or the low number tested.

Fatigue

Classically, fatigue is defined as a reduction in force, relaxation rate, and force generation rate. Figure 5.5 shows that force, force generation rate and relaxation rates do not change in concert during a fatigue protocol. As they do not respond in the same way to the same stimulation, they must be differentially sensitive to stimuli, indicating that these measurements are representative of distinct physiological processes. Mechanisms of disease progression or treatment may preferentially affect one of these measurements over another.

Figures 5.7-5.9 have three parts. The lower graphs show the measurements throughout the whole test. The top panels in figures 5.7-5.9 show the measurements only at select parts of the tests: the initial, maximal, and minimal values. Below these part graphs are the same data in table form. Data are shown in these three ways to emphasize that significance is not consistent in all measurements, and that the precise method of measurement should always be reported.

Figures 5.7 and 5.8 show differences between *mdx* and WT mice that were alluded to in figure 5.4. The lower panel in Figure 5.7 shows that the force of WT muscles is significantly greater than the age-matched *mdx* muscles. Figure 5.9 shows that there is no difference in relaxation rate between the *mdx* and WT muscles. The 43-week old mice have the same force generation rate as the younger counterpart of the same colony (Figure 5.8). However, the relaxation rate is significantly reduced compared to the younger *mdx* mice.

Figure 5.10 shows representative submaximal, unfused mini-tetani from the fatigue protocol. The left panels show a contraction of WT muscle compared to an *mdx* muscle, with the faster rate but decreased total force. The panels on the right of figure 5.10 show contraction from the same *mdx* muscle with a larger force, the same force generation rate but a decreased relaxation rate. Both comparisons show opposing differences in these measurements,

underscoring the point that these values do not coincide. The lower panels show the same contractions as the upper panels represented in rate change. Any point above zero is a force generation rate. It is noticeable here that during contraction, the younger *mdx* muscle is relaxing (rate below zero) more than the wild type muscles or the 43 week-old *mdx* muscle. Another noticeable feature in the left panels is that after the last stimulation, there is more time before the WT muscle relaxes. In the lower left panel, there is a shoulder observable on the WT trace. The contraction is maintained for some time before the muscle relaxes.

Force-Frequency

In figures 5.11 and 5.12, the minimal value refers to the smallest value obtained at a higher frequency than that which produced the greatest value. Both force generation rate and relaxation rate showed some decline toward the end of the test.

Figure 5.11 shows the maximal and minimal force generation rates of the less challenging protocol (FF1) and the more challenging protocol (FF2) with longer periods of contraction (3 seconds vs 0.3 seconds) and less time to recover in between contractions (1 minute instead of 3 minutes). When values of FF1 are compared to the values from FF2, the force generation rate does not change significantly. There is also no significant difference between the minimal and maximal force generation rate in the same protocol.

Relaxation rates are shown in Figure 5.11. Here, the minimal values are significantly less than maximal; the relaxation rate declines dramatically after the maximal relaxation rate was obtained. Comparison of relaxation rates between the more and less challenging protocols reveals a significant decrease.

Passive Tension Tolerance

Figure 5.12 shows the reduction in active contraction as a result of increasing the passive tension. In each of the four groups tested, relaxation rate is the most sensitive to changes in passive tension. In all groups except the irradiated group, the force is the least sensitive to increase in passive tension. In the wild type group, the optimal passive tension may have shifted during the test. The optimal length for contraction during activity has been reported to shift(Rassier and MacIntosh 2002). This may result in an underestimation of the force of WT muscle. This should be considered with the reason that this shift occurred in WT but not the *mdx* muscles.

Throughout the myomechanical test, the relaxation rate is the most sensitive to activity-induced changes. While in most protocols, there is a tendency for relaxation rate to decline, the fatigue protocol shows that the relaxation rate is also subject to increase. In the fatigue test, the magnitude of the FGR and RR are similar (within 30%), but in the FF1 and FF2 the max RR is as more than 250% the FGR and falls to only a fifth of the magnitude of the FGR.

The force generation rate in WT mice is slower than age-matched *mdx* muscles in the fatigue protocol, but is faster in the force frequency protocols. The values for each group are not the same from protocol to protocol, nor should they be. The fatigue protocol tests the ability of the muscle to adapt to persistent submaximal stimulation. The force, force generation rate, and relaxation rate provoked by the force frequency protocols are representative of the maximum capable of that nerve/muscle at a specific stimulation. Since the relaxation rate of the muscles in force-frequency protocols changes significantly for the same muscle, it can be said that the relaxation rate is a measurement of the status of the muscle, which may be related to intracellular calcium depletion, modification of calcium sensitivity of sarcomeric proteins, or

both. Timing of the return to full capacity may be indicative of recovery of intracellular calcium stores or restoration of native calcium sensitivity. This can be disambiguated by performing similar experiments on muscles with genetically altered contractile proteins or calcium handling proteins. Alteration of contractile proteins would change the sensitivity to calcium.

Many mechanisms active in *mdx* muscle are attributed to an increase in intracellular calcium. Three mechanisms lead to the increase in intracellular calcium. First, there are transient microtears in the membrane that are stimulated by stresses on the membrane and allow the influx of calcium. Second, there are significant stretch-induced channels that allow calcium influx in the hyperstressed *mdx* membrane. Third, the sodium-calcium exchanger stays active after a contraction, moving sodium out of the cell that came into the cell via a stretch-induced microtear(Fanchaouy, Polakova et al. 2009).

The increase in force generation rate in young *mdx* muscles has been reported before(Fanchaouy, Polakova et al. 2009). The increase in force generation rate is due to an increase in the phosphorylation in myosin light chain kinase, increased in *mdx* mice because of the increase in intracellular calcium(Smith, Huang et al.). Persistent rapid rounds of regeneration in *mdx* muscle favor the emergence of slow twitch fiber type predominance in *mdx* mice. Myosin light chain kinase is more active in fast twitch muscle, which is why the force generation rate decreases with age.

While the levels of ATP are important in fatigue they change very little during a fatigue protocol, leading some to believe that ATP depletion is not the major cause of fatigue(Allen, Lamb et al. 2008). However, a small reduction in ATP will trigger a stress mechanism, activating chloride and ATP-sensitive potassium channels that reduce the amplitude of action

potential and the calcium that enters the cytoplasm(MacIntosh, Holash et al. ; Allen, Lamb et al. 2008). Classically, fatigue is defined as the reduction in force, force generation rate and relaxation rate. Figure 5.3 shows that this definition is not valid throughout any of the test. Force generation rate increases and then stays higher, and after an initial decrease, the relaxation rate continues to increase.

Cellular mechanisms of potentiation include two possibilities. The first is that early in the series of repeated stimulation, myosin regulatory light chain is phosphorylated, resulting in an increased sensitivity to calcium. The second possibility is similar to what is called 'staircasing' in which small increases of intracellular calcium potentiate a larger force response(Allen, Lamb et al. 2008). In our results, mechanisms of fatigue and potentiation are likely simultaneous.

Since potentiation is elicited at low frequencies and fatigue is elicited at high frequencies, it would be possible to design a test that preferentially provoked one or the other. This would aid the interpretation of the cellular events that contribute to functional properties of the muscles (Rassier and Macintosh 2000).

FIGURES

Figure 5.1: Myomechanical testing protocol.
This figure shows all 5 protocols discussed. The first protocol (A) is twitch, in which a contraction is elicited by a single stimulation. The second is a ten-minute long fatigue protocol (B) in which a 300ms sub-maximal tetanus is evoked at a stimulation rate of 50 Hz. Fatigue is followed by a second bout of twitches. Force-frequency 1 (C) shows eleven 300ms contractions elicited by 10, 30, 40, 50, 80, 100, 120, 150, 180, 200, and 250 Hz, with three minutes of rest time in between each contraction. Force-frequency 2 (D) challenges the muscle further with 3 second long stimulations separated by only one minute. Lastly, passive tension tolerance and recovery (E), tests the ability of the muscle to maintain contraction despite increased length as well as the ability of the muscle to recover from any stretch-induced decrement.

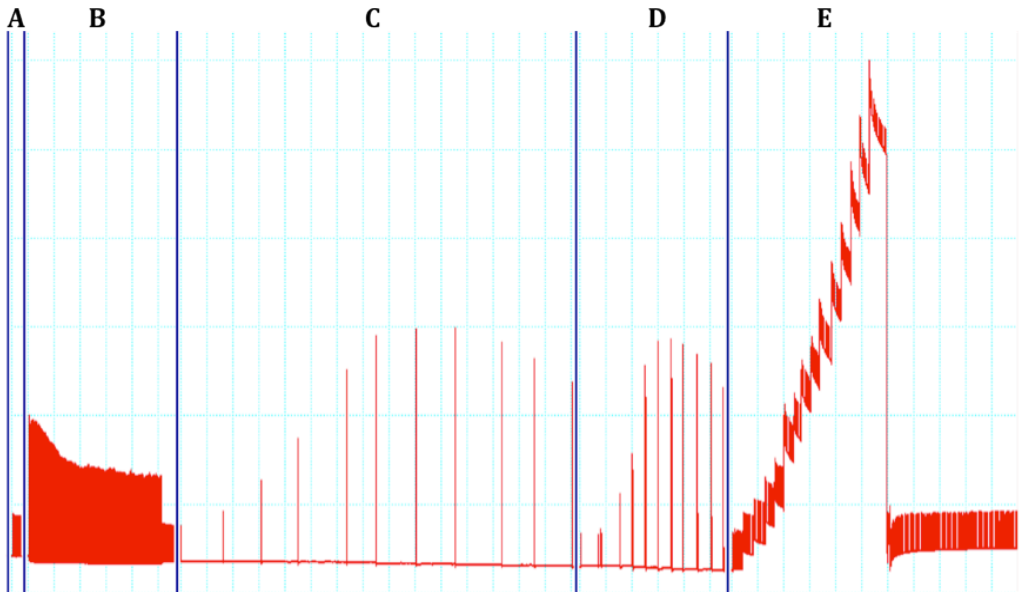

Figure 5.2: Muscle testing platform.
The anesthetized mouse was places on the platform on the supine position with the isolated sciatic nerve and tibialis anterior tied and tagged with thread. The mouse was held in the position by pins at the hip (not visible in this image), chest, just medial to the thigh of the tested leg. The pins medial to the thigh and at the hip held the leg taught, so that movement from the knee was restricted. A needle held the foot just medial to the thread that connected the tibialis anterior to the force transducer. This was the only pin that pierced the skin. The moisture was maintained by Kreb's Henseleit solution drip, positioned by the red prong at the top of the picture and emerging from the tubing. The electrodes stimulated the sciatic from a hook and the ground was held behind the leg, in contact with the fascia and muscle of the posterior proximal muscle.

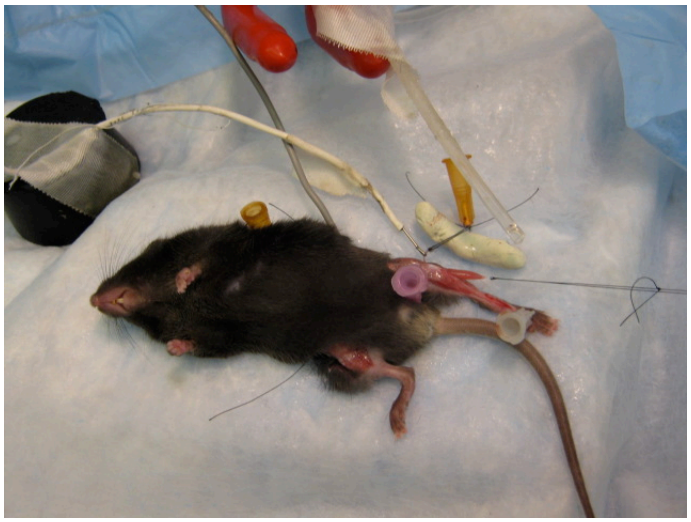

Figure 5.3: TA wet mass and maximal force by age.
A) Maximum force of TA by age. Isometric force of *mdx* untreated mice aged from 4 weeks to 67 weeks. Here, the decline is much smaller. The maximum of 50 grams of force is reached at 40 weeks and declines only to 48 grams at 67 weeks. This maximum represents the point at which regeneration cannot keep up with necrosis in the colony of *mdx* being studied presently. B) Wet mass of tibialis anterior by age, from 3 weeks and 6 days to 67 weeks and 0 days. The mass of the muscle reaches a maximum of 80mg at 40 weeks before declining to 60mg at 67 weeks of age. The best-fit curve shows a maximum at 30 weeks of 70mg and a decline to 60 mg.

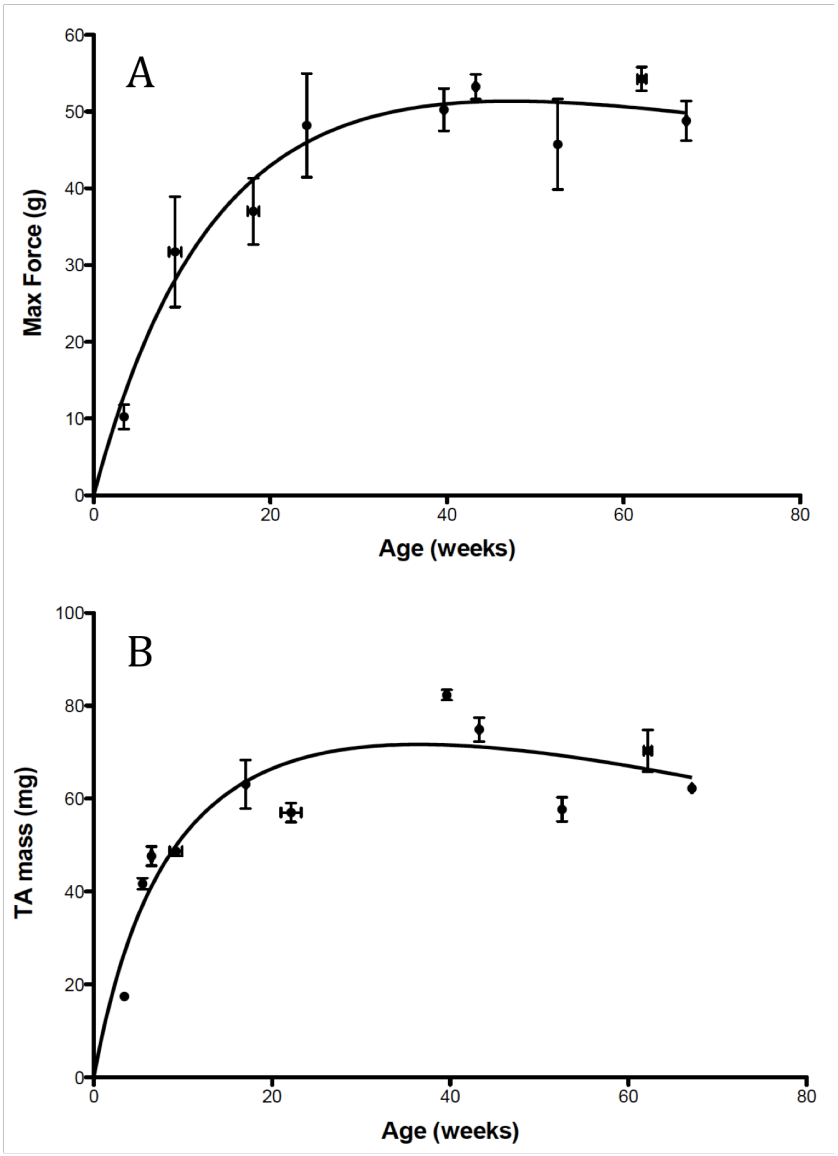

Figure 5.4: Force is not predictive of force generation rate.
This graph shows data from 25 *mdx* and 5 wild type animals. The initial force is plotted over force generation rate for each muscle tested. The trend shows that the force increases with increasing force generation rate. The wild type muscles (red asterisks) are grouped outside of the 95% area, and have a higher force and lower force generation rate than the data from *mdx* muscles. The solid black line is the best linear fit. The 95% confidence interval is shown by the dotted lines above and below the solid line. The black dots represent data from dystrophic muscles.

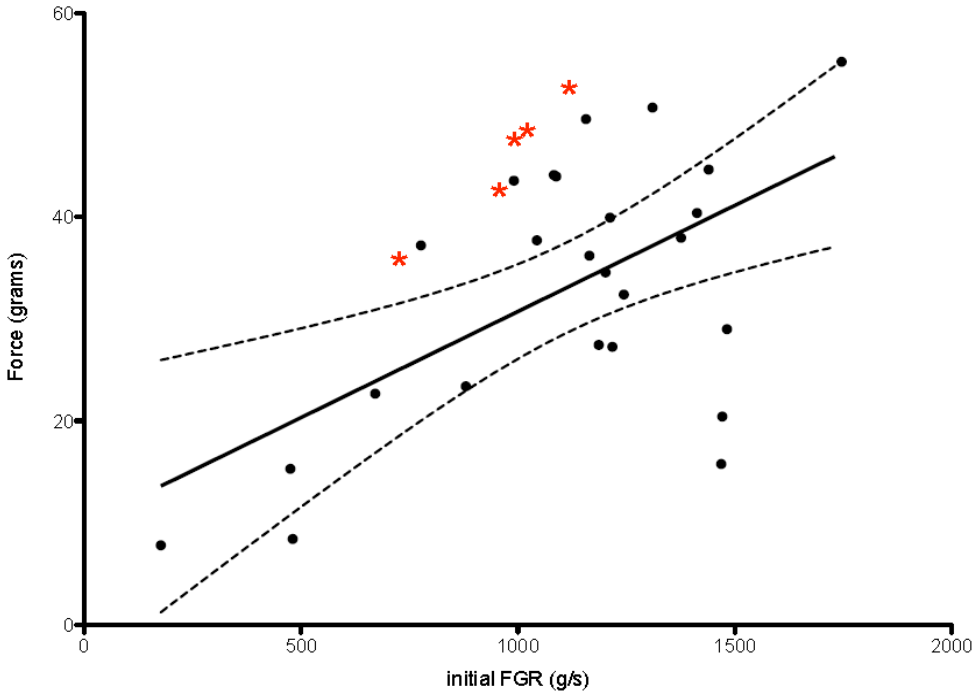

Figure 5.5: The mean force, force generation rate, and relaxation rate of 6-8 week old *mdx* muscles.

This figure shows the distinct patterns of force, force generation rate and fatigue during 8 minutes of fatigue. The force (Gach, Cherednichenko et al.) potentiates 3.7% in the first 36 seconds before a decline to less than 80% of the initial value. The force generation rate (blue) increases 11% of the initial value for the first 36 seconds and then remains elevated, finishing the test 12% higher than the initial value. The magnitude of the relaxation rate (purple) at the beginning of the test is 90% greater than that of the force generation rate. The magnitudes are equal at 78 seconds, and the relaxation rate reaches a minimum at 168 seconds. For the duration of the fatigue test, the relaxation rate increased so that it was 21% greater than the minimum value, but only 65% the initial value. The relaxation rate is far more dynamic than either force or force generation rate throughout the fatigue test.

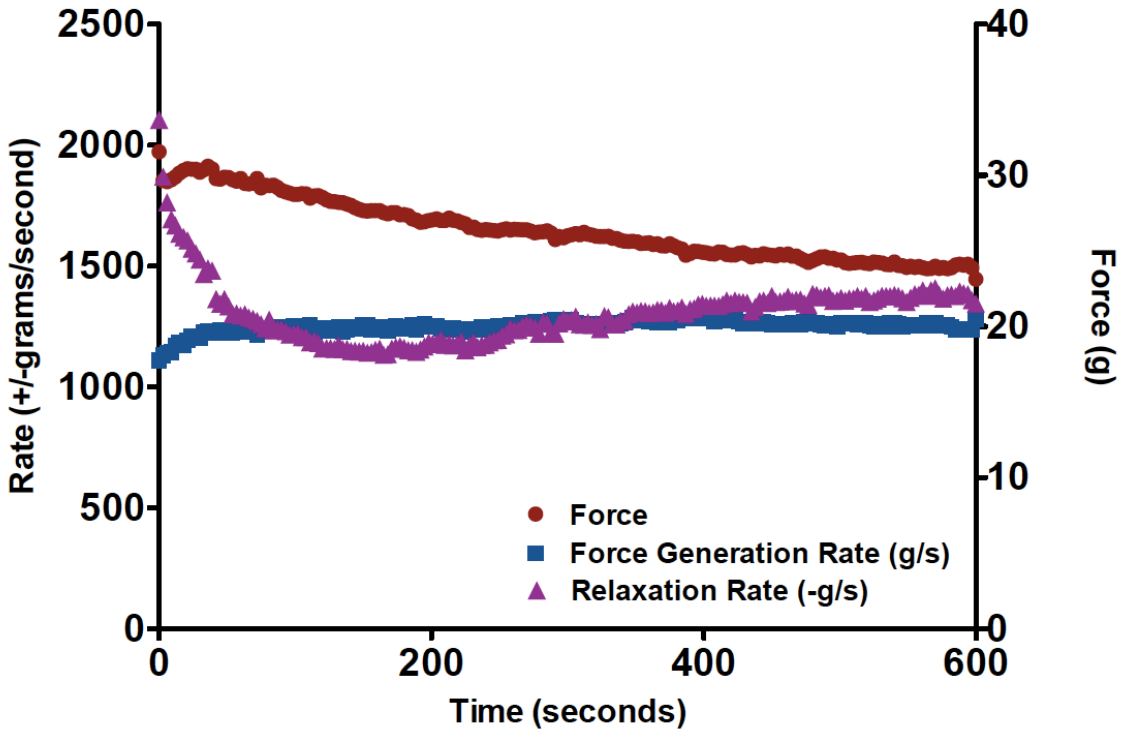

Figure 5.6: Fatigue of force among groups.
There is no difference in the fatigue of muscles in any of these groups. Error bars represent sem.

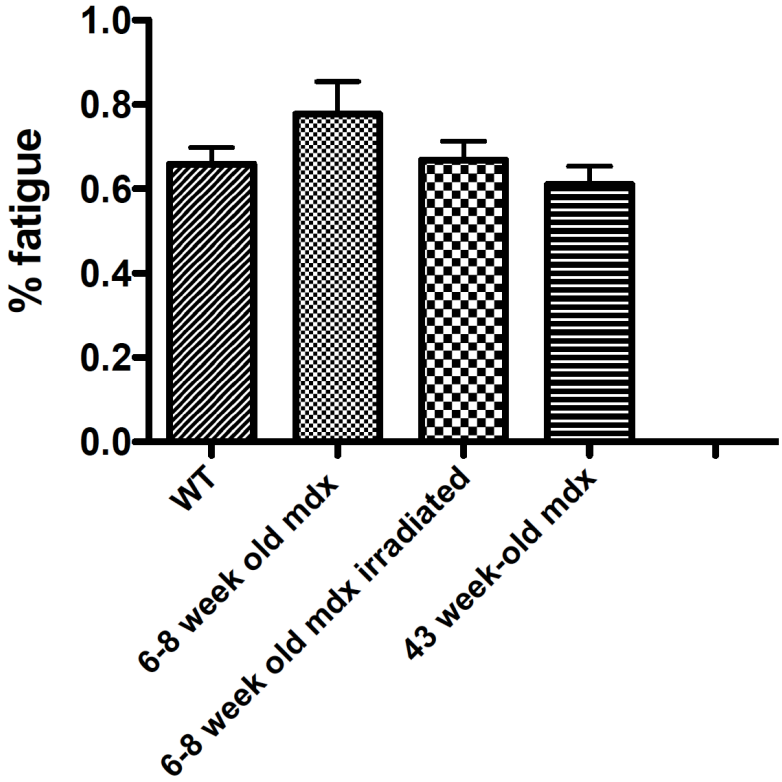

Figure 5.7: Initial, maximal and minimal force during fatigue.
Wild type muscles exert more force initially (A) and maximally (B). The significance of this relationship dissolves by the end of the test. The 43-week-old muscles are also stronger at the beginning of the test but not at the end.

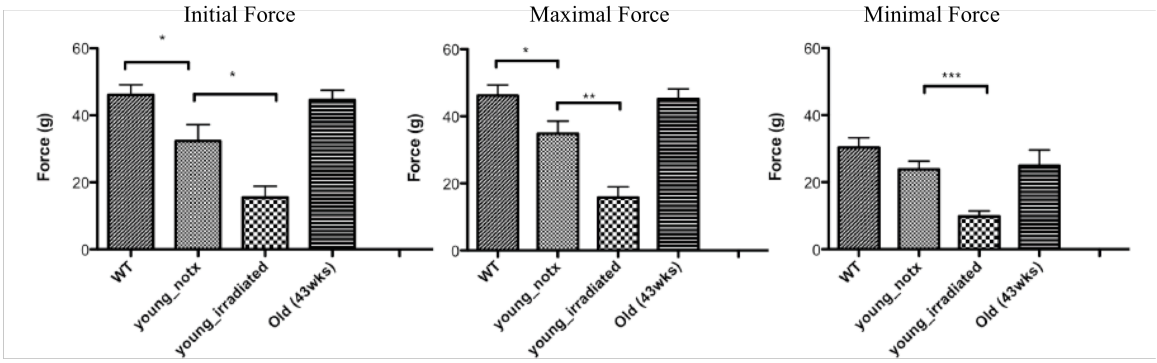

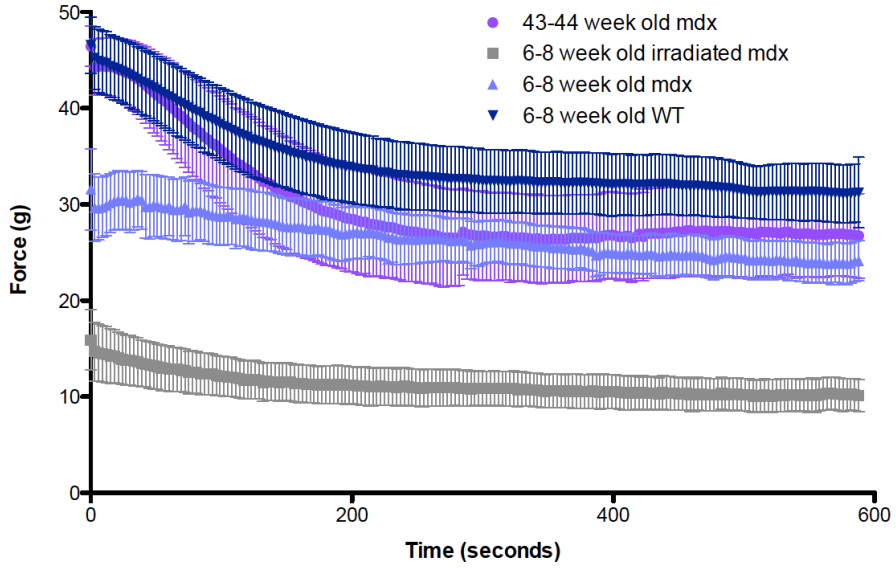

Figure 5.8: Initial, Maximal and Minimal force generation rates during fatigue.
The relationships established among control groups are distinct when measuring force generation rate. The force generation rate is decreased in wild type muscles compared to the age- and sex-matched *mdx* mice throughout most of the protocol. The force generation rates for 43-week old mice are not different from the younger counterparts.

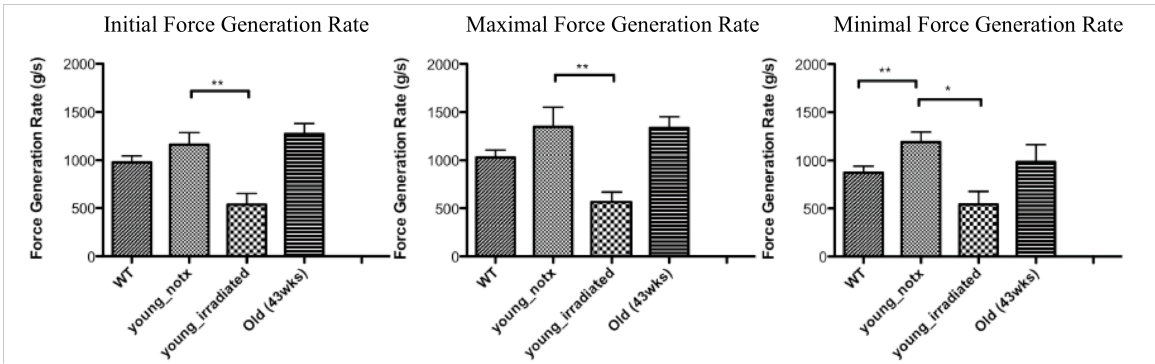

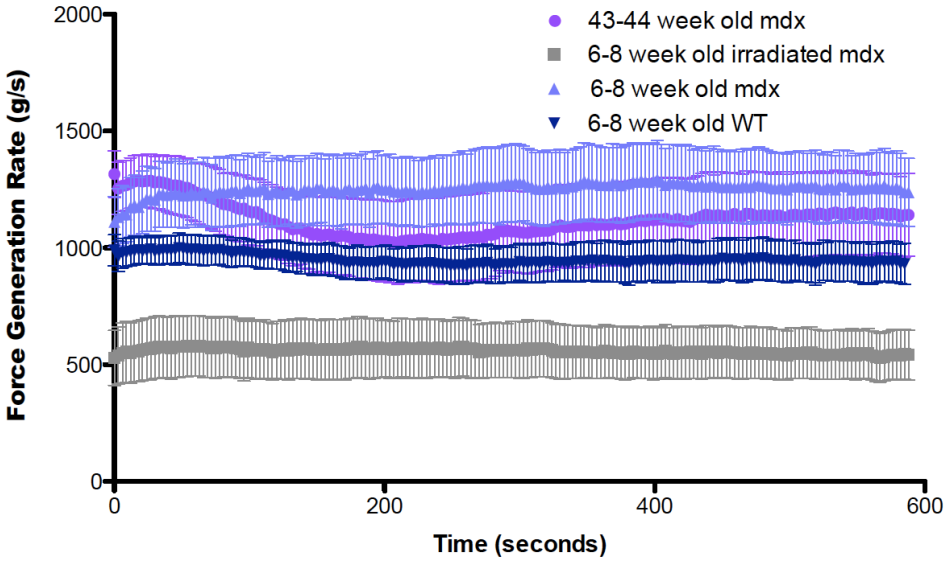

Figure 5.9: Initial, maximal and minimal relaxation rates during fatigue.
The relationship among the groups changes once again when looking at the relaxation rates. The relaxation rate of the 43-week old *mdx* muscles are significantly diminished compared to 6-8 week old *mdx* muscles, whereas the wild and *mdx* relaxation rates are the same throughout the test.

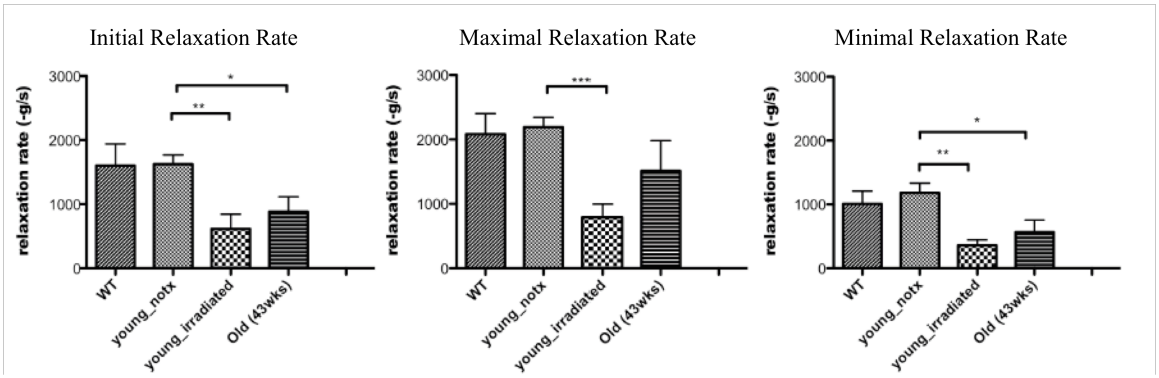

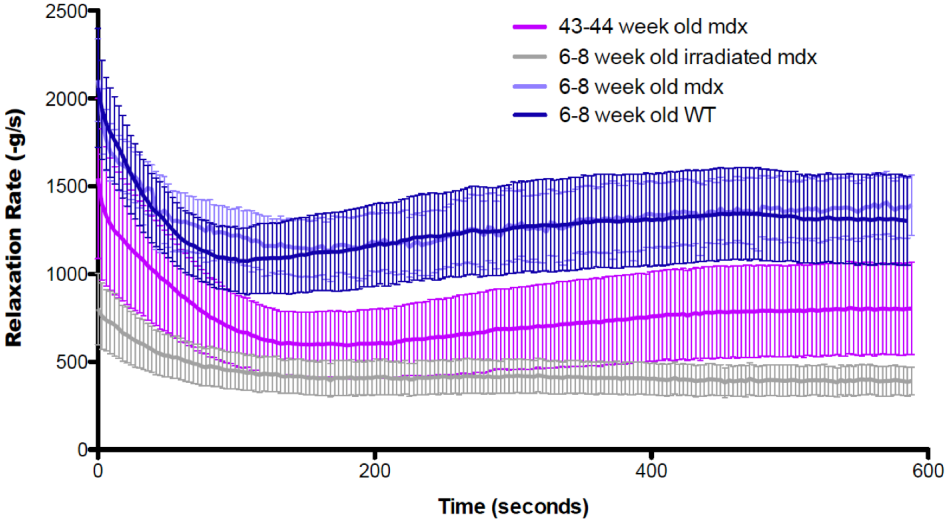

Figure 5.10: *Mdx* versus WT mini-tetanti of fatigue.
A single representative sub-maximal tetanus helps distinguish differences between the muscles. The force of 6-8 week old *mdx* muscle is shown with a WT muscle in A and with a 43-week old muscle in B. The rates of contraction are shown for 6-8 week old *mdx* muscle and WT muscle in C and 6-8 week old *mdx* muscle with 43-week old muscle in B. As reported, the force generation rate is faster in *mdx* muscle compared to wild type.

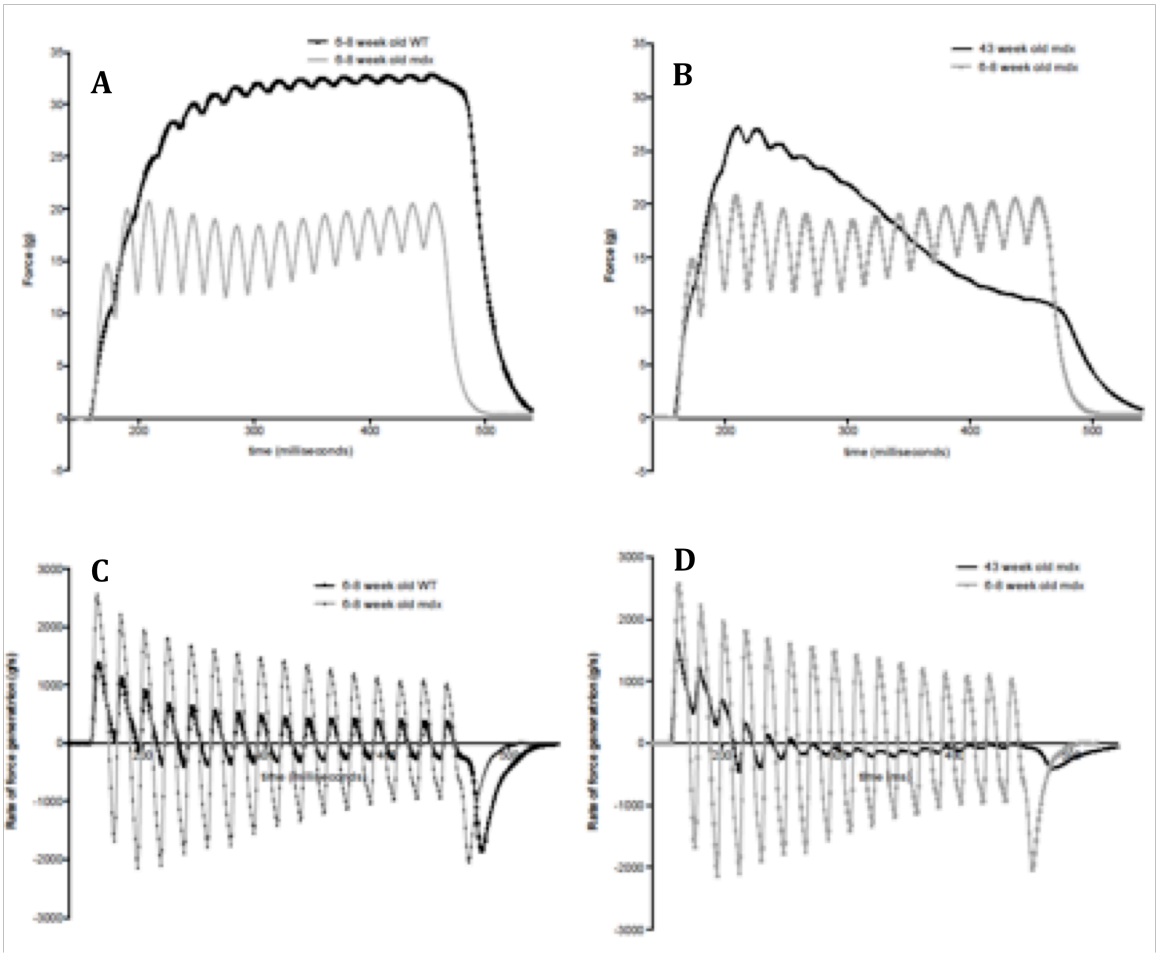

Figure 5.11: Maximal and minimal force generation rates in force frequency protocols. These measurements are obtained from protocols that are more challenging (FF2) and less challenging (FF1) Here we show the maximal (A and C) and minimal (B and D) force generation rates obtained from less challenging (A and B) and more challenging (C and D) protocols. The minimal force generation rate in 43-week old *mdx* muscles was significantly greater in the more challenging protocol than the 6-8 week old *mdx* muscles.

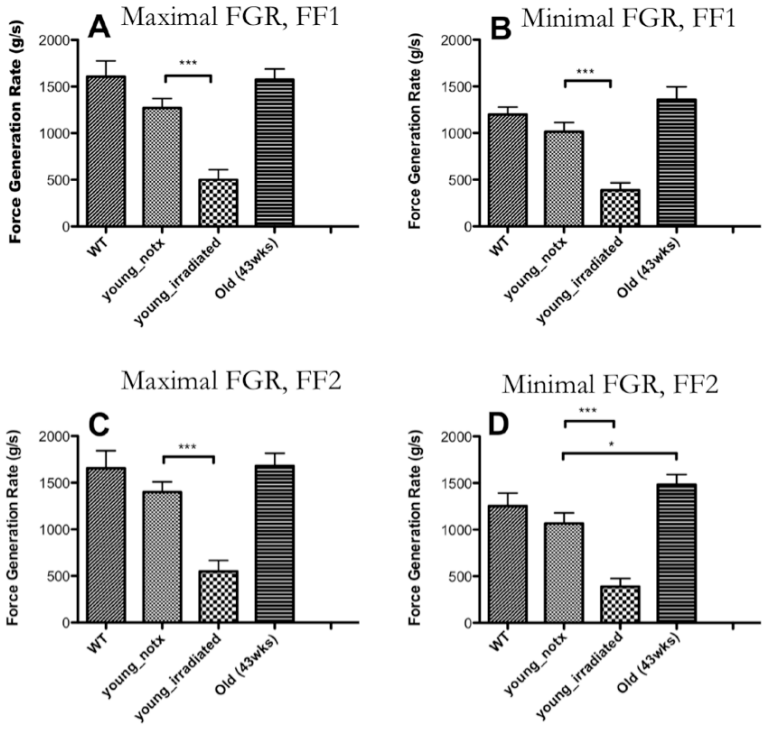

Figure 5.12: Maximal and minimal relaxation rates in force frequency protocols.
These measurements are obtained from protocols that are more challenging (FF2) and less challenging (FF1) The minimal relaxation rate in older mice decreases in both the more and less challenged protocol. The 43-week old *mdx* muscles relax at a slower rate than the 6-8 week old *mdx* muscles. In all groups, there is a decline of relaxation rate with increasing muscle.

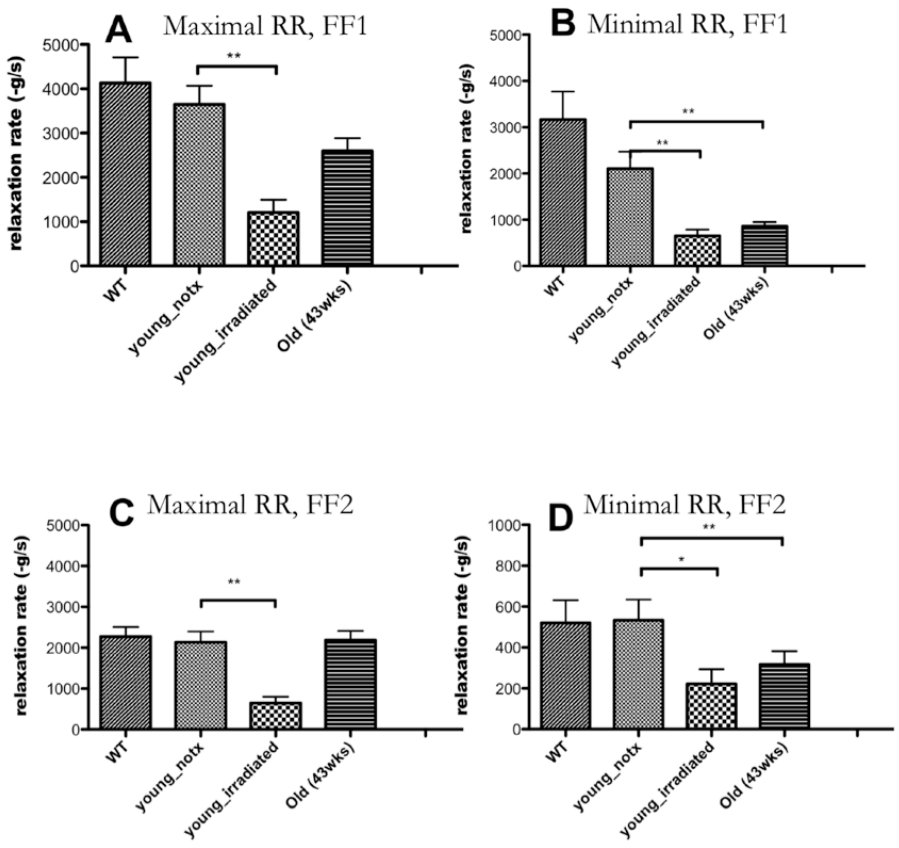

Figure 5.13: Passive Tension Tolerance of Force, Force Generation Rate, and Relaxation Rate

A, B, C, and D represent irradiated muscles, untreated 6-8 week old *mdx* mice, 43 week old untreated *mdx* mice, and 6-8 week old wild type mice, respectively. Relaxation rate is the most sensitive to increases in length. In irradiated muscle, the force generation rate is the least sensitive to increases to passive tension. Error bars show sem.

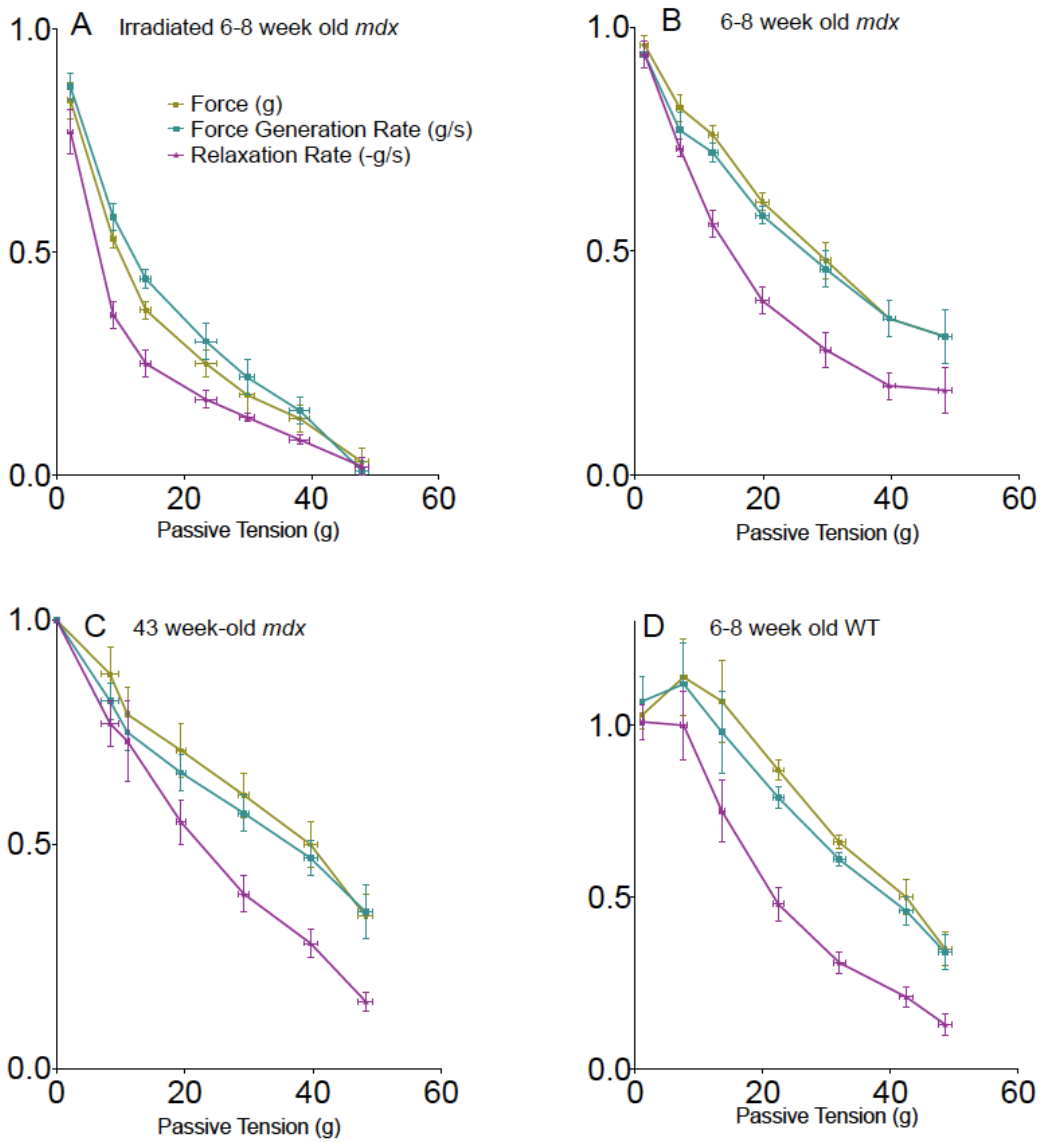

CHAPTER 6: RESTORATION OF SKELETAL MUSCLE FUNCTION IN MUSCLES TREATED WITH SATELLITE CELLS THAT EXPRESS α2δ1

While satellite cell grafts in animals have been more successful than human trials, their success has been limited(Morgan and Partridge 1992; Irintchev, Langer et al. 1997; Peault, Rudnicki et al. 2007). Migration is considered a limiting factor and treatment to enhance migration is underway(Meng, Adkin et al. ; Torrente, El Fahime et al. 2000; Peault, Rudnicki et al. 2007). Here, we select for a subpopulation of satellite cells that we believe will be capable of overcoming this limiting factor.

We believe that α2δ1 is directly involved in the migration and attachment of cells and that it is a harbinger for differentiation. If correct, then satellite cells that express surface α2δ1 at the time of the injection will integrate more fully into the host muscle and contribute to the myogenic phenotype. We expect that these muscles will be larger and stronger than muscles treated with cells without surface α2δ1. To assess whether the donor cells preferentially contribute to kinetic components of the muscle, we monitor force generation rate and relaxation rate in addition to mass and force. The passive tension tolerance is a measure of the ability of the cells to maintain contraction against increasing passive tension.

In vivo, self-renewal of the satellite cell pool allows the muscle to continue responding to damage. In fifteen subjects, we challenge the muscles treated with satellite cell subpopulations by exercising the muscles four weeks after treatment. Ten days after this re-exercise challenge, we measure differences in mass among treated groups.

METHODS:

The hindlimbs of twenty-one to twenty-eight day old male *mdx* mice were positioned for irradiation as shown in Figure 6.1. Within 24 hours of irradiation, the muscles were exercised and injected with sorted satellite cells. Experiments from this section use fluorescent activated cell sorting described in Chapter 2, and the *in situ* myotest described in Chapter 5.

Satellite Cell Isolation and Storage:

Hindlimb muscles from EGFP positive neonates less than three days old are isolated, minced, and enzymatically digested. The isolate is filtered through a 45 μm mesh. Isolated cells are frozen in 10% DMSO in fetal bovine serum and stored at -80ºC in cryovials. At the time of use, cells are reconstituted by thawing at room temperature, rinsed in suspension, centrifuged and re-suspended in plating medium.

Anesthesia:

A ketamine/xylazine mixture is used to anesthetize the mice during irradiation, exercise, injection, and myotest protocols. Achievement of proper anesthetic plane is determined by non-response to toe-pinch. This is usually obtained with 2 mg of ketamine and 0.1 mg of xylazine suspended in 0.25 mL of saline for a 25 gram mouse.

Irradiation of hindlimbs:

Irradiation is applied to prevent the division and differentiation of the host's satellite cells, which would inhibit the activation of the donor satellite cells(Boldrin, Neal et al.). Radiation is delivered by the Clinac iX linear accelerator in UIH Department of Radiation Oncology. Mice are positioned with one leg extended and aligned with only this hindlimb within the zone of x-

ray exposure. The dose of irradiation is 25 γray and is delivered at 2 γray per minute. This is repeated with the contralateral leg.

Muscle stimulation protocol:

Exercise around the time of graft aids in attachment(Roberts and McGeachie 1992). In order to target the muscle with maximal intensity, we use transcutaneous electrical muscular stimulation. The tibialis anterior is very susceptible to injury by exercise(Dellorusso, Crawford et al. 2001). After anesthetizing the subject with ketamine/xylazine and depilating the right posterior distal hindlimb, a Grass Stimulator delivers 1.2 times the voltage necessary to elicit a contraction, at 40 Hz to the tibialis anterior for 40 minutes.

Injection of sorted cells

The tibialis anterior maximally protrudes at approximately one third of the distance from lateral proximal protrusion of the fibula to the lateral malleolus. This point of maximal protrusion coincides with the belly of the muscle, and is the target for cell delivery. The needle is inserted just proximal to this point, so that the tip of the needle is located in the belly of the muscle when the cells are delivered. Hamilton needles and syringes are used for the injection process. Plating media (high-glucose DMEM supplemented with L-glutamine with 20% serum, 1% penicillin/streptomycin and 1% amphotericin-b) is used as vehicle. Forty thousand cells of one subpopulation resuspended in 5 μL of vehicle are injected into the TA. The contralateral TA is injected with vehicle alone.

Re-exercise challenge

To test the ability of donor cells to be reactivated, fifteen mice were exercised via transcutaneous electrical muscular stimulation as described above four weeks after injection of

donor cells. Ten days after this second bout of exercise, the muscles were tested *in situ* as described previously.

Statistics:

For data from force-frequency protocols, the significance was determined by a paired t-test. For values presented in a bar graph, significance is determined by a simple unpaired t-test.

RESULTS

Muscles treated with cells that express α2δ1 are significantly heavier than the contralateral muscle

To get an initial indication of the ability of the donor cells to attach and contribute to mass, we measured the mass of treated, untreated, and control muscles three to four weeks after treatment. The masses of the tibialis anterior of six groups of male mice, aged 6-8 weeks, are shown in Figure 6.2. The three columns on the right represent the mass of muscles that have been irradiated and injected with either vehicle alone, with satellite cells with no surface α2δ1, or with satellite cells with early expression of α2δ1.

There is no difference in the mass of WT and *mdx* muscles. Irradiation reduces the mass by 63%. Treatment of irradiated muscle with vehicle alone increases the mass by 32%. Compared to vehicle alone, there is no difference in the mass of muscles treated with cells that do not express α2δ1. The mass of muscles treated with satellite cells that express surface α2δ1 is significantly greater than both those treated with vehicle alone and those treated with cells without surface α2δ1.

No difference in force, force generation rate or relaxation rate in muscles control or treated muscles during the fatigue protocol

During fatigue, submaximal repeated stimulation challenges the ability of the muscle to adapt to consistent activity. As no significant difference was found among muscles treated with satellite cell subpopulations during the fatigue test, error bars in Figure 6.2 were eliminated. A noteworthy trend shows muscles treated with cells that have surface α2δ1 are faster to relax and faster to generate force. Comparison of results from Chapter 5 places these results firmly between the force of the irradiated muscle and the non-treated 6-8 week old *mdx* muscle for all three measurements.

Muscles treated with cells that express α2δ1 are significantly stronger than the contralateral muscle

The force frequency protocol tests the maximum capability ability of the muscle to generate force at a give stimulation frequency. Figures 6.4a and 6.4b show that, compared to contralateral muscle, muscles treated with satellite cells with surface α2δ1 can exert 28% and 34% more force. Muscles treated with cells without α2δ1 are not stronger than the contralateral muscle (figures 6.4c and 6.4d). There is no significant decrement from the force exerted during FF1 (figures 6.4a and 6.4c) to FF2 (figures 6.4b and 6.4d).

Muscles treated with cells that express α2δ1 contract faster than the contralateral muscle

In order to determine whether the treatment contributes to force generation, we measure the speed with which the muscle contracts at a given frequency. We show that force generation

rate throughout both force-frequency protocols. The force generation rate was the least sensitive to activity-induced changes. In figure 6.5a and 6.5b, we show that muscles treated with cells that express surface α2δ1 do contract faster than the contralateral muscle treated with vehicle. Figures 6.5c and 6.5d show that muscles treated with cells without α2δ1 do not contract more quickly.

Muscles treated with either cell subpopulation relax more quickly than contralateral muscle

The relaxation rate was altered with treatment (Figure 6.6). Muscles treated with cells that express α2δ1 relax more quickly than the contralateral muscle treated with vehicle alone. Figures 6.5c and 6.5d show differences in muscles treated with satellite cells without α2δ1 on the surface. This is the first measurement in which any effect of treatment with this cell type is observed.

There is a distinct difference between relaxation rates provoked by FF1 and FF2. The more challenging protocol provokes a relaxation rate reduced to only one-third of the initial values. In all groups, the optimal frequency of relaxation shifts so that the maximum relaxation rate takes place at a smaller frequency. The optimal frequency for muscles treated with cells that express α2δ1 shifts from 120 Hz to 80 Hz. For the contralateral muscle, the optimal frequency shifts from 100 Hz to 50 Hz. For muscles treated with cells without α2δ1 and the contralateral muscle, the optimal frequency shifts from 100 Hz to 80 Hz.

More passive tension was tolerated by muscles treated with satellite cells that express surface α2δ1.

Figure 6.7A shows the decline in force upon increase in passive tension for wild type and irradiated *mdx* muscles. The passive tension necessary to reduce the force to 50% of the initial value is reported in Figure 6.7B. Muscles treated with cells that contain α2δ1 require more passive tension to reduce the force by half compared to muscles treated with cells that do not express surface α2δ1. Comparison with Figure 5.13 reveals that all of these values are between irradiated *mdx* and non-irradiated *mdx* muscles.

After re-exercise, muscles treated with cells with CD34 had a greater mass.

We tested the ability of the satellite cells to be re-activated by exercising the muscles four weeks after treatment and measuring mass 10 days after re-exercise. Figure 6.8A shows the mass of each group tested. The correlation of increased mass with treatment to α2δ1 was lost. Figure 6.8B shows that muscles treated with cells with CD34 were significantly larger than those treated with cells that did not express CD34 at the time of sorting.

The ratio (treated:contralateral) of the mass of muscles treated with cells without CD34 was 0.80±0.11, with a 95% confidence interval of 0.5157–1.078. This raises the possibility that the mass actually *decreased* in muscles treated with cells without CD34. We plotted the mass of irradiated muscles treated with vehicle at 7 weeks and at 10 weeks on the graph representative of the *mdx* colony (figure 6.9). The blue asterisk represents the mean mass of irradiated muscles treated with vehicle from seven-week-old *mdx* mice. While they are smaller than the

other mice of the same age, it is possible that it is within error. The red asterisk represents the mean mass of irradiated muscles treated with vehicle from ten-week-old mdx mice. Despite being at an age of rapid growth, the mass was significantly smaller than it was at seven weeks.

In order to assess whether the decline in mass was due to injury from intense exercise, we measured the mass of muscles that had been irradiated and injected with vehicle but not re-exercised and compared this to the mass of muscles that had been injected with vehicle and exercised. There was no difference in the mean mass (Figure 6.10) of these two groups, indicating that the reduction in mass was not due to re-exercise challenge.

DISCUSSION:

Muscles that were injected with vehicle were significantly larger than muscles that were irradiated and not injected (Figure 6.2). While it is possible that the needle stick itself caused a protective inflammatory response, it is more likely that the serum in the vehicle was protective against damage. The mass of 6-8 week old *mdx* muscles is not significantly different from the mass of age- and sex-matched WT muscles. Treatment of muscles with cells without α2δ1 does not result in a greater mass, but treatment of muscles with cells that do express surface α2δ1 does increase mass significantly, when compared to muscles injected with vehicle alone or to muscles injected with cells without α2δ1.

Figure 6.3 shows the force (6.3A), force generation rate (6.3B), and relaxation rate (6.3C) of muscles treated with cells with or without α2δ1, and the corresponding contralateral muscles during the fatigue protocol. There are no significant differences in these results. Error bars

are omitted to facilitate the observation of trends. Muscles treated with cells that expressed surface α2δ1 may have exhibited augmented rates of force generation and relaxation. The force was not higher than the contralateral muscle. Force of muscles treated with cells that do not express α2δ1 trends slightly higher.

In figures 6.3A and B, we see that the force of muscles treated with cells that express α2δ1 is significantly greater in both force-frequency protocols. In figures 6.3 C and D, the force of muscles treated with cells that do not express surface α2δ1 is identical to that from the contralateral leg in both protocols. There is an insignificant reduction in the force generated in the less challenging protocol to the more challenging protocol.

The force generation rates of treated muscles compared to the force generation rates of contralateral muscles are shown in figure 6.4. There is no significant difference among groups, but the force generation rate of muscles treated with α2δ1 trend higher than contralateral, while the force generation rate of muscles treated with cells with no α2δ1 are indistinguishable from contralateral. In this test, the force generation rate is less sensitive to differences in treatment than force.

Figure 6.5 shows the relaxation rates of treated and contralateral muscles. Muscles treated with either subpopulation of satellite cells are capable of relaxing more quickly than contralateral muscle. The measurement of relaxation is sensitive enough to detect the contribution from donor cells. Alternatively, these cells contribute uniquely to relaxation rate. In both treatment groups and in contralateral legs, the magnitude of the relaxation rate declines significantly at frequencies greater than 120 or 150 Hz. Comparison of the relaxation rate generated by the

more challenging protocol yields a 50% reduction in relaxation rate from the relaxation rate of the less challenging protocol.

The passive tension applied to a muscle required to reduce the twitch force to half that of the original value is greater in muscles treated with cells with α2δ1 (Figure 6.6). These muscles are capable of generating contraction against greater force than muscles treated with vehicle alone.

Re-exercise challenge

After re-exercise, we found that the satellite cells that express CD34 at the time of the sort were larger than those that did not express CD34. While this seems to disagree with our results from earlier, it is consistent with results from *in vitro* studies that show that CD34 is an early marker of satellite cells and cells with α2δ1 are either more advanced through the process of development or more committed to myogenesis. These cells with α2δ1 differentiate and contribute to mass and force, but remain vulnerable to damage. Whether cells with CD34 were activated at this time or if they were simply protected from damage is unknown.

Despite improved muscle function, the fate of the injected cells remains in question. Functional recovery of muscle could theoretically be achieved by neurogenesis, vasculogenesis, or myogenesis. It has been shown that satellite cells are capable of differentiating into neurons, endothelital cells (Tamaki, Uchiyama et al. 2005) and adipocytes. Muscle regeneration requires angiogenesis and neurogenesis in order to properly supply the new muscle(Roberts and McGeachie 1990). This would require the outgrowth of existing vessels, and the activation of local pericytes. In these experiments, proliferation of pericytes was eliminated by irradiation of the muscles, requiring both migration of cells from other parts of

the body or that the injected cells are multipotent. This creates the possibility of increased function due to cell type without the commitment to myogenesis.

FIGURES

Figure 6.1: Irradiation of hindlimbs of mdx host mice.
After being anesthetized, the mice were arranged so that only their hindlimbs were within the irradiation beam. The beam here is represented by the light. The red laser is used to align the mice with the irradiation beam. This procedure was done separately for each leg. Each leg was irradiated for 12.5 minutes, at 2 γray per minute.

Figure 6.2: Mass of treated and control muscles.
The mass of wild type tibialis anterior muscles is greater than that of sex- and age-matched *mdx* muscles. Irradiation of *mdx* muscles causes a dramatic decrease in mass. Injection of vehicle in irradiated, *mdx* muscle increases the mass significantly, to19.1mg. Injection of cells with α2δ1 suspended in vehicle into irradiated *mdx* muscle does not significantly increase mass. Treatment of irradiated *mdx* muscle with cells that express surface α2δ1 increases the mass of muscle. The increase in mass is significant when compared either to muscle treated with vehicle or cells without α2δ1. In order as shown, from left to right, the mean and sem of the mass of muscles for each group are 36.48±1.66mg, 34.43±3.61mg, 13.12±1.48mg, 18.24±1.17mg, 18.68±1.20mg, and 22.50±1.32mg, with n=6, 4, 6, 29, 14, and 16.

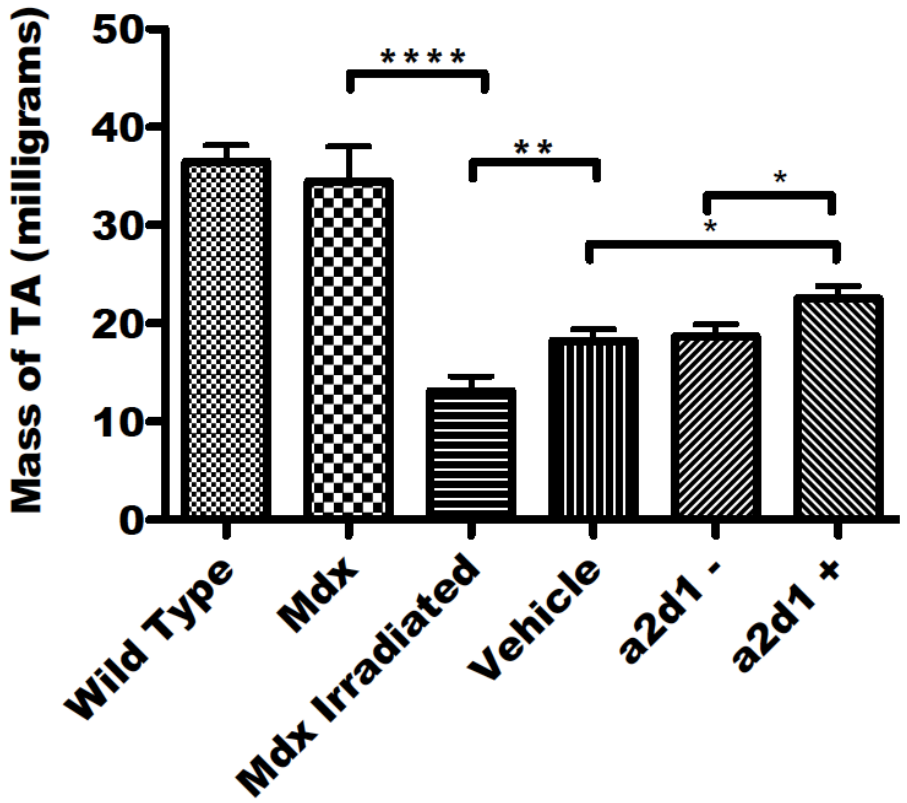

Figure 6.3: Fatigue behavior of muscles treated with satellite cells that express surface α2δ1 and muscles treated with cells that do not express surface α2δ1. No error bars are shown because these differences are not significant. The trend shows that α2δ1 has a marginally greater force generation rate and relaxation rate, but not less force during this fatigue test.

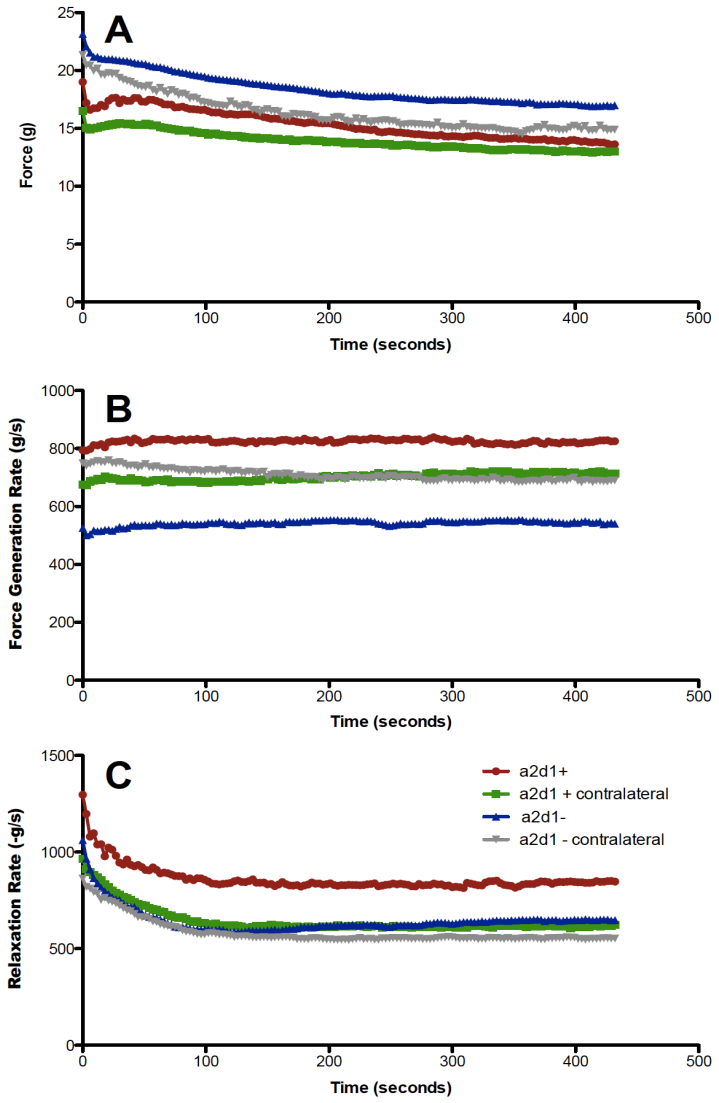

Figure 6.4: Force of muscles treated with satellite cells that express surface α2δ1 (A and B) and muscles treated with satellite cells without α2δ1 (C and D) in a less challenging force-frequency protocol (A and C) and a more challenging force-frequency protocol (B and D). The gray line represents the force from the treated tibialis anterior, and the black line represents the contralateral leg. Error bars represent sem.

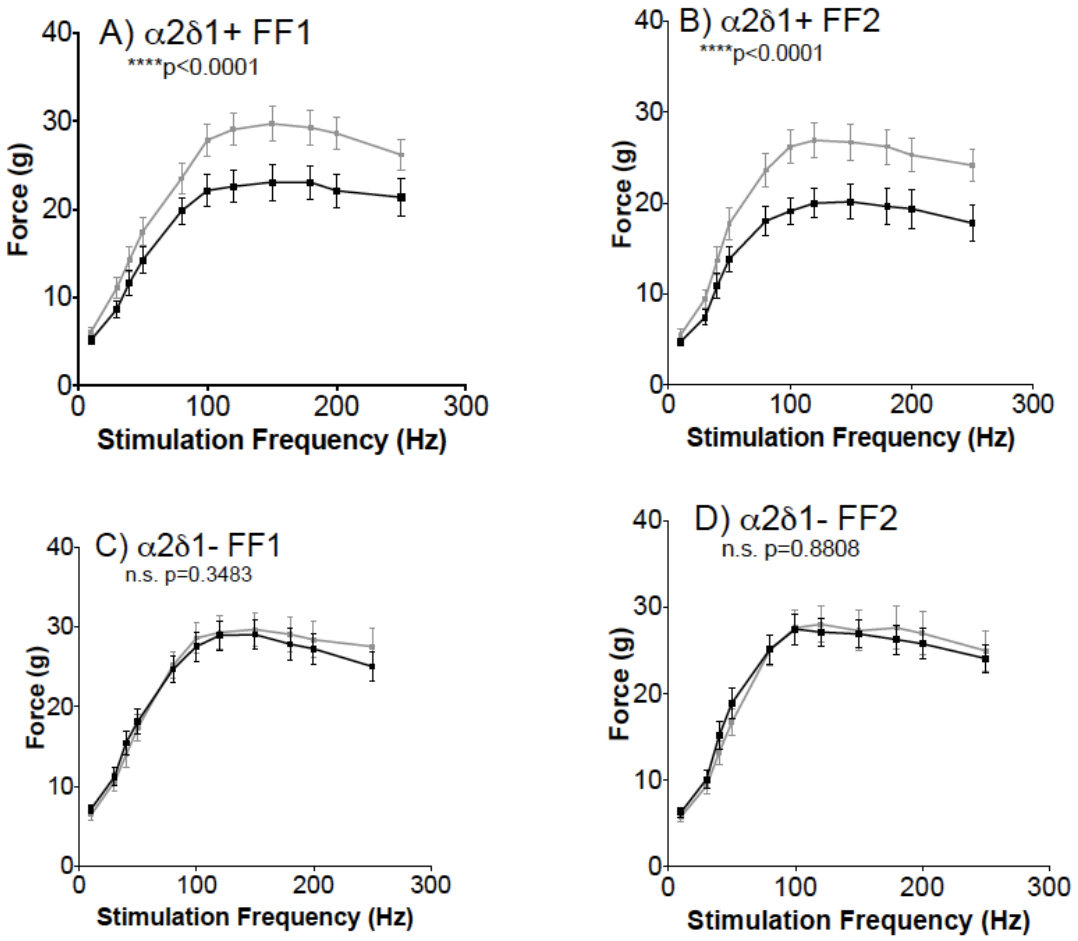

Figure 6.5: Force generation rate of muscles treated with satellite cells that express surface α2δ1 (A and B) and muscles treated with satellite cells without α2δ1 (C and D) in a less challenging force-frequency protocol (A and C) and a more challenging force-frequency protocol (B and D). The gray line represents the force from the treated tibialis anterior, and the black line represents the contralateral leg. Error bars represent sem.

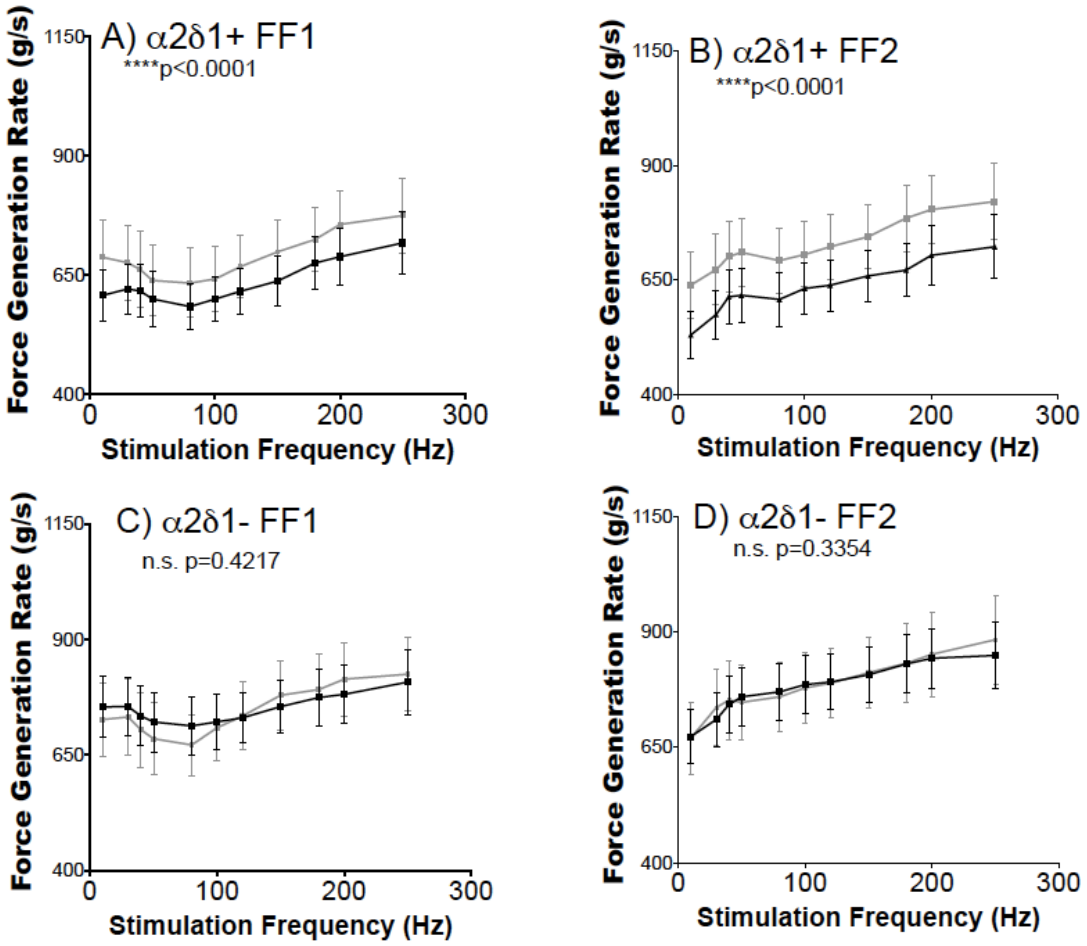

Figure 6.6: Relaxation rate of muscles treated with satellite cells that express surface α2δ1 (A and B) and muscles treated with satellite cells without α2δ1 (C and D) in a less challenging force-frequency protocol (A and C) and a more challenging force-frequency protocol (B and D). The gray line represents the force from the treated tibialis anterior, and the black line represents the contralateral leg. Error bars represent sem.

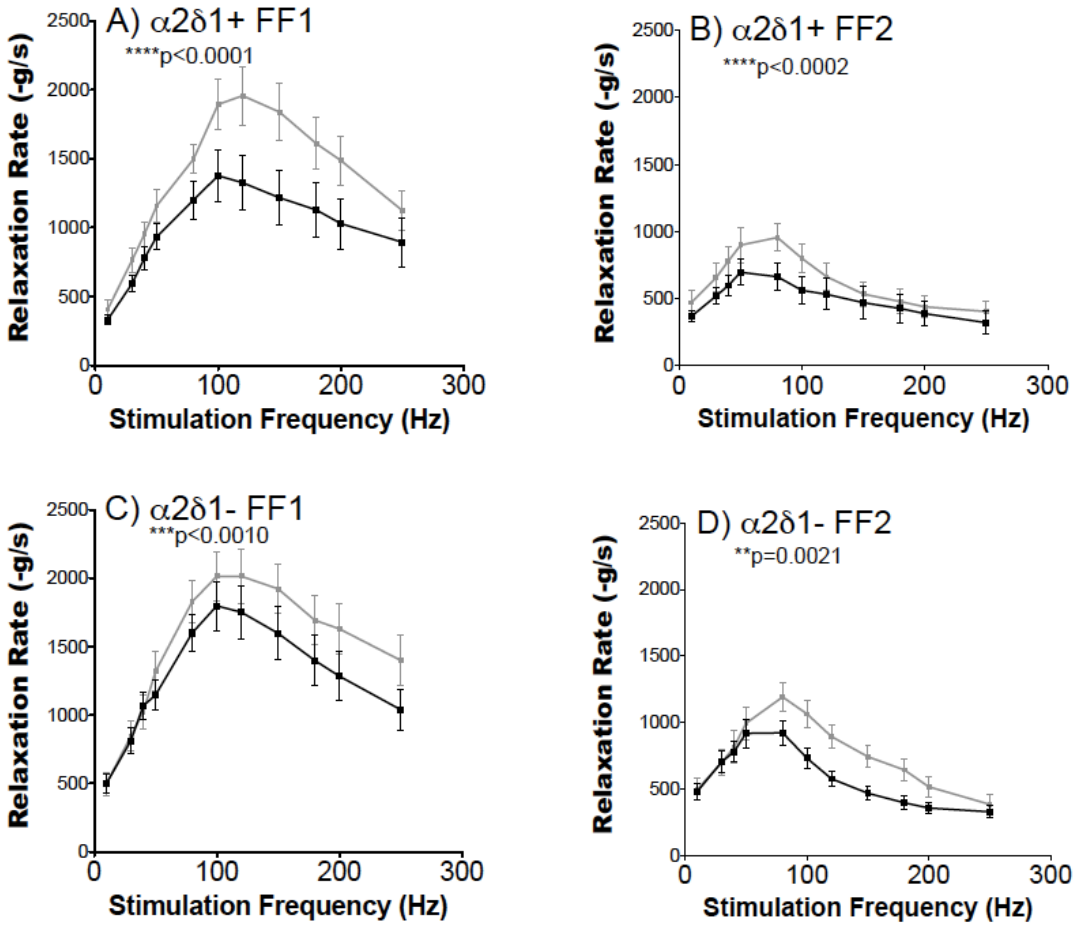

Figure 6.7: Passive tension tolerance of muscles treated with cells that have α2δ1 are capable of maintaining their contraction with significantly greater passive tension. Force of the active contraction is reduced as passive tension increases beyond the optimal passive tension. This relationship is shown for *mdx* irradiated mice (dashed line) and age-matched wild type mice (A). The passive tension applied to the muscle required for active force to be reduced by 50% is shown in B. Muscles treated with cells that express α2δ1 can more effectively preserve their ability to contract against passive tension. The passive tension required for the active contraction to be reduced by 50% of the initial value is 15.75±1.57g, 17.14±2.22g, 23.00±1.20g, and 29.06±2.03g for muscles treated with vehicle, cells without α2δ1, cells with α2δ1, and for WT muscles, with n=27, 14, 8, and 7 muscles, respectively.

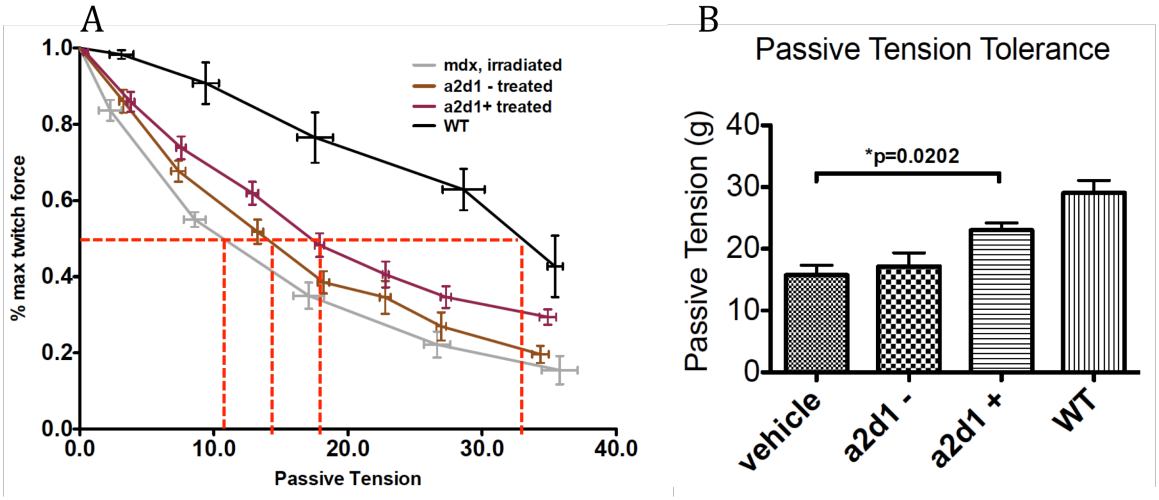

Figure 6.8: Mass of treated muscles 10 days after re-exercise challenge. Ten days after re-exercise challenge, the mass of muscles treated with cells that have both α2δ1 and CD34 is significantly greater than muscles treated with cells without CD34 but with α2δ1 and muscles treated with cells without CD34 or α2δ1 (A). Mass of muscles treated with vehicle, cells with α2δ1f only, neither α2δ1 nor CD24 (negneg), cells with both α2δ1 and CD34 (pospos), and cells with only CD34 is 13.47±1.58mg, 11.85±2.28mg, 8.53±4.43mg, 17.80±1.24mg and 17.80±2.89mg respectively. A correlation between increased mass and treatment with cells with α2δ1 is lost. Muscles treated with cells that have CD34 have a significantly greater mass than muscles treated with cells that do not express CD34, regardless of whether they also expressed α2δ1. The ratio of mass of treated:untreated muscles for those muscles treated with CD34+ cells is 1.273±0.10, with a 95% CI of 1.047 to 1.498. For muscles treated with cells without CD34, the ratio is 0.80±0.11, with a 95%CI of 0.516 to 1.078)

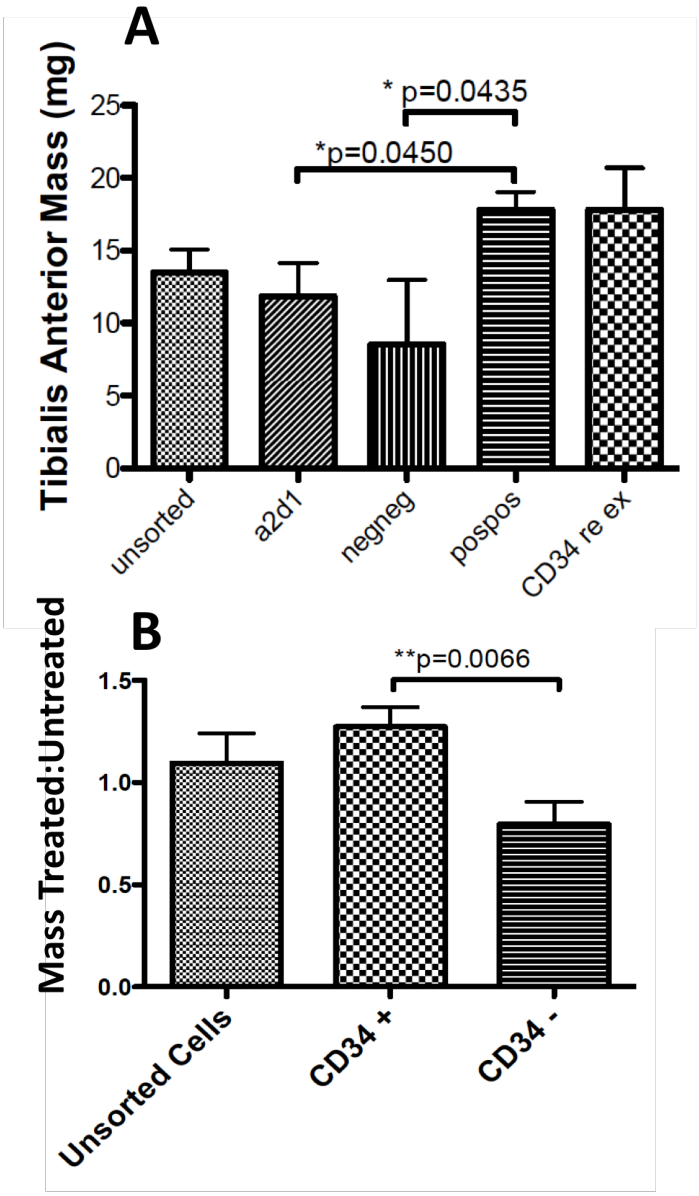

Figure 6.9: Mass decline after irradiation and re-exercise.
The mean mass of the muscles tested at 6-8 weeks is shown by the blue asterisk. The mass of the muscles tested at 10 weeks is shown by the red asterisk. This difference in mass of 6-8 week old treated muscle compared to 10 week-old treated muscle (18.24±1.17 vs. 12.59±1.15, n=29 and 18 respectively) is significant (p=0.006). This decline in mass occurs even at an age that normally coincides with rapid growth.

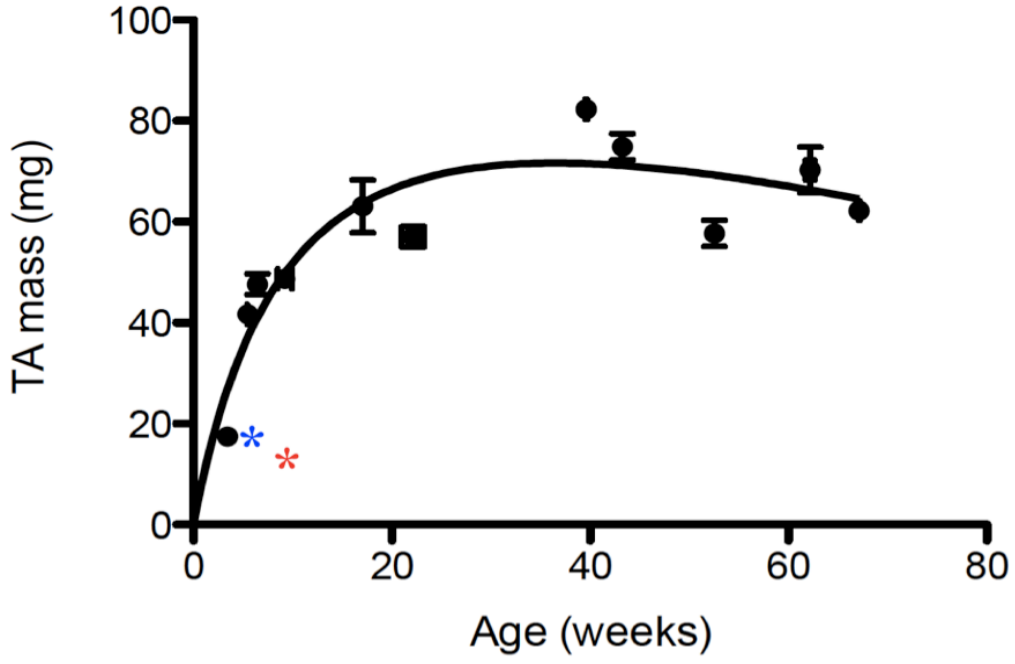

Figure 6.10: Exercised and non-exercised mass of tibialis anterior treated with vehicle at 10 weeks

To investigate whether the decrease in mass of tibialis anterior from 7 weeks to 10 weeks was attributable to the damage caused by re-exercise challenge, we compare the mass of muscles treated with only vehicle of exercised and non-exercised muscles. The mass of treated muscles exercised and not exercised at 10 weeks of age. There is no difference in the mass of exercised (13.47±1.58mg) and non-exercised (14.28±2.46mg) muscle, indicating that mass decline was not due to exercise. Error bars represent sem.

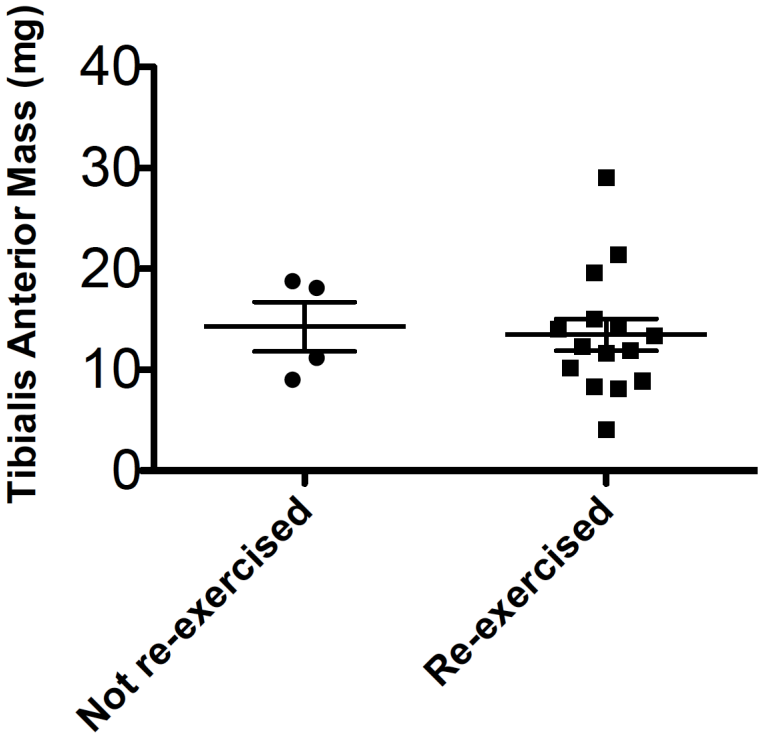

CONCLUSIONS

We assert that satellite cells that exhibit early expression of α2δ1 provide a clear advantage during critical times of a satellite cell graft. Compared to contralateral muscle, muscles treated with cells that express surface α2δ1 exhibited greater force of contraction and relaxation rate, and these muscles were better able to maintain contraction against increasing passive tension.

In this work we also asked why this may be the case. We found that over fifty percent of newly isolated satellite cells express α2δ1, and that expression of α2δ1 takes place much earlier than the pore-forming subunits of the calcium channel, strongly suggesting that the role of α2δ1 at this early period is independent of its role with the calcium channel. Cells that express surface α2δ1 express more myogenin than MyoD two days after the sort, consistent with the idea that they are further along in the process of differentiation or that these cells are willing to commit to the myogenic process. These same cells elongate earlier than other subpopulations. *In vivo*, these cells attached to the host muscle and provided a measureable increase in mass and force, and an increase in relaxation rate.

Primitive satellite cells express CD34 on the cell surface. Myotubes express surface α2δ1 and not CD34. The timing of the decrease in CD34 and increase in α2δ1 is unknown. The *in vivo* experiment results together with results from the re-exercise challenge are consistent with the idea that cells that express CD34 lag behind in differentiation, and that cells with α2δ1 are ahead in the process. Whether the $CD34^+$ cells populations do differentiate *in vivo* is not specifically addressed in this work, and so it is equally possible that these cells do not differentiate or contribute to muscle function after re-exercise. Initially, increased mass and

force correlate with the presence of α2δ1, as these cells are in the process of differentiation. These new myofibers are more susceptible to cell death than cells that did not differentiate after injection, were further behind in the differentiation process, or did not differentiate and therefore avoided susceptibility to contraction-induced death.

The mass of the muscle continues to decline after irradiation. This decline is not due to the bout of stimulation. While treatment with 40,000 satellite cells seems to have supplemented the damage done with irradiation, it was not sufficient to compensate for the loss of host satellite cells. Cells positive for α2δ1 would contribute most to compensation for muscle injury. More work will have to be performed to understand whether $CD34^+$ cells play a beneficial role in regeneration.

The relaxation rate is the most functionally sensitive parameter of the measurements taken. During fatigue, relaxation rate changes 40% from initial value, while force and force generation rate only changed 8% and 3% respectively. Relaxation rate changed most dramatically throughout the force frequency protocols, during which the relaxation rate ranges from more than 250% of the magnitude of the force generation rate and falls to only a fifth of the magnitude of the force generation rate. In the treated muscles, the only significant difference measured in the muscles treated with cells that do not express α2δ1 was in the relaxation rates. Measurements of relaxation rate are more sensitive than measurements of force or force generation rate.

Treatment with a ligand of α2δ1, thrombospondin, causes an increase in proliferation rate of C2C12 cells and an increase of migration rate of primary satellite cells. This may be accomplished by acceleration of the expression levels of total Jnk1 as cells are coming out of

quiescence. Chapter 3 shows that effect of early expression of α2δ1 is most measureable in the first few days after plating. Treatment with TSP increases migration over 4 days, and increases proliferation in just 24 hours.

FUTURE DIRECTIONS

Here, we propose that α2δ1 is a marker of a myogenic cell. Identification of a myogenic cell by a surface marker is still a topic of research. CD34, syndecan 3 and 4, M-cadherin are just a few markers of myogenic cells that have been suggested(Chapman, Balakrishnan et al.). The same issue arises with each of these markers: there are myogenic cells that do not have the marker, and there are cells that express the marker that are not myogenic. Identifying myogenic precursors is reasonably complicated. There is disagreement about the origin of adult muscle progenitors. Through each stage of differentiation, the cell markers change(Kallestad and McLoon ; Asakura, Seale et al. 2002; Qu-Petersen, Deasy et al. 2002; Tamaki, Akatsuka et al. 2002; Collins, Olsen et al. 2005). To date, the best marker for satellite cells is Pax7. All cells with Pax7 are myogenic satellite cells, but there are myogenic cells that do not express Pax 7(Bosnakovski, Xu et al. 2008). The sensitivity of identifying myogenic cells with the α2δ1 surface marker would be addressed by determining the coincidence of α2δ1 with Pax7. This could be done by a series of cell sorting experiments, during which either a four way sort is performed based on the expression of Pax7 and α2δ1 or Pax7 cells could be isolated and a 2-way sort could be performed. We would expect a high coincidence of expression.

Despite the observed increase in myogenesis of cells that express α2δ1 *in vitro*, the fate of these satellite cells *in vivo* was not directly witnessed. Immunohistochemistry could be carried out in these muscles. The donor cells are labeled with EGFP and dystrophin. The cell type would be determined by distribution and by colocalization.

The question remains: how significant is the impact of the interaction between α2δ1 and TSP in regenerating skeletal muscle? Proof of the significance of the interaction could be achieved by knockout and reintroduction experiments, in which the phenotype induced by a knockout can be reversed by treatment with the element knocked out. Satellite cell migration and proliferation measured in conditioned media from macrophages of TSP-1 knockouts could be measured, treated with TSP-1 and then measured again. Similar experiments have been performed in the CNS, in which conditioned media from TSP-1 knockout astrocytes fail to cause proliferation or differentiation of neural progenitor cells(Lu and Kipnis).

Energetics of protein interaction would help predict the probability of this interaction. The association constants of α2δ1 with other ligands have been studied. The relationship of the strength of binding and function of α2δ1 is an active topic of research(Mortell, Anderson et al. 2006), in which k_d is correlated with neuropathic pain assay. A patent for a high throughput method of detecting ligands of α2δ1 is in process in Canada(2013). This expedited structure-activity relationship (SAR) method has been used to identify 45 ligands to α2δ1 and quantify their binding strengths(Chen, Stearns et al. 2006). This experiment could be modified to correlate the strength of binding of α2δ1 to our migration assay.

We report that treatment with TSP increases migration of primary cells, but we do not know whether the migration is chemotactic (directional) or random. Time-lapse photography of primary satellite cells would allow for a description of migratory patterns of these subpopulations of cells. Additionally, a device such as the NANIVID (NANo IntraVital

Imaging Device) could be employed. This device can create a steady concentration gradient over several hours, which is necessary to provoke chemotaxis(Raja, Gligorijevic et al.).

Thrombospondin-1 secretion by induced macrophages polarized from bone marrow-derived cells was discussed in Chapter 4. It remains to be seen whether satellite cell co-culture with these polarized macrophages migrate and proliferate to an extent that mirrors the amount of TSP-1 that they produce. Further, these types of cells could be cultured with subpopulations of satellite cells. We expect that satellite cells that express surface α2δ1 would respond most to M1 macrophages, as they secrete the most TSP-1.

The migration assay was successful only when we plated and passaged the cells once. This limited the experiments that could be performed, as levels of CD34 and α2δ1 are expected to change over a short time course, and it is likely that splitting the cells would accelerate this change. Genetic methods of enriching α2δ1 could be useful for maximizing the effect of TSP treatment.

There is ample room to understand better the relationship between the cellular events and *in vivo* tests. Testing muscles altered calcium handling proteins or altered sarcomeric proteins and would aid our ability to accurately interpret results from the test. In the age of translational research, it is important to know what calcium handling alterations are measureable *in vivo*.

REFERENCES

Adams, J. C. and J. Lawler "The thrombospondins." Cold Spring Harb Perspect Biol **3**(10): a009712.

Adams, J. C. and J. Lawler (1994). "Cell-type specific adhesive interactions of skeletal myoblasts with thrombospondin-1." Mol Biol Cell **5**(4): 423-37.

Adams, J. C. and R. P. Tucker (2000). "The thrombospondin type 1 repeat (TSR) superfamily: diverse proteins with related roles in neuronal development." Dev Dyn **218**(2): 280-99.

Alden, K. J. and J. Garcia (2002). "Dissociation of charge movement from calcium release and calcium current in skeletal myotubes by gabapentin." Am J Physiol Cell Physiol **283**(3): C941-9.

Allen, D. G., G. D. Lamb, et al. (2008). "Skeletal muscle fatigue: cellular mechanisms." Physiol Rev **88**(1): 287-332.

Allen, D. G., B. T. Zhang, et al. "Stretch-induced membrane damage in muscle: comparison of wild-type and mdx mice." Adv Exp Med Biol **682**: 297-313.

Arnold, L., A. Henry, et al. (2007). "Inflammatory monocytes recruited after skeletal muscle injury switch into antiinflammatory macrophages to support myogenesis." J Exp Med **204**(5): 1057-69.

Asakura, A., M. Komaki, et al. (2001). "Muscle satellite cells are multipotential stem cells that exhibit myogenic, osteogenic, and adipogenic differentiation." Differentiation **68**(4-5): 245-53.

Asakura, A., P. Seale, et al. (2002). "Myogenic specification of side population cells in skeletal muscle." J Cell Biol **159**(1): 123-34.

Banks, G. B. and J. S. Chamberlain (2008). "The value of mammalian models for duchenne muscular dystrophy in developing therapeutic strategies." Curr Top Dev Biol **84**: 431-53.

Bauer, C. S., A. Tran-Van-Minh, et al. "A new look at calcium channel alpha2delta subunits." Curr Opin Neurobiol **20**(5): 563-71.

Beauchamp, J. R., L. Heslop, et al. (2000). "Expression of CD34 and Myf5 defines the majority of quiescent adult skeletal muscle satellite cells." J Cell Biol **151**(6): 1221-34.

BERTELLI, F. U. K., BROWN, JASON PETER (United Kingdom), DISSANAYAKE, VISAKA (Sri Lanka), SUMAN-CHAUHAN, NIRMALA (United Kingdom) GEE, NICOLAS STEVEN (United Kingdom) (2013). C. I. P. Office. Canada.

Blaauw, B., M. Canato, et al. (2009). "Inducible activation of Akt increases skeletal muscle mass and force without satellite cell activation." FASEB J **23**(11): 3896-905.

Boldrin, L., A. Neal, et al. "Donor satellite cell engraftment is significantly augmented when the host niche is preserved and endogenous satellite cells are incapacitated." Stem Cells **30**(9): 1971-84.

Bosnakovski, D., Z. Xu, et al. (2008). "Prospective isolation of skeletal muscle stem cells with a Pax7 reporter." Stem Cells **26**(12): 3194-204.

Canti, C., M. Nieto-Rostro, et al. (2005). "The metal-ion-dependent adhesion site in the Von Willebrand factor-A domain of alpha2delta subunits is key to trafficking voltage-gated Ca2+ channels." Proc Natl Acad Sci U S A **102**(32): 11230-5.

Chapman, M. R., K. R. Balakrishnan, et al. "Sorting single satellite cells from individual myofibers reveals heterogeneity in cell-surface markers and myogenic capacity." Integr Biol (Camb) **5**(4): 692-702.

Chen, C., B. Stearns, et al. (2006). "Expedited SAR study of high-affinity ligands to the alpha(2)delta subunit of voltage-gated calcium channels: Generation of a focused library using a solution-phase Sn2Ar coupling methodology." Bioorg Med Chem Lett **16**(3): 746-9.

Collins, C. A., I. Olsen, et al. (2005). "Stem cell function, self-renewal, and behavioral heterogeneity of cells from the adult muscle satellite cell niche." Cell **122**(2): 289-301.

De Jongh, K. S., C. Warner, et al. (1990). "Subunits of purified calcium channels. Alpha 2 and delta are encoded by the same gene." J Biol Chem **265**(25): 14738-41.

De Luna, N., E. Gallardo, et al. "Role of thrombospondin 1 in macrophage inflammation in dysferlin myopathy." J Neuropathol Exp Neurol **69**(6): 643-53.

Dellorusso, C., R. W. Crawford, et al. (2001). "Tibialis anterior muscles in mdx mice are highly susceptible to contraction-induced injury." J Muscle Res Cell Motil **22**(5): 467-75.

Dimchev, G. A., N. Al-Shanti, et al. "Phospho-tyrosine phosphatase inhibitor Bpv(Hopic) enhances C2C12 myoblast migration in vitro. Requirement of PI3K/AKT and MAPK/ERK pathways." J Muscle Res Cell Motil **34**(2): 125-36.

Dolphin, A. C. "Calcium channel auxiliary alpha2delta and beta subunits: trafficking and one step beyond." Nat Rev Neurosci **13**(8): 542-55.

Dolphin, A. C., C. N. Wyatt, et al. (1999). "The effect of alpha2-delta and other accessory subunits on expression and properties of the calcium channel alpha1G." J Physiol **519 Pt 1**: 35-45.

Dooley, D. J., C. P. Taylor, et al. (2007). "Ca2+ channel alpha2delta ligands: novel modulators of neurotransmission." Trends Pharmacol Sci **28**(2): 75-82.

Douglas, L., A. Davies, et al. (2006). "Do voltage-gated calcium channel alpha2delta subunits require proteolytic processing into alpha2 and delta to be functional?" Biochem Soc Trans **34**(Pt 5): 894-8.

Elia, D., D. Madhala, et al. (2007). "Sonic hedgehog promotes proliferation and differentiation of adult muscle cells: Involvement of MAPK/ERK and PI3K/Akt pathways." Biochim Biophys Acta **1773**(9): 1438-46.

Eroglu, C., N. J. Allen, et al. (2009). "Gabapentin receptor alpha2delta-1 is a neuronal thrombospondin receptor responsible for excitatory CNS synaptogenesis." Cell **139**(2): 380-92.

Fanchaouy, M., E. Polakova, et al. (2009). "Pathways of abnormal stress-induced Ca2+ influx into dystrophic mdx cardiomyocytes." Cell Calcium **46**(2): 114-21.

Flucher, B. E. and C. Franzini-Armstrong (1996). "Formation of junctions involved in excitation-contraction coupling in skeletal and cardiac muscle." Proc Natl Acad Sci U S A **93**(15): 8101-6.

Flucher, B. E., J. L. Phillips, et al. (1991). "Dihydropyridine receptor alpha subunits in normal and dysgenic muscle in vitro: expression of alpha 1 is required for proper targeting and distribution of alpha 2." J Cell Biol **115**(5): 1345-56.

Foster, K., H. Foster, et al. (2006). "Gene therapy progress and prospects: Duchenne muscular dystrophy." Gene Ther **13**(24): 1677-85.

Gach, M. P., G. Cherednichenko, et al. (2008). "Alpha2delta1 dihydropyridine receptor subunit is a critical element for excitation-coupled calcium entry but not for formation of tetrads in skeletal myotubes." Biophys J **94**(8): 3023-34.

Garcia, J. "The calcium channel alpha2/delta1 subunit interacts with ATP5b in the plasma membrane of developing muscle cells." Am J Physiol Cell Physiol **301**(1): C44-52.

García, K., L. Grajales, et al. (2011). The α2/δ Subunit of Calcium Channels - A Multitasking Protein.

Garcia, K., T. Nabhani, et al. (2008). "The calcium channel alpha2/delta1 subunit is involved in extracellular signalling." J Physiol **586**(3): 727-38.

Garside, V. C., A. S. Kowalik, et al. "MIST1 regulates the pancreatic acinar cell expression of Atp2c2, the gene encoding secretory pathway calcium ATPase 2." Exp Cell Res **316**(17): 2859-70.

Glass, D. J. "PI3 kinase regulation of skeletal muscle hypertrophy and atrophy." Curr Top Microbiol Immunol **346**: 267-78.

Govoni, A., F. Magri, et al. "Ongoing therapeutic trials and outcome measures for Duchenne muscular dystrophy." Cell Mol Life Sci.

Grajales, L., J. Garcia, et al. "Induction of cardiac myogenic lineage development differs between mesenchymal and satellite cells and is accelerated by bone morphogenetic protein-4." J Mol Cell Cardiol **53**(3): 382-91.

Hack, A. A., M. E. Groh, et al. (2000). "Sarcoglycans in muscular dystrophy." Microsc Res Tech **48**(3-4): 167-80.

Heckmatt, J., E. Rodillo, et al. (1989). "Management of children: pharmacological and physical." Br Med Bull **45**(3): 788-801.

Hendrich, J., A. T. Van Minh, et al. (2008). "Pharmacological disruption of calcium channel trafficking by the alpha2delta ligand gabapentin." Proc Natl Acad Sci U S A **105**(9): 3628-33.

Hibino, H., R. Pironkova, et al. (2003). "Direct interaction with a nuclear protein and regulation of gene silencing by a variant of the Ca2+-channel beta 4 subunit." Proc Natl Acad Sci U S A **100**(1): 307-12.

Hoffman, E. P., E. Reeves, et al. "Novel approaches to corticosteroid treatment in Duchenne muscular dystrophy." Phys Med Rehabil Clin N Am **23**(4): 821-8.

Hoppa, M. B., B. Lana, et al. "alpha2delta expression sets presynaptic calcium channel abundance and release probability." Nature **486**(7401): 122-5.

Ieronimakis, N., G. Balasundaram, et al. "Absence of CD34 on murine skeletal muscle satellite cells marks a reversible state of activation during acute injury." PLoS One **5**(6): e10920.

Irintchev, A., M. Langer, et al. (1997). "Functional improvement of damaged adult mouse muscle by implantation of primary myoblasts." J Physiol **500 (Pt 3)**: 775-85.

Kallestad, K. M. and L. K. McLoon "Defining the heterogeneity of skeletal muscle-derived side and main population cells isolated immediately ex vivo." J Cell Physiol **222**(3): 676-84.

Kottlors, M. and J. Kirschner "Elevated satellite cell number in Duchenne muscular dystrophy." Cell Tissue Res **340**(3): 541-8.

Kuang, S. and M. A. Rudnicki (2008). "The emerging biology of satellite cells and their therapeutic potential." Trends Mol Med **14**(2): 82-91.

Kukkar, A., A. Bali, et al. "Implications and mechanism of action of gabapentin in neuropathic pain." Arch Pharm Res **36**(3): 237-51.

Lesault, P. F., M. Theret, et al. (2012). "Macrophages improve survival, proliferation and migration of engrafted myogenic precursor cells into MDX skeletal muscle." PLoS One **7**(10): e46698.

Lu, Z. and J. Kipnis "Thrombospondin 1--a key astrocyte-derived neurogenic factor." FASEB J **24**(6): 1925-34.

MacIntosh, B. R., R. J. Holash, et al. "Skeletal muscle fatigue--regulation of excitation-contraction coupling to avoid metabolic catastrophe." J Cell Sci **125**(Pt 9): 2105-14.

Majack, R. A., S. C. Cook, et al. (1986). "Control of smooth muscle cell growth by components of the extracellular matrix: autocrine role for thrombospondin." Proc Natl Acad Sci U S A **83**(23): 9050-4.

Manzur, A. Y. and F. Muntoni (2009). "Diagnosis and new treatments in muscular dystrophies." J Neurol Neurosurg Psychiatry **80**(7): 706-14.

Mauro, A. (1961). "Satellite cell of skeletal muscle fibers." J Biophys Biochem Cytol **9**: 493-5.

Mendell, J. R., J. T. Kissel, et al. (1995). "Myoblast transfer in the treatment of Duchenne's muscular dystrophy." N Engl J Med **333**(13): 832-8.

Meng, J., C. F. Adkin, et al. "Contribution of human muscle-derived cells to skeletal muscle regeneration in dystrophic host mice." PLoS One **6**(3): e17454.

Meriane, M., P. Roux, et al. (2000). "Critical activities of Rac1 and Cdc42Hs in skeletal myogenesis: antagonistic effects of JNK and p38 pathways." Mol Biol Cell **11**(8): 2513-28.

Miller, R. G., K. R. Sharma, et al. (1997). "Myoblast implantation in Duchenne muscular dystrophy: the San Francisco study." Muscle Nerve **20**(4): 469-78.

Morgan, J. E. and T. A. Partridge (1992). "Cell transplantation and gene therapy in muscular dystrophy." Bioessays **14**(9): 641-5.

Mortell, K. H., D. J. Anderson, et al. (2006). "Structure-activity relationships of alpha-amino acid ligands for the alpha2delta subunit of voltage-gated calcium channels." Bioorg Med Chem Lett **16**(5): 1138-41.

Morton, M. E. and S. C. Froehner (1989). "The alpha 1 and alpha 2 polypeptides of the dihydropyridine-sensitive calcium channel differ in developmental expression and tissue distribution." Neuron **2**(5): 1499-506.

Nabhani, T., T. Shah, et al. (2005). "Skeletal muscle cells express different isoforms of the calcium channel alpha2/delta subunit." Cell Biochem Biophys **42**(1): 13-20.

Novak, M. L. and T. J. Koh "Macrophage phenotypes during tissue repair." J Leukoc Biol **93**(6): 875-81.

Partridge, T. A., J. E. Morgan, et al. (1989). "Conversion of mdx myofibres from dystrophin-negative to -positive by injection of normal myoblasts." Nature **337**(6203): 176-9.

Peault, B., M. Rudnicki, et al. (2007). "Stem and progenitor cells in skeletal muscle development, maintenance, and therapy." Mol Ther **15**(5): 867-77.

Perdiguero, E., V. Ruiz-Bonilla, et al. (2007). "Genetic analysis of p38 MAP kinases in myogenesis: fundamental role of p38alpha in abrogating myoblast proliferation." EMBO J **26**(5): 1245-56.

Perez-Ruiz, A., V. F. Gnocchi, et al. (2007). "Control of Myf5 activation in adult skeletal myonuclei requires ERK signalling." Cell Signal **19**(8): 1671-80.

Politano, L. and G. Nigro "Treatment of dystrophinopathic cardiomyopathy: review of the literature and personal results." Acta Myol **31**(1): 24-30.

Protasi, F., C. Franzini-Armstrong, et al. (1997). "Coordinated incorporation of skeletal muscle dihydropyridine receptors and ryanodine receptors in peripheral couplings of BC3H1 cells." J Cell Biol **137**(4): 859-70.

Qu-Petersen, Z., B. Deasy, et al. (2002). "Identification of a novel population of muscle stem cells in mice: potential for muscle regeneration." J Cell Biol **157**(5): 851-64.

Raja, W. K., B. Gligorijevic, et al. "A new chemotaxis device for cell migration studies." Integr Biol (Camb) **2**(11-12): 696-706.

Rassier, D. E. and B. R. Macintosh (2000). "Coexistence of potentiation and fatigue in skeletal muscle." Braz J Med Biol Res **33**(5): 499-508.

Rassier, D. E. and B. R. MacIntosh (2002). "Sarcomere length-dependence of activity-dependent twitch potentiation in mouse skeletal muscle." BMC Physiol **2**: 19.

Risher, W. C. and C. Eroglu "Thrombospondins as key regulators of synaptogenesis in the central nervous system." Matrix Biol **31**(3): 170-7.

Roberts, P. and J. K. McGeachie (1990). "Endothelial cell activation during angiogenesis in freely transplanted skeletal muscles in mice and its relationship to the onset of myogenesis." J Anat **169**: 197-207.

Roberts, P. and J. K. McGeachie (1992). "The effects of pre- and posttransplantation exercise on satellite cell activation and the regeneration of skeletal muscle transplants: a morphometric and autoradiographic study in mice." J Anat **180 (Pt 1)**: 67-74.

Smith, I. C., J. Huang, et al. "Posttetanic potentiation in mdx muscle." J Muscle Res Cell Motil **31**(4): 267-77.

Spurney, C. F., A. Sali, et al. "Losartan decreases cardiac muscle fibrosis and improves cardiac function in dystrophin-deficient mdx mice." J Cardiovasc Pharmacol Ther **16**(1): 87-95.

Stodieck, L. S., B. J. Greybeck, et al. "In vivo measurement of hindlimb neuromuscular function in mice." Muscle Nerve **45**(4): 536-43.

Taktak, D. M. and P. Bowker (1995). "Lightweight, modular knee-ankle-foot orthosis for Duchenne muscular dystrophy: design, development, and evaluation." Arch Phys Med Rehabil **76**(12): 1156-62.

Tamaki, T., A. Akatsuka, et al. (2002). "Identification of myogenic-endothelial progenitor cells in the interstitial spaces of skeletal muscle." J Cell Biol **157**(4): 571-7.

Tamaki, T., Y. Uchiyama, et al. (2005). "Functional recovery of damaged skeletal muscle through synchronized vasculogenesis, myogenesis, and neurogenesis by muscle-derived stem cells." Circulation **112**(18): 2857-66.

Tamayo, T., L. Grajales, et al. "Commitment of Satellite Cells Expressing the Calcium Channel alpha2delta1 Subunit to the Muscle Lineage." J Signal Transduct **2012**: 460842.

Tanabe, T., K. G. Beam, et al. (1988). "Restoration of excitation-contraction coupling and slow calcium current in dysgenic muscle by dihydropyridine receptor complementary DNA." Nature **336**(6195): 134-9.

Torrente, Y., E. El Fahime, et al. (2000). "Intramuscular migration of myoblasts transplanted after muscle pretreatment with metalloproteinases." Cell Transplant **9**(4): 539-49.

Tremblay, J. P. and J. T. Vilquin (2001). "[Transplantation of normal or genetically modified myoblasts for the treatment of hereditary or acquired diseases]." J Soc Biol **195**(1): 29-37.

Turk, R., E. Sterrenburg, et al. (2005). "Muscle regeneration in dystrophin-deficient mdx mice studied by gene expression profiling." BMC Genomics **6**: 98.

Vandesompele, J., K. De Preter, et al. (2002). "Accurate normalization of real-time quantitative RT-PCR data by geometric averaging of multiple internal control genes." Genome Biol **3**(7): RESEARCH0034.

Watkins, S. C., G. W. Lynch, et al. (1990). "Thrombospondin expression in traumatized skeletal muscle. Correlation of appearance with post-trauma regeneration." Cell Tissue Res **261**(1): 73-84.

Zhang, Y., Y. Yamada, et al. "The beta subunit of voltage-gated Ca2+ channels interacts with and regulates the activity of a novel isoform of Pax6." J Biol Chem **285**(4): 2527-36.

VITA

EDUCATION

B.S. in Neurobiology, Physiology, and Behavior, UC Davis June 2005

B.S. in Materials Science and Engineering, UC Davis, June 2005

M.S. in Materials Science and Engineering, UC Davis September 2008

Undergraduate GPA 3.52, Graduate GPA 3.85

M.D. and Ph.D. in progress at the University of Illinois, Chicago, graduation in May, 2015

Ph.D. successfully defended in July, 2013

AWARDS AND RECOGNITIONS

Outstanding Undergraduate Researcher, UC Davis, 2004

Deans List, College of Letters and Science, and College of Engineering, 2002-2005

RESEARCH EXPERIENCE

Bridge to Baccalaureate (NIH) summer researcher 2001 and 2002

Undergraduate Researcher from 2003-2005 in the lab of Professor Amiya Mukherjee, College of Engineering, UC Davis

Graduate Researcher from 2006-2008, also in the lab of Professor Amiya Mukherjee, PhD, College of Engineering, UC Davis

Graduate Researcher from 2009-2013, Department of Physiology and Biophysics, Professor Jesuú García-Martínez, M.D., Ph.D.

TEACHING EXPERIENCE

Teaching Assistant, Mechanics of Materials EMS 172, UC Davis Fall 2005

Physiology Tutor, UIC COM, 2011-2013

Physiology Instructor, Summer Pre-Matriculation Program, Urban Health Program, UIC, 2010-2013

VITA (CONTINUED)

INSTITUTIONAL SERVICE

Student Advisory Committee, Medical Scientist Training Program, 2008-2010

Graduate Student Representative

Physiology and Biophysics Graduate Student Association 2010-2013

PRESENTATIONS

N. A. Mara, T. Tamayo, A.V. Sergueeva, X. Zhang, A. Misra, A.K. Mukherjee, Microstructure/High Temperature Mechanical Behavior Relationship in Cu/Nb Nanoscale Multilayers; Mechanics of Nanoscale Materials and Devices Symposium, Materials Research Society Conference, Spring 2006

N. A. Mara, T. Tamayo, X. Zhang, A. Misra, A.K. Mukherjee, Tensile Deformation of Cu/Nb Multilayers at Elevated Temperatures presented at Los Alamos National Laboratory as part of a symposium on nanoscale metallic multilayers, March 20, 2006.

T. Tamayo, A.V. Servueeva, Umberto Anselmo-Tamburini, A.K. Mukherjee, Effect of Volume Fraction of the High-Temperature Mechanical Behavior of Bimodal FCC Metals presented at the Materials Research Society Conference, San Francisco, Spring, 2007

T. Tamayo, Jennifer Kwan, Therapeutic potential of satellite cells in Duchenne Muscular Dystrophy, University Of Illinois at Chicago, Center for Cardiovascular Research Seminar Series, April 14, 2011

T. Tamayo, "Enriching Satellite Cells with a2d1 Promotes Differentiation" Biophysical Society Conference, San Diego, Monday Feb 27th, 2011 Presentation B620

T. Tamayo, J. Kwan "Metabolism & effects of inflammation on renal transplant survival/function in Obese Patients" UIC Center for Clinical and Translational Science and the Medical Scientist Training Program, April 23, 2013

VITA (CONTINUED)

PUBLICATIONS

N. A. Mara, A.V. Sergueeva, T. Tamayo, X. Zhang, A. Misra and A. Mukherjee, "High Temperature Mechanical Properties of Cu/Nb Nanoscale Multilayers at Diminishing Length Scales", Thin Solid Films, v 515, n 6, Feb 12, 2007, p 3241-3245.

The α2/δ Subunit of Calcium Channels - A Multitasking Protein Authors / Editors: Kelly Garcia, Liliana Grajales, Tammy Tamayo, and Jesús García (University of Illinois at Chicago, Chicago, IL, USA) Series: Protein Biochemistry, Synthesis, Structure and Cellular Functions Binding: Online Book Pub. Date: 2011 4th quarter ISBN: 978-1-62100-532-2

Tammy Tamayo, Liliana Grajales, and Jesús García, "Commitment of Satellite Cells Expressing the Calcium Channel α2δ1 Subunit to the Muscle Lineage," Journal of Signal Transduction, vol. 2012, Article ID 460842, 8 pages, 2012. doi:10.1155/2012/460842

Cantuti-Castelvetri L, Maravilla E. Marshall M. Tamayo T, D'Auria L, Monge J, Jeffries J, Sural-Fehr T, Lopez-Rosas A, Li G, Garcia K, van Breeman R, Vite C, Garcia J, Bongarzone ER, "Mechanism of Neuromuscular Dysfunction in Krabbe Disease," J Neurosci;35(4):1606-1616

Tammy Tamayo, Eben Eno, Carlos Madrigal, Ahlke Heydemann, Kelly García, Jesús García, "Functional *In Situ* Assessment of Muscle Contraction in Wild Type and *mdx* Mice," Muscle and Nerve, accepted

APPENDIX

Permission to Reprint Copyright Material

Dear Dr. Tamayo,

Thank you for your email. I would like to let you know that all articles published in Hindawi journals are released under a "Creative Commons Attribution License," enabling the unrestricted use, distribution, and reproduction of an article in any medium, provided that the original work is properly cited. The authors of the article, along with any interested reader, are free to view, print, and download any articles published in the journal.

You do not need any permission to use them. However, you must cite the original source of the article to ensure proper attribution.

For more information about how to cite this article, you can use the following URL:

http://www.hindawi.com/journals/jst/2012/460842/cta/

Please feel free to contact me if you have further inquiries.

Best regards,

Rana

From the linked page:
"Copyright © 2012 Tammy Tamayo et al. This is an open access article distributed under the Creative Commons Attribution License, which permits unrestricted use, distribution, and reproduction in any medium, provided the original work is properly cited."
From their copyright page:
"Copyright
Open Access authors retain the copyrights of their papers, and all open access articles are distributed under the terms of the Creative Commons Attribution License, which permits unrestricted use, distribution and reproduction in any medium, provided that the original work is properly cited.
The use of general descriptive names, trade names, trademarks, and so forth in this publication, even if not specifically identified, does not imply that these names are not protected by the relevant laws and regulations.
While the advice and information in this journal are believed to be true and accurate on the date of its going to press, neither the authors, the editors, nor the publisher can accept any legal responsibility for any errors or omissions that may be made. The publisher makes no warranty, express or implied, with respect to the material contained herein."